NUNA CLÁUDIA PEIXOTO DE ARAÚJO

INTERPLAY BETWEEN MINERALIZATION AND INFLAMMATION IN OSTEOARTHRITIS: GLA-RICH PROTEIN AND MARINE BIOACTIVE COMPOUNDS AS NEW THERAPEUTIC APPROACHES

UNIVERSIDADE DO ALGARVE

2023

NUNA CLÁUDIA PEIXOTO DE ARAÚJO

INTERPLAY BETWEEN MINERALIZATION AND INFLAMMATION IN OSTEOARTHRITIS: GLA-RICH PROTEIN AND MARINE BIOACTIVE COMPOUNDS AS NEW THERAPEUTIC APPROACHES

Doutoramento em Ciências Biomédicas

Trabalho efetuado sob a orientação de: Professora Doutora Dina Simes,

e co-orientação de:

Doutora Carla Viegas

Doctor Cees Vermeer

UNIVERSIDADE DO ALGARVE

2023

Interplay between mineralization and inflammation in osteoarthritis:
Gla-rich protein and marine bioactive compounds as new therapeutic approaches

Declaração de autoria de trabalho

Declaro ser a autora deste trabalho, que é original e inédito. Autores e trabalhos consultados estão devidamente citados no texto e constam da listagem de referências incluída.

À minha adorável filha, Jojo!

Agradecimentos

Como em qualquer percurso desafiante da vida, o apoio que nos é dado é imprescindível e de grande reconhecimento!

Assim, gostaria de iniciar agradecendo à Professora Doutora Dina Simes e à Doutora Carla Viegas, por me terem acolhido no seu grupo de investigação 'Functional Biochemistry and Proteomics' e me terem apoiado na planificação e execução deste projeto. Foram sempre muito presentes quer na transmissão do seu conhecimento científico, quer na orientação do trabalho. Nesta fase final, o seu empenho e dedicação foram da maior relevância e estou-lhes grata pela persistência e encorajamento constantes. Acrescento também, os bons momentos de partilha em termos pessoais, que se foram proporcionando ao longo dos anos e que contribuiram para que tudo fosse mais prazeroso.

Agradeço ao Doutor Acácio Ramos, o principal responsável pela colheita de material biológico do projeto, que sempre me recebeu no Hospital Particular do Algarve com grande entusiasmo e que se mostrou sempre disponível para colaborar nos estudos bem como esclarecer qualquer dúvida que pudesse surgir.

Agradeço também à Doutora Joana Magalhães, do Grupo de Bioingeniería Tisular y Terapia Celular – Coruña, pela sua recetividade e empenho, quer na análise de material biológico, quer na disponibilizaçao de culturas celulares. O seu contributo e incentivo foram também enormes no acompanhamento deste trabalho, em vários momentos de avaliação relativamente ao progresso do trabalho,integrando a comissão de acompanhamento deste doutoramento. Agradecimentos ao Doutor Francisco Blanco por permitir a colaboração entre o seu grupo de investigação (Grupo de Bioingeniería Tisular y Terapia Celular) e o nosso.

Agradeço ao Professor Doutor José Belo por se ter mostrado disponível e ter participado na avaliação periódica do estado de desenvolvimento do meu doutoramento, fazendo parte da comissão de acompanhamento.

Ainda relativamente ao apoio na componente científica, agradeço à Professora Doutora Anjos Macedo pelo seu contributo nos estudos de microscopia e pela sua dedicação, paciência e entusiasmo. Um agradecimento ao Professor Doutor António P. Matos pelo seu conhecimento na área, de grande utilidade em algumas das conclusões deste projeto.

Gostaria de agradecer à Professora Doutora Ana Grenha, pelos conhecimentos transmitidos na área de nanoencapsulação. Pela sua disponibilidade e dedicação. Um agradecimento especial para o Jorge Pontes pela sua dedicação, persistência e empenho incansáveis e pela sua boa disposição!

À Professora Doutota Eva Zubía, agradeço as amostras de compostos de origem marinha disponibilizados e a sua disponibilidade.

I want to express my gratitude to Doctor Cees Vermeer for providing me with the opportunity of either directly or indirectly access his extensive knowledge about Vitamin K.

Agradecimentos ao Doutor José Enriquez por permitir a colaboração entre o Departamento de Anatomia Patológica do Centro Hospitalar do Algarve e o nosso laboratório, e em particular à Técnica Alexandra Teixeira, que realizou todas as inclusões de tecidos em parafina do projeto e alguns dos cortes histológicos.

Agradeço aos meus colegas de laboratório, que me recepcionaram, Sofia Cavaco, Lúcia e Rúben, que foram cruciais no início deste projeto. Mais tarde, juntou-se a Inês e a Catarina Marreiros, com quem eu gostei muito de partilhar o laboratório e a quem reconheço grandes qualidades pessoais e como investigadora!

Obrigada a todos os que se cruzaram neste percurso e que me apoiaram de alguma maneira… Amiga Liliane, pelo apoio e bons momentos, Vera, Monya, Daniela... Um agradecimento especial para a minha amiga Marta, sempre presente e grande companheira!

Fora da Universidade, agradeço a amizade em forma de incentivo e encorajamento de quem me rodeia, destacando a presença constante da Jani e Nanda. Um agradecimento particular à Luci, pelo acompanhamento em momentos-chave!

À minha 'família' mais próxima, em especial à minha filha Jojo e à minha querida mãe, as forças motrizes (!) desta caminhada, o meu sentido 'Obrigada'.

A produção deste trabalho teve o financiamento da Fundação para a Ciência e Tecnologia (SFRH/BD/111824/2015), à qual expresso os meus agradecimentos.

Abstract

Osteoarthritis (OA) is a prevalent joint disorder with significant global impact, characterized by limited treatment options and challenges in early diagnosis. This research aimed to address a deeper understanding of the onset and progression of OA, while exploring novel therapeutic strategies. Pathologic calcification and inflammation, associated with degradation of cartilage extracellular matrix, are prominent features observed in OA. Gla-Rich Protein (GRP), a vitamin K-dependent protein, has recently shown promising potential in possessing anti-inflammatory and anti-mineralization properties in articular cells, suggesting its role in the interplay between inflammation and mineralization in OA. Based on that, we developed chitosan-based nanoparticles to encapsulate GRP, aiming to enhance its bioavailability and thereby facilitating its application in functional assays. These nanoparticles effectively delivered GRP and retained its anti-inflammatory activity in human activated macrophages (THP-1 MoM) and chondrocytes. The novel nanoformulation demonstrated promising potential for therapeutic applications in chronic inflammatory diseases. Furthermore, we developed an experimental pipeline in order to evaluate potential OA-modifying compounds and their effects on inflammation and mineralization. The pipeline involved a series of activity assessments, starting from a simpler cell-based model of OA and progressing to a more complex co-culture model based on human cartilage. This progressive approach allowed us to examine potential drugs as mediators of inflammation and mineralization, mimicking the early disease stages and providing valuable insights into the complex pathological processes involved in OA progression. In the search for new active compounds to treat OA, we investigated the utilization of a marine bioactive compound, amentadione (YP), in the context of OA treatment, using the established pipeline. Amentadione exhibited strong anti-inflammatory effects, by downregulating key inflammatory mediators such as cyclooxygenase 2 (COX-2) and interleukin 6 (IL-6), and also demonstrated the ability to regulate nuclear factor κB (NF-κB) signaling pathways. By decreasing matrix metalloproteinase-3 (MMP3) levels and chondrocyte hypertrophic differentiation factors, Col10 and Runx2, YP contributed to cartilage homeostasis. These findings highlight the high therapeutic potential of amentadione as a cartilage protective factor in OA.

In summary, this research highlights the therapeutic potential of both GRP and marine bioactive compound YP in the management of inflammatory responses in OA. The utilization

of novel drug delivery systems, including chitosan-based nanoparticles, along with the comprehensive evaluation of compounds using the established experimental pipeline, offers the possibility of better understanding the underlying disease mechanisms and to explore new potential active compounds in OA.

Keywords: Osteoarthritis , Gla-Rich Protein, Marine Bioactive Compounds, Inflammation, Mineralization, Ectopic calcification, Nanoencapsulation, 3D OA model.

Resumo

A osteoartrite (OA) é uma doença da articulação, prevalente e com impacto global significativo, que combina a quase inexistência de um diagnóstico precoce, com tratamentos limitados e direcionados maioritariamente para combater a sintomatologia. Este projeto teve como objetivo uma melhor compreensão sobre a iniciação da OA e sua progressão, assim como a exploração de novas estratégias terapêuticas. Para tal, um sistema sequencial de testes que mimetizam uma fase inicial da doença foi desenvolvido e aplicado para a investigação de novos agentes com potencial atividade na OA. Calcificação patológica e inflamação, associadas à degradação da matriz extracelular, são características proeminentes observadas na OA. Gla-Rich Protein (GRP), uma proteína dependente de vitamina K, mostrou recentemente potenciais atividades anti-inflamatórias e anti-mineralizantes em células articulares, podendo desempenhar um papel na interação entre a inflamação e a mineralização na OA. Com base nisso, e conhecendo algumas limitações da GRP, desenvolvemos pela primeira vez, nanopartículas à base de quitosano para encapsular a GRP, visando aumentar a sua biodisponibilidade e estabilidade, facilitando assim a sua aplicação em ensaios funcionais. Essas nanopartículas revelaram-se efetivas na entrega da proteína GRP, a qual reteve a sua atividade anti-inflamatória em macrófagos ativados (THP-1 MoM) e condrócitos. A nova nanoformulação demonstrou um potencial promissor para aplicações terapêuticas em doenças inflamatórias crónicas. Posteriromente, desenvolvemos uma sequência de ensaios experimentais na perspetiva de avaliar o potencial de alguns compostos como modificadores da doença, focando nos seus efeitos anti-inflamatórios e anti-mineralizantes. Essa sequência de testagem envolve uma série de avaliações de atividade, que têm início num modelo mais simples de OA, baseado em células, e progredindo para um modelo mais complexo, de co-cultura celular e explantes de cartilagem humana. Esta abordagem experimental contínua e progressiva permitiu examinar a atividade de alguns compostos enquanto mediadores da inflamação e mineralização, tentando reproduzir as condições dos estadios iniciais da doença e fornecendo informações valiosas sobre os complexos processos patológicos envolvidos na progressão da mesma. Assi, na busca de novos compostos ativos para o tratamento da OA, investigámos a atividade de um composto marinho bioativo, amentadiona, no contexto do tratamento da OA e usando o sistema experimental de testagem estabelecido. A amentadiona revelou capacidade anti-inflamatória e melhorou a homeostase da cartilagem. Reduziu os principais mediadores inflamatórios, como ciclooxigenase 2 (COX-2) e interleucina 6 (IL-6), e também demonstrou a capacidade de regular as vias de sinalização do fator nuclear κB (NF-κB). Esses resultados demonstram

potencial terapêutico da amentadiona como fator protetor da cartilagem na OA.

Em suma, esta pesquisa destaca o potencial terapêutico da GRP, na sua forma livre e nanoencapsulada, e do composto bioativo marinho amentadiona na modulação de respostas inflamatórias na OA. A utilização de novos sistemas de entrega de compostos ativos, incluindo nanopartículas à base de quitosano, juntamente com a avaliação abrangente de compostos usando a sequência experimental de testes aqui estabelecida, oferece a possibilidade de entender melhor os mecanismos subjacentes da doença e explorar a potencialidade da atividade de novos compostos na OA.

Palavras-chave: Osteoartrite, Gla-Rich Protein, Compostos marinhos bioativos, Inflamação, Mineralização, Calcificação patológica ou ectópica, Nanoencapsulação, Modelo 3D de co-cultura para OA.

Table of Contents

Figure Index

Table Index

Abbreviation list

3D	Three-dimensional
Aa	Amino acid
ADAMTS	A disintegrins and metalloproteinases with thrombospondin motifs
ACR	American College of Rheumatology
AE	Association efficiency
AF	Arthritis Foundation
ALP	Alkaline phosphatase
ANOVA	Analysis of variance
BCP	Basic calcium phosphate
BMP	Bone morphogenetic protein
Bp	Base pairs
BSA	Bovine serum albumin
CBB	Coomassie brilliant blue
CBME	Centro de Biomedicina Molecular e Estrutural
CCMar	Centro de Ciências do Mar
CDC	Centre for Disease Control and Prevention
CDMP	Cartilage-derived morphogenetic proteins
cDNA	Complementary DNA
cGRP	γ-carboxylated GRP
CHUAC	Complejo Hospitalario Universitario a Coruña
CIBER	Centro de Investigación Biomédica en Red
CID	Chronic Inflammatory Diseases
CKD	Chronic kidney disease
cMGP	γ-carboxylated MGP
CNG	ucGRP-loaded CS/TPP nanoparticles
CNP	Chitosan (CS)/TPP nanoparticles
Col1a1	Type I collagen
Col2a1	Type II collagen
Col10a1	Type X collagen
COMP	Cartilage oligomeric matrix protein
COX-2	Cyclooxygenase 2
CPP	Calciprotein particles
CPPD	Calcium pyrophosphate dehydrate
CRP	C-reactive protein
CRPM	C-reactive protein metabolite
CRTAC1	Cartilage acidic protein 1
CS	Deacetylated chitosan
CT	Computed Axial Tomography
Ctr	Control
CTX-II	C-terminal cross-linked telopeptide of type II collagen
CVD	Cardiovascular diseases
Cy C	Cystone C
Cyd G	Cystodione G
Cyd K	11-Hydroxyamentadione
DALYs	Disability-adjusted life years
DAMPs	Damage-associated molecular patterns

DMEM	Dulbecco's modified Eagle's medium
DMOADs	Disease-modifying osteoarthritis drugs
DNA	Deoxyribonucleic acid
Dp-ucMGP	Dephosphorylated and undercarcoxylated MGP
DTT	Dithiothreitol
DXM	Dexamethasone
E	Extinction coefficient
ECM	Extracellular matrix
EDAC	1-Ethyl-3-(3-dimethylaminopropyl) carbodiimide hydrochloride
EDTA	Ethylenediamine tetraacetic acid
ELISA	Enzyme-linked immunosorbent assay
ESR	Erythrocyte sedimentation rate
EVs	Extracellular vesicles
FBS	Fetal bovine serum
FBP	Functional Biochemistry and Proteomics
FC	Fluorescein labelled chitosan
FCT	Fundação para a Ciência e Tecnologia
FCNG	GRP-loaded FC/TPP nanoparticles
FCNP	Fluorescein labelled chitosan (FC)/TPP nanoparticles
GAG	Glycosaminoglycans
Gas6	Growth arrest-specific protein 6
GBD	Global Burden of Disease
GGCX	γ-glutamyl carboxylase
Gla	γ-carboxyglutamic acid
Glc-Gal-Pyd	Glucosyl-galactosyl-pyridinoline
Gln	Glutamine
Glu	Glutamate
GRP	Gla-rich protein
HAP	Hydroxyapatite
HE	Hematoxylin-eosin
HFLS	Human fibroblast-like synoviocytes
HIF-2α	Hypoxia-inducible factor 2α
IF	Immunofluorescence
IGF	Insulin-like growth factor
IHC	Immunohistochemistry
IkBα	Nuclear factor of kappa light polypeptide gene enhancer in B-cells inhibitor, alpha
IL	Interleukin
K	Quinone form of vitamin K
K1	Phylloquinone
K2	Menaquinones
KH2	Vitamin K hydroquinone
KL	Kellgren-Lawrence
KO	Vitamin K 2,3-epoxide
LC-MS/MS	Liquid chromatography-MS/MS
LDS	Lithium dodecyl sulphate
LPS	Lipopolysaccharide
MCM	Conditioned media
MGP	Matrix Gla protein
MK	Menaquinone

MK-n	Menaquinone with a n number of prenyl repeats
MMP	Matrix metalloproteinase
MPSs	Microphysiological systems
MS	Mass spectrometry
MVs	Matrix vesicles
MW	Molecular weight
NF-κB	Nuclear factor κB
NO	Nitric oxide
NOS	Nitric oxide synthase
NSAIDs	Nonsteroidal anti-inflammatory drugs OA Osteoarthritis
NTA	Nanoparticle Tracking Analysis
OARSI	Osteoarthritis Research Society International
OC	Osteocalcin
O/N	Overnight
OPN	Osteopontin
Osx	Osterix
PBS	Phosphate buffered saline
PCR	Polimerase chain reaction
PdI	Polydispersity index
PG	Prostaglandin
pI	Isoelectric point
Pi	Inorganic phosphate
PPi	Inorganic pyrophosphate
PRGP	Proline-rich Gla proteins
PY	Process yield
RA	Rheumatoid arthritis
RNA	Ribonucleic acid
ROS	Reactive oxygen species
RP-HPLC	Reverse phase-high performance liquid chromatography
RT	Room temperature
RT-PCR	Reverse transcription-polymerase chain reaction
Runx2	Runt-related transcription factor 2
SD	Standard deviation
SDS-PAGE	Sodium dodecyl sulphate-polyacrylamide gel electrophoresis
SO	Safradin-O
Sox9	SRY-box 9
TBST	Tris buffered saline
TEM	Transmission electron microscopy
TGF-β	Transforming growth factor β
THP-1 MoM	THP-1 macrophage cells
TLR	Toll-like receptors
TMG	Transmembrane Gla proteins
TNFα	Tumour necrosis factor α
TPP	Tripolyphosphate
ucGRP	Undercarboxylated GRP
UCMA	Upper zone of growth plate and cartilage matrix associated protein, former unique cartilage matrix associated protein
ucMGP	Undercarboxylated MGP
ucOC	Undercarboxylated OC
VEGF	Vascular endothelial growth factor

VKDP	Vitamin K-dependent protein
VKOR	Vitamin K epoxide reductase
VKR	Vitamin K reductase
VSMCs	Vascular smooth muscle cells
WHO	The World Health Organization
Wnt	Wingless/Int
YP	Amentadione
YLD	‘Years lived with disease’

Chapter 1

General introduction

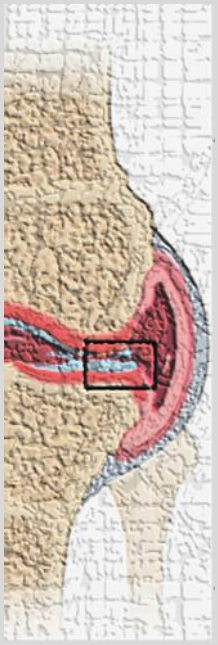

© Nuna Araújo

Chapter 1 – General introduction

This introductory chapter includes a brief description and contextualization of osteoarthritis (OA), describing OA physiopathology, diagnosis and epidemiologic state. It outlines the interplay of inflammation and ectopic calcification in the progression of the disease and the necessity for new therapeutic approaches for this common complex degenerative condition, and reviews the stated approaches to circumvent the pathology and to study OA.

1.1 Chronic Inflammatory Diseases (CID) and Osteoarthritis

According to The World Health Organization (WHO), chronic inflammatory diseases (CIDs) are the most significant cause of death worldwide, being identified as the major threat to human health (1). The prevalence of diseases associated with chronic inflammation is anticipated to increase for the next 30 years, and presently, 3 of 5 people die due to CIDs. Among them, osteoarthritis (OA), arthritis, cardiovascular diseases (CVD), chronic kidney disease (CKD), diabetes, neurodegenerative disorders and cancer are leading causes of death and disability, globally (2).

Inflammation is part of the organism mechanism of protection that can be either manifested as acute, starting rapidly and becoming severe in a short period of time, or as persistent, evolving for a chronic state. Chronic inflammation is usually referred as a slow and long-term inflammation, lasting for several months to years and might lead to organ dysfunction, incapacity and life risk (2).

Osteoarthritis is the most common chronic degenerative disease of the joint, that compromises life quality and can cause disability. Although the disease pathophysiology is still not totally unveiled, it is accepted that the trigger of OA may be multifactorial and that inflammation has an important role in the initiation, progression and severity of OA, as it is implicated in a wide range of biomechanical alterations and immune responses (2-3). There are several risk factors associated with OA, such as gender, obesity, age, genetic profile and mechanical factors (5). OA is considered a whole joint disease, affecting many tissues of the articulation, including subchondral bone, cartilage, ligaments and the synovium, and all are intervenients in the complex process of joint remodeling and degeneration. There are some histopathological features that are commonly present during the development of the disease,

such as the articular cartilage damage, subchondral bone sclerosis and osteophyte formation, joint capsule hypertrophy and periarticular muscle dysfunction, as well as inflammation of the synovium (5).

1.2 Osteoarthritis epidemiology: a state of the evidence

Osteoarthritis epidemiology has faced an income of data deriving not only from recent clinical studies approaching osteoarthritis patients, but also from world organisations that have been putting a lot of efforts and resources on reporting and sensitizing for this pathology. The evolution of modern health-care systems and the increasing insights into the pathogenesis of pain in osteoarthritis, boosted its diagnostics and consequently the medical reporting. It is important to note, however that although there are considerable and recent data regarding this pathology, the estimates of osteoarthritis are still quite far from the reality, and do not estimate the true dimension of the problem (5-6).

Despite the global efforts of some of the most relevant organizations regarding this matter, as the Centre for Disease Control and Prevention (CDC) (8), the Arthritis Foundation (AF) (9) and World Health Organization (WHO) (10), osteoarthritis does not feature in global strategic plans for non-communicable diseases, even though commonly coexists with heart disease, diabetes, and mental health problems and can worsen the morbidity and mortality associated with these conditions (10-12). This can be partially explained by the fact that OA does not result in direct death, despite its significant impact on life quality. Due to the fact that measuring non-fatal health loss is one of the most complex endeavors in population health research, the disease is still an under-recognized chronic condition and generally neglected (11,13).

Adding to the imprecise accounting of this pathology, it is also important to note that both reported prevalence and incidence rates vary across studies, due to the various definitions of OA that are used: symptomatic, radiographic, self-reported, or doctor diagnosed. In general, prevalence estimates for symptomatic OA tend to be lower than radiographic OA as its diagnosis is defined by a combination of symptoms such as pain and stiffness, and radiographic (15). A systematic review showed that the reported prevalence of osteoarthritis in individual studies depended on the definition of osteoarthritis used, as well as on the age categories, countries of origin, and sex distribution of the study population (16). Also, patients with

osteoarthritis frequently report that their concerns are underestimated, delaying or disregarding osteoarthritis diagnosis (17).

Global changes of demographic structure and lifestyle are affecting the epidemiological data in general and pointing the society for the true life-impact of this pathology. The trends to having an elderly population, the higher rates of obesity observed worldwide along with increasing numbers of joint injuries are the main reasons. Additionally, social determinants, access to health care, all have impacts on the raising of the disease burden, particularly in high-income countries (6). This can be seen in the latest results from WHO Geneva 2020 report (18). While in 2000 OA was considered the 17th highest cause of 'years lived with disease' (YLD) in the whole world, in 2019 it climbed the rank to the 13th position demonstrating the growing health impacts on society.

Parallel to WHO reports, the Global Burden of Disease (GBD) project has been a remarkable contributor of data and statistics for osteoarthritis, in recognising the importance of OA to population health and health systems globally. Safiri *et al.* made a practical and recent review, covering only the OA data from the most recent GBD report from 2017 (19). Although Spanish and UK general practice registry data have been used to report on the incidence of osteoarthritis in the general population (19), the GBD project not only estimates the most reliable global incidence, but also the prevalence of OA, covering a total of 195 countries in its study (19-20). Results from the GBD study showed that, from 1990 to 2017, there was a 102 % increase in crude incidence rate of OA (21-22).

Recent data registered 41,5 million new OA diagnostics, with women being disproportionately affected by the condition (23), namely 24,4 million of women to 17,1 million men. Nearly 18 million YLD were due to OA, and regarding the disability-adjusted life years (DALYs), equivalent of one year of full health, the numbers reported were around 1 million cases for both sexes which reflects the burden of this disease in the everyday life (24). Another relevant data from GBD report showed that musculoskeletal disorders were the first cause of YLDs in comparison to 21 other cause categories, including 354 diseases and injuries (24).

Clinically, the knee is the most common site of osteoarthritis, followed by the hand and hip. This was confirmed by 2019 GBD data, where osteoarthritis affected 7 % of the global population, around 527 million people worldwide, with knee osteoarthritis having a substantial account for this number with 4 %, followed by hand osteoarthritis with 1.9 % and hip osteoarthritis with 0.44 % (23).

Despite the more accurate data, a limitation of GBD report regarding OA is important

to note. It estimates largely hip and knee OA, since these are the common sites of OA in larger joints and considered the cause of the greatest disability. Furthermore, the GBD study 2017 only included the symptomatic knee OA, radiologically confirmed, which tended to collect relatively late cases, due to the discordance between symptomatic and radiographic changes (19).

A recent systematic review and meta-analysis estimated the global prevalence of knee OA based on 9,440,250 participants from 34 countries. Their results showed that global prevalence of knee OA was 22.9 % in individuals aged 40 and over. The continent with highest prevalence of knee OA was Africa 21.0 %, followed by Asia with 19.2 %, Europe and North America had a prevalence of 13.4 % and 15.8 %, respectively (25). This supports the growing tendency of OA in low-income and lower middle-income countries (25).

Several observational and interventional studies have showed in a smaller scale the OA burden, perceiving how the global estimates continue to underscore its position as a leading cause of disability worldwide. Wallace IJ *et al*. demonstrated that the prevalence of knee OA has doubled since the mid-20th century in the United States (26).

In Portugal, a 2005 national report of an observational study about the most prevalent chronic diseases, identified that 24 % of the participants reported suffering from some form of rheumatic disease (27). Other important data is presented by the *Observatório Nacional das Doenças Reumáticas* in 2010, where estimated radiographic knee osteoarthritis in subjects older than 40 years, was 56.9 % in men and 57.7 % in women; radiographic hip osteoarthritis was 54.8 % in men and 24.5 % in women. In 2013, *Liga Portuguesa Contra as Doenças Reumáticas* estimated that 6 % of the Portuguese population had the disease (28). More recently, Branco *et al*. conducted a study (29) with 10661 participants, where the prevalence for knee OA was 12.4 %, hand OA was 8.7 % and hip OA was 2.9 %. They concluded that musculoskeletal diseases are highly prevalent in Portugal and are associated not only with significant physical function but mental health impairment, leading to greater consumption of health resources.

Over the years many studies have investigated the association between knee OA and premature mortality, leading to conflicting results. This is mostly due to differences in OA diagnostic. For instance, *Kluzek et al.* (30) published results based on a cohort population of 821 Caucasian women, showing that knee pain, with or without radiographic OA, was associated with premature all-cause and cardiovascular (CVD) specific mortality. In 2019, a study with a community-based cohort including Afro American and Caucasian adults ≥45 years of age, included 4182 participants with nearly 15 years of follow-up, in which 1822 deaths

occurred (31). An analysis by *Turkiewicz et al*. (32) using a large database from the Swedish Healthcare Register also showed an increased risk for cardiovascular death for knee and hip OA patients with a doctor-diagnosis, during 9–11 years of follow-up, respectively.

Arthritis is a serious disease resulting in enormous societal and personal impact. Combined, these studies call for improved strategies to decrease OA global burden, and more important, they point into the direction that OA contributes to an unfavourable clinical outcome due to limitations in physical function and activity.

Musculoskeletal disorders, including OA, are highly prevalent and are expected to increase worldwide (33). Because of its function-impairing nature, its impact on society is quite substantial both in terms of its epidemiology and its economic effect. In fact, the health-care costs, together with the personal costs for patients with osteoarthritis, such as loss of income and the subsequent reductions in personal savings, greatly surpass the direct health-care costs (34).

OA is a major public health challenge, and an increasing burden in most countries. It is expected to continue with increased life expectancy and ageing of the global population. Improving population and policy maker awareness of risk factors, including overweight and injury, and the importance and benefits of OA management, together with providing health services for an increasing number of people living with OA, are recommended for management of the future burden of this condition.

1.3 Osteoarthritis diagnosis

Currently, the diagnosis of OA is generally made by medical history, physical examination of the affected joint and radiographic evaluations. Except in the advanced stages, there is usually uncertainty about the diagnosis of OA. The American College of Rheumatology (ACR) developed criteria for the classification of Knee osteoarthritis in 1986, and later for osteoarthritis of the hand and hip. These criteria, combines clinical and radiological data and have since, been routinely used in all clinical and epidemiological studies on osteoarthritis and are now a fully accepted standard (33-34).

Regarding the assessment of osteoarthritis severity, two of the most widely used radiographic classification systems are the Kellgren and Lawrence (KL) system and the Osteoarthritis Research Society International (OARSI) atlas criteria. The OARSI classification

system is considered more suitable for categorizing joint space width, whereas the KL system is used to assess the overall OA status of the joint. Kellgren and Lawrence (37) published a method of grading osteoarthritis of the knee in 1957 (**Table 1. 1**), which has been widely used in clinical and epidemiological studies to categorize the status of the joint. The KL classification system grades OA from a 0, in which 0 corresponds to healthy joints and 4, to end stage OA (**Table 1. 1**), and the most adequate treatment for each OA patient is defined according to the obtained classification degree (38). However, some authors have questioned its validity, as it relies mainly on the presence of osteophytes and does not adequately assess the importance of the joint space impingement (39). Also, OA may be developing silently at early stages, without the typical symptoms and radiographic changes manifestations, and the articular cartilage destruction may become irreversible during that subclinical phase (40).

Table 1.1 Grades of Radiological Osteoarthritis (Adapted from Kellgren and Lawrence (35).

GRADE	FEATURES
0	Absence of osteophytes
1	Minimal osteophytes and joint space narrowing
2	Minimal osteophytes, possible joint space narrowing, cysts and sclerosis
3	Moderate, well-defined osteophytes with definitive joint space narrowing, sclerosis and possible bony deformity
4	Severe OA with large osteophytes, marked joint space narrowing, sclerosis and definitely bony deformity

The principal clinical manifestations of this pathology are joint pain, limitation of movement, crunching and occasionally, variable degrees of swelling or even synovial effusion (14,39). Other signs and symptoms are joint deformity and malalignment, instability and stiffness of the joint. The most frequently affected joints are the knees, hand, hips and small joints of the spine as well as of the foot. The clinical expression is highly variable depending on the joint affected and the time of disease progression. Although the course is usually slow and progressive, patients often suffer painful exacerbations triggered by trauma, overload, periarticular complications or blockages due to meniscal degeneration or articular free bodies (42).

Except in the inflammatory phases, the usual blood tests in patients with primary OA show normal results (43). The erythrocyte sedimentation rate (ESR) is part of the routine general analysis carried out and it allows to distinct between conditions of inflammatory origin from those of mechanical origin, where the acute phase reactants are within the limits of normality or slightly elevated. In primary OA, the analytical determination of C-reactive protein (CRP) does not provide any additional data, and present normal values (44). In inflammatory phases, a moderate elevation of ESR and/or CRP may be detected. Blood tests can be an important tool to confirm or rule out metabolic causes (45).

Normal radiography remains the imaging technique of first choice in the study of patients with OA, as the characteristic tetrad of OA consists of joint space impingement, marginal osteophytes, subchondral bone sclerosis and subchondral geodes. In early stages, only discrete joint impingement or isolated osteophytes may be seen. In advanced stages there is irregularity of the subchondral bone, even with direct contact between adjacent cysts, severe subchondral sclerosis and misalignment of the joint axes, with joint deformity (**Figure 1.1**) (46).

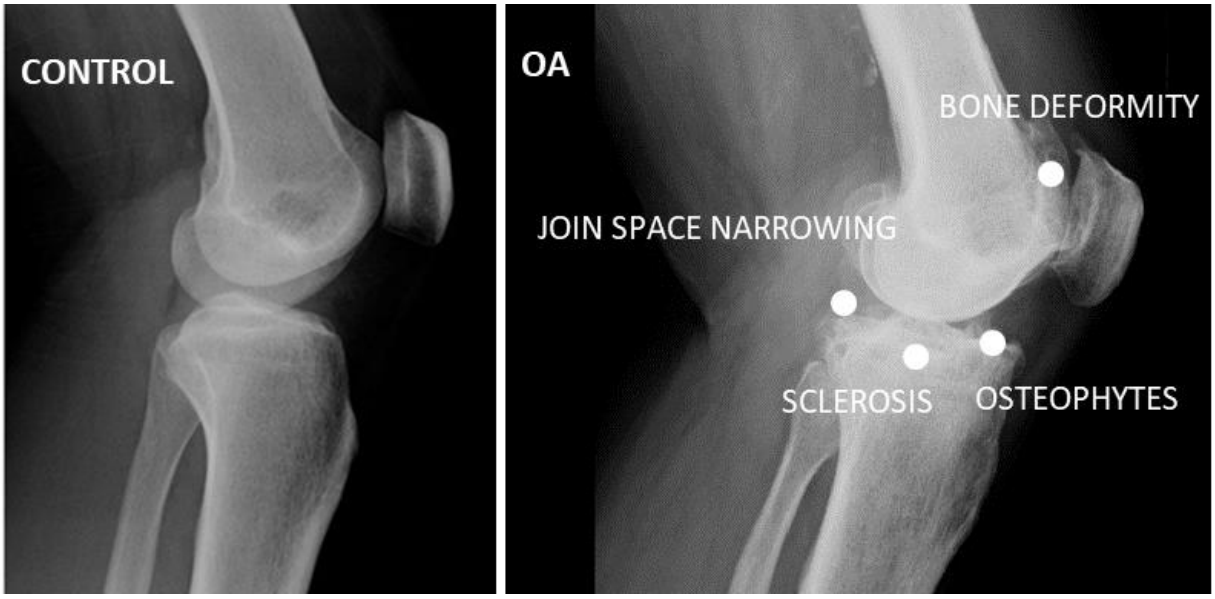

Figure 1.1 Radiographs of healthy (Control) and Kellgren-Lawrence (KL) osteoarthritic knees (OA). Radiographs of the osteoarthritic knee (KL, grade 4) reveal the presence of osteophytes, joint space narrowing, sclerosis and bony deformities (adapted from (45)).

The correlation between radiological alterations and clinical manifestations (basically pain and stiffness when starting movements) is not always as expected and depends on the

joints studied, being higher in knees, hips and lumbar spine, and low in hands and cervical spine (47). Occasionally, additional imaging tests are necessary to complete the study and confirm or exclude the findings obtained by radiology. Ultrasound is a useful technique for the study of frequent complications in OA, especially to confirm the existence of popliteal Baker cysts and of synovial effusion. Ultrasound is a useful technique with precise indications and is also able to detect intra-articular free bodies, sometimes suggesting synovial chondromatosis (48). Bone scintigraphy and Computed Axial Tomography (CT) may be indicated in the case of suspected occult bone lesions (49).

Overall, clinical history, physical examination and radiology are usually sufficient for the diagnosis, staging and prognosis of patients with OA. In cases of suspected secondary OA of metabolic origin, laboratory studies may be useful. In rare cases, more sophisticated techniques are required (50). Arthroscopy, with or without synovial biopsy, is useful in cases of suspected intra-articular free bodies, synovial chondromatosis or meniscopathy. In these cases, the procedure also has therapeutic applications, as it allows removal of foreign bodies or regularization of the meniscal surface, and induces a clinical improvement in many patients, sometimes for a long time (51) .

Given the slow clinical and radiological progression of OA, biochemical markers of OA activity and progression would be highly desirable. These markers would have prognostic value and would also allow the effectiveness of anti-osteoarthritic drugs to be monitored. To this end, the levels of some degradation molecules derived from cartilage degeneration and synovial membrane inflammation have been studied, yet advances in the field of OA biomarkers still remain challenging (52). Several OA biomarkers are recognized, but most of these molecules represent advanced stages of OA and only a few, early stages of the disease (53). Since OA is believed to start at cartilage level, markers of cartilage damage are considered of most importance to reveal early OA stages (52). Serum cartilage oligomeric matrix protein (COMP) is representative of cartilage turnover, and it was associated with increased severity of OA. Col2a1 has been associated with articular cartilage damage, and one of the suggested early OA biomarkers is urine C-terminal cross-linked telopeptide of type II collagen (CTX-II), marking joint damage and increased risk of rapid OA progression (54). Indeed, higher urine levels of CTX-II may be linked to stage 1 of the KL classification system (54). Nevertheless, the question whether urine CTX-II levels are exclusively a cartilage degradation biomarker is still uncertain. Matrix metalloproteinases (MMPs), such as MMP13, that regulates enzymatic cartilage extracellular matrix degradation, have been related with patients with OA (55). Also,

biomarkers studied for synovial inflammation such as glucosyl-galactosyl-pyridinoline (Glc-Gal-Pyd) are correlated with synovial membrane damage.

Recently, proteomics investigation showed that cartilage acidic protein 1 (CRTAC1) is a promising biomarker in the diagnose and in estimating severity in hand, hip, and knee OA (55-56). Additionally, structural variations of glycosaminoglycans from the extracellular cartilage matrix were shown to differentiate OA from non-OA cartilage, and C-reactive protein metabolite (CRPM) and collagen metabolites may help discriminate subsets of OA patients (58).

Along with an early diagnosis, OA prevention may be considered to improve the global state of the disease. OA prevention should be directed towards avoiding modifiable risk factors such as obesity, repetitive stress on the same joint or severe joint trauma. Excess body weight increases the mechanical load on the joints, altering joint biomechanics and causing increased stress and suffering in the joint. In this context, it is important to focus on diet in obese patients as an appropriate measure to prevent degenerative joint disease (59). Also, the relationship between OA of the knees and hand, and jobs involving repetitive and constant movements of these joints is well documented (60).

1.4 Pathophysiology of osteoarthritis

The pathogenesis of osteoarthritis is complex and involves mechanical, metabolic and inflammatory factors, which ultimately result in structural modifications and failure of the articular synovial joint. Synovial joints are constituted by articular cartilage, ligaments, subchondral bone, periarticular muscles and a synovial cavity, filled with synovial fluid and surrounded by an outer and inner fibrous membrane (**Figure 1.2**). Articular joints are responsible for the bone movement and load absorption, and during OA development, a dynamic imbalance occurs between the damage and repair of joint tissues, with emphasis on the articular cartilage, and culminating in the articulation failure.

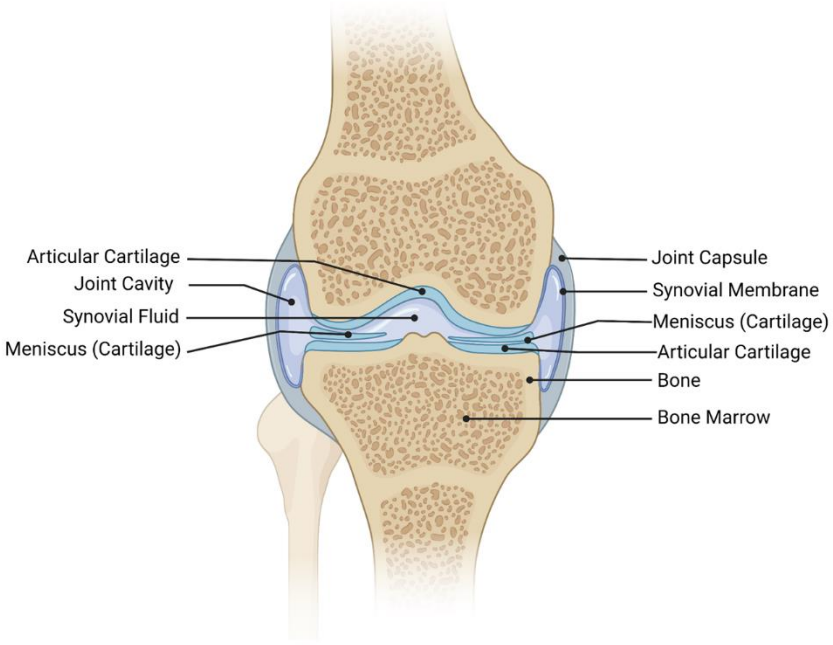

Figure 1.2 Schematic representation of the main articular joint constituents: articular cartilage, joint cavity, joint capsule, synovial fluid, synovial membrane, meniscus, bone and bone marrow (adapted from (60)).

Articular cartilage is a thin connective tissue comprising the articular joint at the end of two bones, responsible for a low friction surface for articulation and for minimizing the impact of mechanical forces. This function is facilitated by a layer of proteoglycan lubricin and hyaluronic acid on the articular surface, substances produced by both chondrocytes and synovial cells. Chondrocytes is the unique cell type present in the cartilage, organized within a three-dimensional extracellular matrix (ECM), composed of a collagen network, predominantly of collagen type II (Col2a1) (61) and proteoglycans, mainly aggrecan (62). Chondrocytes are responsible for maintaining the matrix components, by synthesising glycosaminoglycans (GAG), proteoglycans and other non-collagen molecules. At the cartilage, the 3D organization of the matrix components in the superficial layer and the high content of proteoglycans contribute to the absorption of the mechanical impact (63). Cartilage is an avascular tissue, and the oxygen and nutrients required are available from the vascular supply in the joint capsule, synovium and subchondral bone. Mechanical load is necessary for cartilage homeostasis, as it induces fluid movement between the cartilage and the synovial fluid, promoting the diffusion of molecules across cartilage, enabling its nutrition (64). The cartilage tissue is heterogeneous in its composition and physical characteristics, with the thickest part of articular cartilage being non-mineralized, whereas the thinnest and deepest tissue layer, the interface with subchondral

bone, being characterized by hypertrophic chondrocytes, able to express high levels of Col10a1 and suitable to be calcified (**Figure 1.3**) (65). The non-mineralized cartilage can be divided into three distinct zones: the superficial, the intermediate and the radial. Each cartilage zone is characterized by distinct ECM composition and organization, as well as by different phenotypic and gene expression patterns of the resident chondrocytes (**Figure 1.3**) (66).Chondrocytes differ in their phenotype and distribution over the cartilage, being larger and with a hypertrophic appearance in the deep subchondral bone zone, and more flattened or fibroblastic-like, in the superficial zone (**Figure 1.3)** (67). In a non-stressed steady state, chondrocytes are quiescent cells and there is very little turnover of the collagen network.

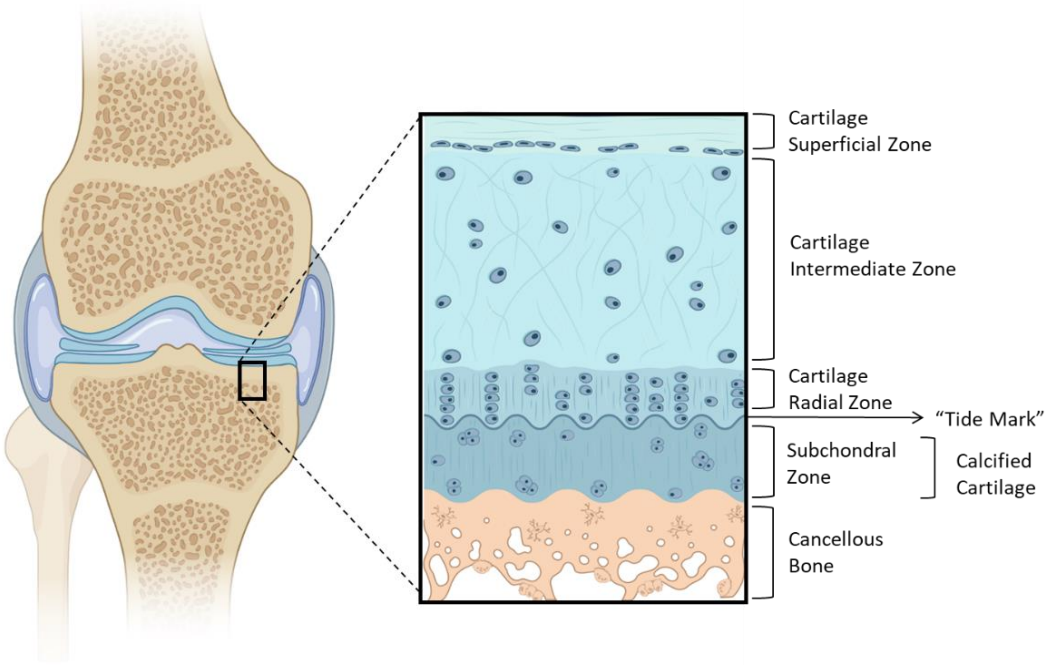

Figure 1.3 Schematic representation of healthy cartilage organization. Each cartilage zone has a distinct chondrocyte phenotype and organization. (Adapted from Martel-Pelletier *et al.* (301)).

Cartilage is a complex specialized structure, and in cases of OA, various cellular changes take place, disrupting the delicate balance of cartilage homeostasis. During OA progression, in the attempt to keep the equilibrium between catabolic and metabolic factors, chondrocytes are 'activated' to a catabolic phenotype, adopt a hypertrophic state and become apoptotic, in case of severe OA. Hypertrophic chondrocytes produce less GAGs, reducing the hydrostatic pressure within the ECM and therefore increasing cartilage vulnerability to wear-

and-tear-induced injuries to the collagen network. Any disturbance in the collagen complex is not able to be repaired and compromises ECM integrity (66). In response to ECM disruption, chondrocytes exhibit increased synthetic activity and cell proliferation, generating pro-inflammatory mediators and matrix degradation products, amplifying ECM degradation and mineralization (5,68) (**Figure 1.4**). Hypertrophic chondrocytes are responsible for higher expression levels of matrix metalloproteases (particularly, MMP-1 and MMP-13), a disintegrin and metalloproteases with thrombospondin motifs (ADAMTS-4 and ADAMTS-5), runt-related transcription factor 2 (Runx2), type X collagen and interleukin (IL-1β), all contributing to cartilage degeneration with implications on its integrity (69). The maintenance of articular chondrocytes in a mature state, without undergoing hypertrophic differentiation and apoptosis, is therefore a way to avoid or at least delay any cartilage imbalance and consequently cartilage degradation.

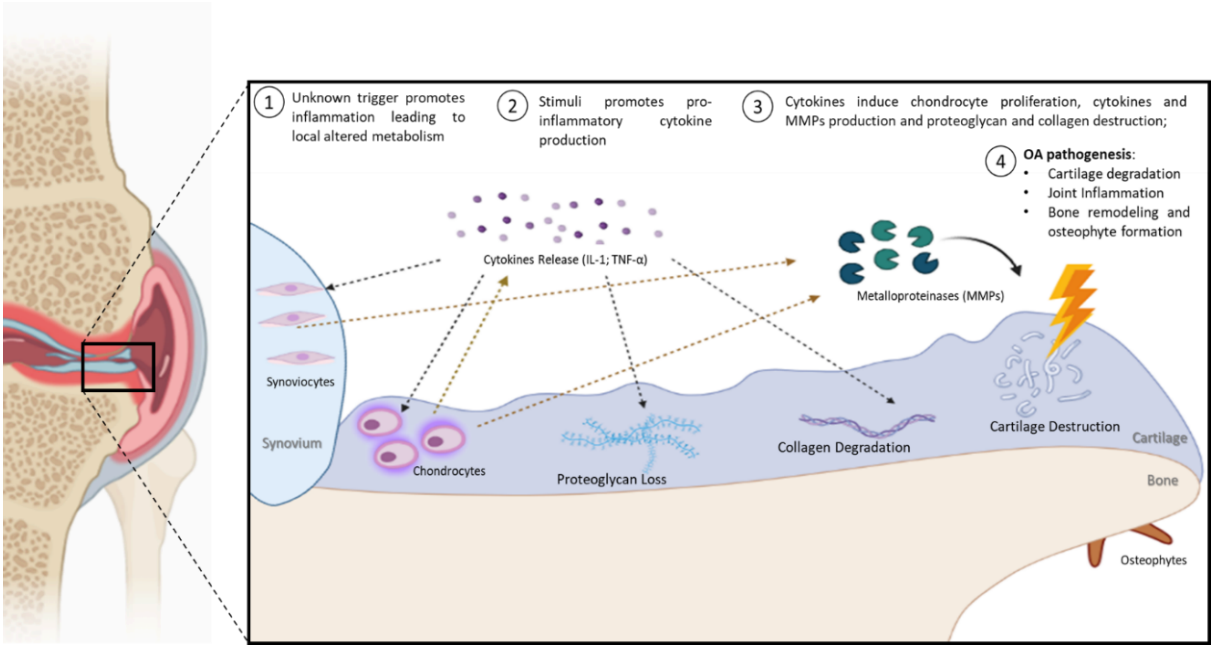

Figure 1.4 The pathogenesis of OA. In response to various stimuli in osteoarthritis (OA), chondrocytes undergo phenotypic changes and express mediators that initiate a destructive cycle of cartilage degradation. Inflammatory factors reach the synovium and trigger an inflammatory process, leading to the production of more inflammatory factors by synovial macrophages and fibroblasts, potentiating the inflammatory event and the cartilage destruction. IL-1, interleukin-1; MMPs, metalloproteinases; OA, osteoarthritis (adapted from (69)).

Interaction between cartilage, synovium and bone in AO

Endochondral ossification is a natural process of mammalian bone growth, a physiological process required for bone formation from cartilage scaffolds, that are gradually replaced by bone. Mesodermal cells are converted into cartilage-producing cells before bone formation begins. It involves chondrocyte and osteoblast differentiation and tissue vascularization (62). In both situations, OA and endochondral ossification, hypertrophic chondrocytes stimulate invasion of cells from the subchondral bone (70). Vascular invasion occurs concomitantly, osteoblasts and osteoclasts become activated and start to replace cartilage with bone tissue, generating a sclerotic bone phenotype.

From a molecular perspective, during endochondral ossification, chondrocytes proliferate, with some undergoing hypertrophy, characterized by an increase in cell size and changes in gene expression. Runx2 is a critical transcription factor involved in the differentiation of hypertrophic chondrocytes. It regulates the expression of genes associated with osteoblast differentiation, extracellular matrix remodeling and mineralization. Bone morphogenetic protein 2 (BMP2) is a member of the transforming growth factor-beta (TGF-β) superfamily and plays a crucial role in endochondral ossification. BMP2 promotes chondrocyte hypertrophy, stimulates the production of matrix-degrading enzymes, and induces the expression of osteogenic markers. The Wnt signaling pathway, particularly the canonical Wnt/β-catenin pathway, is implicated in endochondral ossification. Activation of this pathway influences chondrocyte differentiation, matrix remodeling, and bone formation. Wnt ligands bind to cell surface receptors, leading to the stabilization and translocation of β-catenin into the nucleus, where it regulates gene expression. As hypertrophic chondrocytes progress, they undergo a process of mineralization or calcification. This involves the deposition of hydroxyapatite crystals, primarily composed of calcium and phosphate, within the extracellular matrix. The precise mechanisms underlying calcification are complex and not yet fully elucidated, but it is believed to involve the release of matrix vesicles (MVs) from hypertrophic chondrocytes. These MVs provide nucleation sites for mineralization and promote the deposition of hydroxyapatite crystals. Understanding the interplay between these factors, Runx2, BMP2, Wnt/β-catenin signaling, and the process of calcification by matrix vesicles can shed light into the differentiation and calcification processes within hypertrophic chondrocytes, both in normal situations and in the context of conditions like osteoarthritis (OA).

In OA, this process of bone remodeling and repair lead to the development of

subchondral bone resorption and to bone core damages, reducing its main supportive function. Additionally, deregulation of chondrocyte function and ECM degradation, stimulates the adjacent synovium. During the inflammatory process of synovitis, cytokines, adipokines and damage-associated molecular patterns (DAMPs) attach to the synovial membrane, activating fibroblast-like synoviocytes proliferation, that along with synovial macrophage recruitment, secrete additional pro-inflammatory cytokines and chemokines, which sustain inflammation and contribute to cartilage degeneration and subchondral bone changes, in a cyclic way (71). Cytokines interleukin 1β (IL-1β) and tumor necrosis factor α (TNFα) can activate ECM degeneration by activation of toll-like receptors (TLRs), expressed by chondrocytes. The activation of such receptors, increase the expression of downstream inflammation-related genes via nuclear factor kappa B (NF-κB) signalling, including MMPs and NOS, intensifying the cartilage degeneration (66). Furthermore, synovium lymphocytes induce the production of chemokines by synovium fibroblasts and chondrocytes (66), through the increase of IL-15 and IL-17 levels. At the articular cartilage, an inflammatory cascade is activated through nuclear factor kappa B (NF-κB), stress-induced and mitogen-activated protein kinase (MAPK) pathways, which also triggers matrix degradation via MMPs, in particular MMP-13, nitric oxide synthase 2 (NOS-2), Ciclo-oxigenase-2 (COX-2), hypoxia-inducible factor 2α (HIF-2α) and ADAMTS-4,5 (5). NF-κB also indirectly contributes to premature chondrocyte differentiation, by regulating Wnt/β-catenin and Runx2 signaling. In fact, NF-kB has a pivotal role in regulating inflammatory processes, chondrocyte and osteoclast differentiation and activation, making it a therapeutic target in OA treatment (65).

As a result of ECM remodeling and increased chondrocyte apoptosis, also secretion of reactive oxygen species (ROS), prostaglandins (PG) and nitric oxide (NO) occurs, generating oxidative stress. ROS and other catabolic metabolites activate the innate immune response through the complement cascade, one of the major effector mechanisms of immune system activation in OA, complementing the antibodies and phagocytic cells systems (72).

Ultimately, subchondral bone also undergoes profound structural variations in OA, experimenting excessive and repetitive mechanical stress. Hypertrophic chondrocytes express vascular endothelial growth factor (VEGF) to sustain the process of endochondral bone remodeling. Osteophyte formation, on the other hand, emerges as an effort to restore proper mechanical loading through the mechanism of endochondral bone formation. This response is stimulated by the release of TGFβ and BMP2 from synoviocytes and chondrocytes (73).

Thus, among the various tissues present and significant to the joint function, there is

cross talk that promotes and amplifies the inflammatory and degenerative outcome by aggravating cartilage degradation, the appearance of osteophytes and synovial fibrosis (74).

1.4.1 The inflammation and pathological calcification synergy in the development of OA disease

Calcification can range from physiological to pathological, associated with uncontrolled mineralization of soft tissues, including articular cartilage. The trigger to pathological or ectopic mineralization of soft tissues is not completely disclosed: aging, genetics, ECM alterations, calcium, dysregulation of phosphate (Pi) and pyrophosphate (PPi) metabolism, hypertrophic differentiation of articular chondrocytes, cell apoptosis, modulation of growth factors, inflammatory mediators, may be included as potential calcifying promoters (75-76). The balanced interplay between mineralization inhibitors and mineralizing promoters, must be highly regulated, enabling calcification at physiological sites, but preventing initiation and intensification of pathological calcification process to avoid excessive and uncontrolled mineral deposits (77). When these regulatory mechanisms fail, inappropriate mineralization of soft tissues occurs, and ectopic mineralization causes a range of disorders not only in cartilage, but also in other parts of the body, including arteries, skin, muscles and kidney. Abnormal calcification of connective tissues is associated with a chronic low-grade pro-inflammatory state in age-related diseases such as cardiovascular disease (CVD), kidney disease and osteoarthritis (OA). In the case of OA, this ectopic calcification occurs mainly at the level of the joint cartilage (78), but is also observed in other OA joint soft tissues such as the meniscus, synovium and tendons. Ectopic calcification initiation might be associated with matrix vesicles (MVs), secreted from hypertrophic chondrocytes within the ECM. Calcium crystals are formed inside MVs and then proliferated to the matrix (77). At the core of this mineralization are, in addition to hydroxyapatite crystals [$Ca_{10}(PO_4)_6(OH)_2$] also present in physiological calcification, other types of calcium-phosphate crystals. In the situation of high Pi concentrations and low PPi, the formation of basic phosphate crystals (BCP) is prevalent, while the presence of high levels of PPi promote the formation of calcium pyrophosphate di-hydrate (CPPD) crystals and inhibit the nucleation of BCP crystals (75). The cartilage damage by calcium phosphate crystals is observed and confirmed by the presence of more than 80 % of BCP crystals in the osteoarthritic cartilage. Nevertheless, whether BCP crystals act as initiators, as intervenients in the progression of OA, or as an outcome of cartilage damage at a late stage

of the disease, has been debated. Apart from that, there are evidence that pathological calcification is closely correlated with the extent of joint destruction in OA (79-80), and that cartilage calcification occurs as an active process in promoting crystal-induced stress (76, 81-82). Moreover, calcification modifies cartilage integrity and homeostasis, as calcium-containing crystals, after being cell internalized via endocytosis or phagocytosis, have a direct effect on chondrocytes and synoviocytes. They stimulate synoviocytes proliferation and potentiate the production of inflammatory cytokines. As mentioned before, IL-1β and TNFα stimulate the synthesis of ROS and prostaglandin E2 (PGE2), involved in the promotion of inflammatory mediators and MMPs, potentiating the process of articular inflammation, cartilage degradation and chondrocyte activation and death (83-84). In turn, apoptotic cells are able to release proteolytic enzymes and pro-mineralizing apoptotic bodies likely to enhance crystal-induced stress, that will aggravate cartilage degradation and potentiate ectopic calcification, in a vicious sequence (**Figure 1.5**) (81).

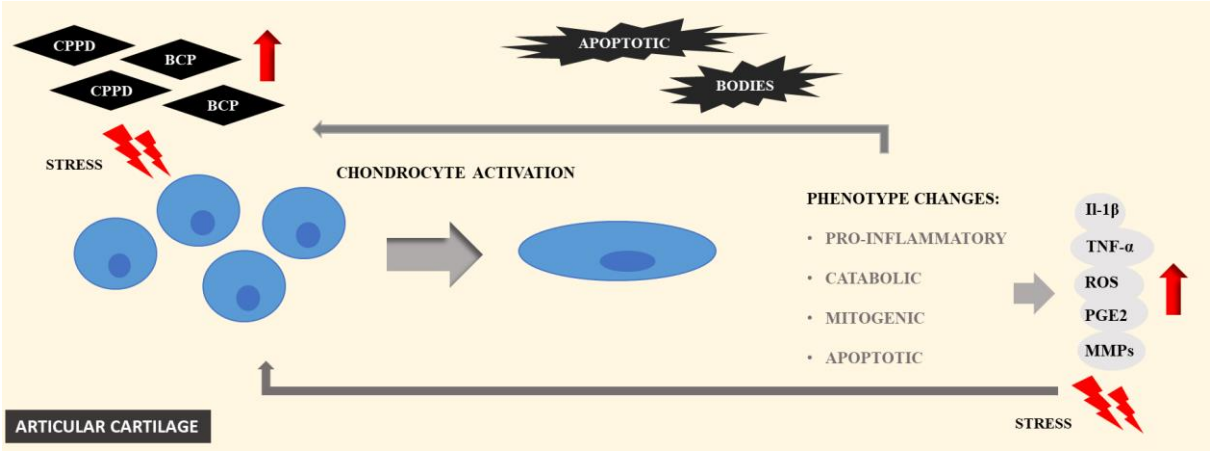

Figure 1.5 Mineral and inflammatory agents in the OA pathologic cycle, at cartilage level. Calcium-containing crystal (basic calcium phosphate, BCP, and Calcium pyrophosphate dehydrate, CPPD) stimulate the proliferation of synoviocytes and activation of chondrocytes, enhancing the production of inflammatory cytokines. This process intensifies articular inflammation, cartilage degradation and further pro-mineralizing apoptotic bodies release, in a damaging cycle.

1.5 Prevention and treatment of Osteoarthritis

There is no curative therapeutic approach for OA and the treatment available must be individualised and varies according to the joint affected, in the sense of relieve pain, improve functional capacity and prevent progression of the disease. Overall, osteoarthritis therapy

should be carried out in a stepwise manner, initially with preventive and non-pharmacological measures, then with the addition of drugs and, in the event of a lack of response, by resorting to surgery (85).

Non-pharmacological approaches include the application of preventive measures to pursuit of what has been called "joint economy". It might require a lifestyle change, including rehabilitation to facilitate healthy body composition, moderate physical activity, and the optimization of an appropriate nutraceutical treatment (86-87).

Available pharmacological treatment is mainly directed to symptoms relief, which is characterized by analgesics or anti-inflammatory drugs as a first choice, depending on the intensity of pain and co-morbidity (88). Weak opioids such as tramadol are very commonly used alone or in combination with paracetamol, reserved for cases where anti-inflammatory drugs have contraindications. Major opioids can also be very effective, especially transdermal fentanyl, in some cases of severe pain (89). Non-steroidal anti-inflammatory drugs (NSAIDs), usually coxibs, are generally recommended to be used for as short time and at the lowest possible dose because of the digestive and cardiovascular risks (90). Coxibs may have fewer toxic effects on the gastrointestinal track, as they are selective cyclo-oxygenase inhibitor drugs of the type 2 (91). Slow-acting drugs for symptomatic relief of osteoarthritis (SYSADOAS), include glucosamine, chondroitin sulphate and diacerein, and act by providing nutrients for matrix synthesis by chondrocytes, yet none of these have been recognised as an osteoarthritis modifying drug (92). Topical analgesics, such as capsaicin, blocks the pain stimuli (93) and local injections of intra-articular administration of corticosteroids is indicated in patients with joint effusion in large joints or severe pain refractory to oral treatment (94). In addition, viscosupplementation with intra-articular hyaluronic acid has a dual effect, acting on the one hand as a joint lubricant and on the other as a cartilage trophic factor (95).

Surgery is indicated primarily for patients with severe symptomatic osteoarthritis whose pain has not responded to medical treatment, who have severe pain at rest and who have increasing limitations in activities of daily living. With the surgery intervention, it is expected to restore the joint function and produce a regression of cartilage, bone and synovial lesions. It is not only used as a last resort, when all other therapies have failed, but in certain cases, it slows down the process in the early stages (96).

Currently, research has been focused on new techniques to replace damaged parts or replace them by regenerating cartilage. Among the surgical options available to treat deep chondral lesions are bone marrow stimulation techniques, chondrocyte therapies of

implantation of autologous chondrocytes, and tissue replacement therapies such as osteochondral autologous transplantation (97).

With the development of cell therapy, experiments are being carried out that seek the regeneration of certain tissues/areas. In the case of osteoarthritis, adipose cells derived from rabbit stem cells have been studied and used to see if it is possible to attenuate the progression of synovial activation and joint destruction (97). The implantation of autologous chondrocytes allows to generate cells that are capable of synthesizing type I collagen, combating cartilage damage, *in vitro*. Currently, despite the anticipation that the generated cartilage would be identical to the original, it exhibits altered functionality, displaying reduced resistance and increased susceptibility to damage. To circumvent this limitation, non-degradable matrix formats, such as polylactic acids (PLA) or polyglycholic acids (PGA), are used for chondrocytes growing before implantation takes place. So far, this technique is only carried out at the experimental level and on animal models (98).

Advances have been made in cartilage tissue engineering, in the sense of finding a scaffold that provides adequate biomechanical properties, biocompatibility and a favorable environment for the cells growing, but it has not yet been possible to obtain the support that contributes to the cartilage tissue repair and that fully complies with its functions as an extracellular matrix (99). Many natural and synthetic biodegradable biomaterials have been studied, and among the materials used are ceramic substitutes (100), nano-hydroxyapatite alone or combined with other materials (101), acellular cartilage matrices, collagen I, PLA and PGA biopolymers, alginate, AH, peptide hydrogels, among others (102-103). Although hydroxyapatite has excellent properties, its use has been limited, since it has presented mechanical deficiencies (104). Currently, research is being done on materials that behave as the ECM in cartilage tissue engineering, and among these, chitosan has been a good option since it has properties such as biocompatibility, biodegradability and non-cytotoxicity. It also has a high affinity to bone cells, its structure is similar to GAGs (105), and its products of degradation are involved in the synthesis of joint components (106).

1.6 Prospection of potential active entities in osteoarthritic inflammation

There is still no drug recognised as an osteoarthritis modifier, despite the many lines of research

(107). Although there has been some progress in developing new molecules aimed at repairing cartilage and bone or treating inflammation and pain, there are currently no effective drugs approved for OA (97), making the search for new potential molecules a priority to address the growing burden of OA. In this search for new agents, a biochemical marker for clinical use, indicative of the metabolic activity of cartilage and with the potential to determine different disease severity profiles, similar to those already available for bone (108), could certainly facilitate the process. OA can be caused by various factors such as heredity, obesity, trauma, congenital or developmental anomalies (109) and so, high heterogeneity is expected in the onset and progression of the disease. Like that, personalised approaches based on validated common characteristics of OA patients may be helpful in the development of OA models, in the search of disease-modifying osteoarthritis drugs (DMOADs), or in the determination of the efficacy of a treatment targeted at OA subgroups. Moreover, OA-specific biomarkers will be critical for accurately classifying each patient's phenotype to help predict appropriate interventions. Recently, different metabolic phenotypes were found in healthy, early and late OA cohorts using mass spectrometry (21,110-111) which may represent a promising step towards personalised health approaches.

1.6.1 Current models used in the search for new active agents and drug treatment

Typically, the sequence of the drug development pipeline begins with the isolated/developed potential active compounds in targeting the underlying pathophysiology of OA, such as inflammation, cartilage degradation, and subchondral bone changes being tested in 2D or 3D *in vitro* disease models. *In vitro* 2D models allow researchers to control certain variables and conditions, which can lead to more reproducible and consistent results. They are also relatively inexpensive and can be used for rapid screening of a large number of compounds. However, 2D *in vitro* models often do not accurately reflect the complex interactions that occur *in vivo*, and the results may not translate well to human clinical trials. Generally, the candidates that show efficacy without cytotoxicity are further tested in animal models before finally one or two drugs enter human clinical trials. *In vivo* animal models allow the interactions between different tissues and organs in a living system, which can provide a more accurate representation of the human body. However, *in vivo* models are more expensive and time-consuming than *in vitro* models, and there may be ethical concerns associated with animal testing. Drug development is indeed a time-consuming and costly process, and most drugs fail in clinical trials, mainly due

to limitations in preclinical testing that can compromise information on safety and efficacy (112). Moreover, when the clinical phase is reached, traditional drug testing models lack the individual characteristics of clinical trial participants. Therefore, it is important to simultaneously invest more in preclinical models that better mimic the OA physiologic context, develop new approaches to improve and accelerate drug development, and ideally, move towards a "personalized OA testing approach". In this sense, it would be very valuable to validate biomarkers that allow patients to be classified into groups, based on endotypes or phenotypes. By studying the specific aetiologies and pathologies, drug candidates and test models could be directed to patient groups, providing a more capable system for the development of new effective DMOADs. There is evidence that cell-cell crosstalk between cartilage, bone and synovium, is a major contributor to the pathogenesis of OA and such communication is also thought to play a key role in preventing or reversing OA, after treatment. Multi-tissue physiological models, such as microphysiological systems (MPSs), designed to replicate the microenvironment *in vivo*, mimicking the physiological conditions of the target tissue or organ, can improve the accuracy and relevance of preclinical studies (113-114). Also explant-based models (115), to study the effects of drugs on multiple cell tissue types simultaneously, and animal models (116), should have greater power in predicting drug toxicity and efficacy in clinical trials. In addition, the OA models need to be versatile and able to generate different types of pathological responses, as more comprehensive tools are needed to further evaluate OA models and the effect of treatments. Currently, most studies use limited parameters such as MMP-13 expression, loss of GAG and the presence of pro-inflammatory cytokines to indicate disease state. However, at least 1500 genes have been found to be differentially expressed in chondrocytes isolated from intact and damaged areas (117). Therefore, "omic"-based methods may facilitate future advances, although currently such studies are rarely conducted when testing DMOADs. Complete characterization of models not only improves patient classification and provides insight into the accuracy of modelling, but can also reveal potential harmful or beneficial effects of treatments that cannot be detected by analyzing the 'known' targets alone. To further validate the models that allow prediction of the efficacy of novel therapeutic interventions in humans, it is also important to first evaluate the effects of agents with known clinical efficacy. This validation step justifies moving forward in the search for new drugs. Ideally, one should start with the 'gold standard", i.e. a drug with recognized treatment efficacy. To date, however, there are no FDA-approved DMOADs, and numerous late-stage clinical trials have failed to show efficacy (109). We can study the effect of these failed drugs in the OA models and compare the results with clinical observations.

Ideally, the effective models should be able to reproduce the deficits of the failed drug. In conclusion, clinically relevant and personalized models of OA are urgently needed to enhance our understanding of the pathogenesis of joint diseases in humans and facilitate the discovery and development of novel drug treatments.

1.6.2 Vitamin K and VKDP's: Gla-rich protein (GRP), a 'dual' mediator in osteoarthritis

During OA progression, pro-inflammatory cytokines and inflammatory mediators are overexpressed, contributing to the degradation of articular cartilage, with the accumulation of specific extracellular matrix (ECM) degradative enzymes. Increased ECM remodeling, along with chondrocyte differentiation and apoptosis, are responsible for ECM disturbance, resultant in continuing loss of articular cartilage. In reverse, cartilage degradation potentiates pathologic calcification, aggravating the pro-inflammatory responses in a vicious cycle of inflammatory and calcifying stimuli and responses (66,68,118). Comprehensively, since ectopic cartilage calcification is strongly linked to the progression of OA (76), it is expected that preventing it, could help to slow or even stop the progression of the disease. As such, inhibitors of calcification such as vitamin K and the extra-hepatic vitamin K-dependent proteins (VKDPs), osteocalcin (OC), matrix Gla protein (MGP) and Gla-rich protein (GRP) are being explored as potential therapeutic targets in calcification-dependent diseases, such as OA (119).

Vitamin K is a lipid-soluble vitamin, that may occur in nature in form of phylloquinone, vitamin K1, or a series of menaquinones (MKs), designated as vitamin K2. Both forms have a common core structure, a 2-methyl-1,4-naphthoquinone ring and an apolar isoprenoid side chain in their chemical structure, that differs in length and degree of saturation (120). Phylloquinone has one unsaturated bond and contains a phtyl side chain (121). Menaquinones are composed by a side chain with repeating 'n' isoprene residues, and are denominated as MK-n (**Table 1.2**) (120-121). Vitamin K vitamers differ in source, absorption rates, tissue distribution, bioavailability and target activity. While phylloquinones are found in plants, algae or cyanobacteria, menaquinones (with the exception of MK-4) are produced by bacteria and majorly obtained nutritionally, from fermented food and liver, and additionally synthesized by intestinal bacteria (120)**.**

Although K1 is the major type of vitamin K present on a typical western diet, MK-4 is the major form of vitamin K present in animal tissues (122), accumulated in the extrahepatic

tissues and resultant from Vitamin K1 interconversion (122). Although vitamin K1 and K2 are obtained mainly dietary, supplementation is increasing in importance (123). Menadione, commonly known as vitamin K3, is not a natural form of vitamin K. Instead, it is considered a byproduct of the breakdown of vitamin K1 and serves as a precursor to tissue MK-4 in circulation, acting as a pro-vitamin (124).

Table 1.2 Chemical structures of Vitamin K1, K2 and K3. Vitamin K1 contains a phytyl side chain with an unsaturated bond and vitamin K2 (MK-n), a side chain with repeating isoprene residues.

	Vitamin K1 (Phylloquinone)	**Vitamin K2** (Menaquinone, MK-n)	**Vitamin K3** (Menadione)
Chemical Structure	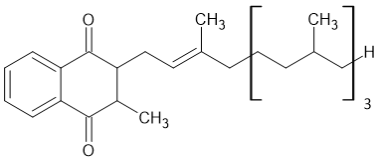	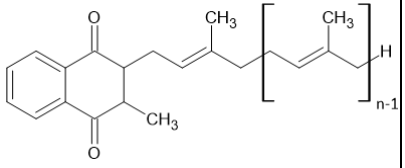	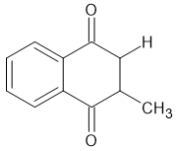
Source	Vegetables	Fermented Foods	Synthetic

The main biological function associated to Vitamin K, since its first identification (125) is related with the activation of of hepatic blood clotting factors. Vitamin K acts as a cofactor for the enzyme γ-glutamyl carboxylase (GGCX), in the post-translational modification of vitamin K-dependent proteins (VKDPs), through the conversion of glutamic acid residues (Glu) into γ-carboxyglutamic acid (Gla) residues, capable of binding calcium and calcium phosphate mineral (125). In the reaction catalyzed by GGCX, the hydroquinone form of vitamin K is converted to its epoxide form and further vitamin K epoxide reductase (KO) converts vitamin K epoxide back to its reduced form (KH_2). This cycle in known as the 'K cycle' and is catalyzed by the enzymes vitamin K epoxide reductase and vitamin K reductase (119) (**Figure 1.6**).

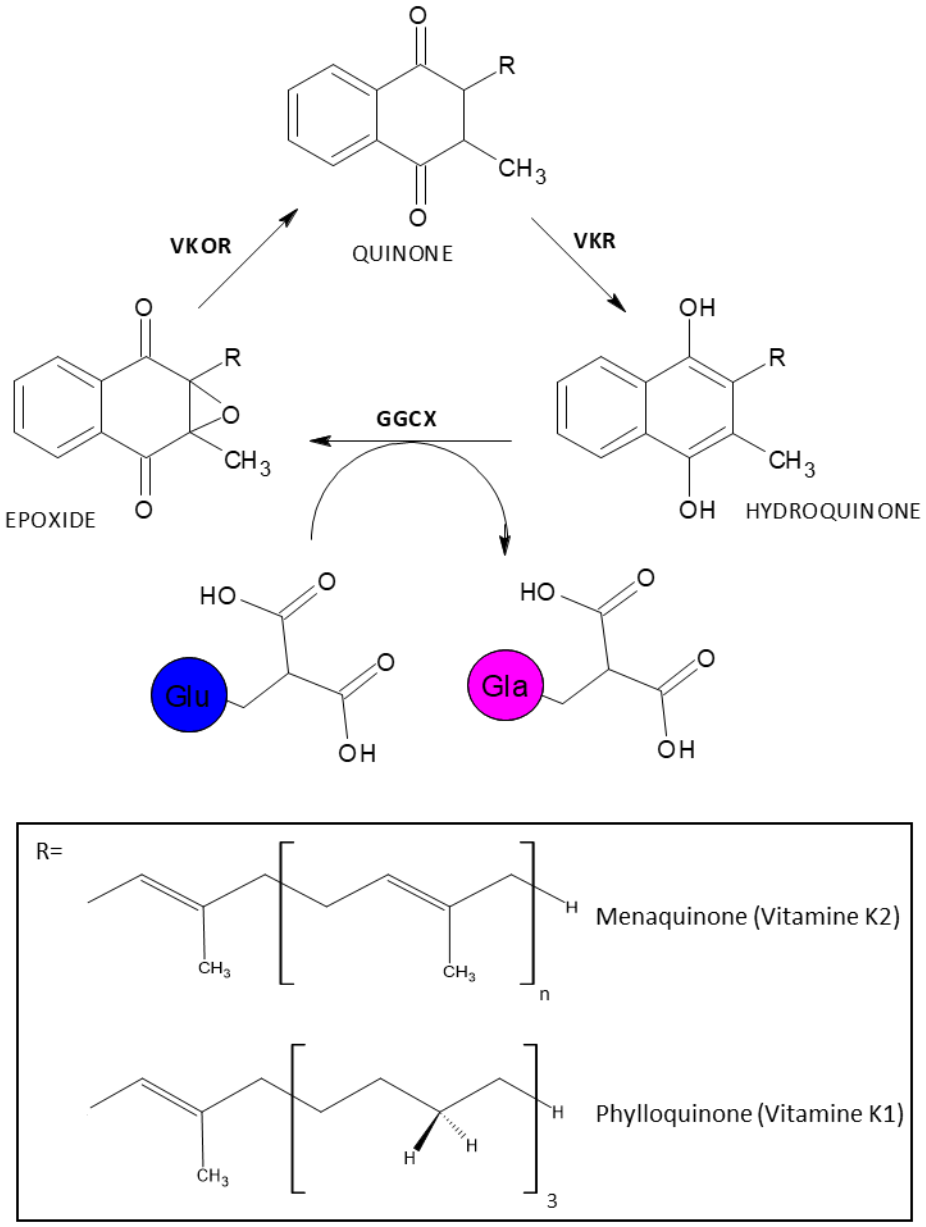

Figure 1.6 Vitamin K Cycle: the vitamin quinone is reduced to its hydroquinone form by vitamin K reductase (VKR). During γ-carboxylation of Glu residues to Gla residues by γ-glutamyl carboxylase (GGCX), vitamin K hydroquinone is converted into its epoxide function. Vitamin K epoxide is further reduced by vitamin K epoxide reductase (VKOR).

Nevertheless, the biological role of this vitamin is now known to be much extensive and vitamin K has been related with many biological processes and pathological conditions. Vitamin K may exert its effect directly by affecting skeletal tissue gene expression or as a co-factor in the post-translational modification of extra hepatic VKDPs (119), matrix Gla protein (MGP), osteocalcin (OC), Gla-rich protein (GRP), growth arrest-specific protein 6 (Gas6), and periostin (Postn), contributing to cartilage calcification inhibiting. Despite that, novel roles have

emerged for vitamin K, independent of its role in VKDPs carboxylation. Vitamin K has been shown to act also as an anti-inflammatory compound by suppressing of the NF-κB signal transduction, and to have a protective effect against oxidative stress by blocking the generation of ROS (**Figure 1.7**). Vitamin K seems to be also involved in tumor progression inhibition (126-129) and transcriptional regulation of osteoblastic and osteoclastic genes (128) .

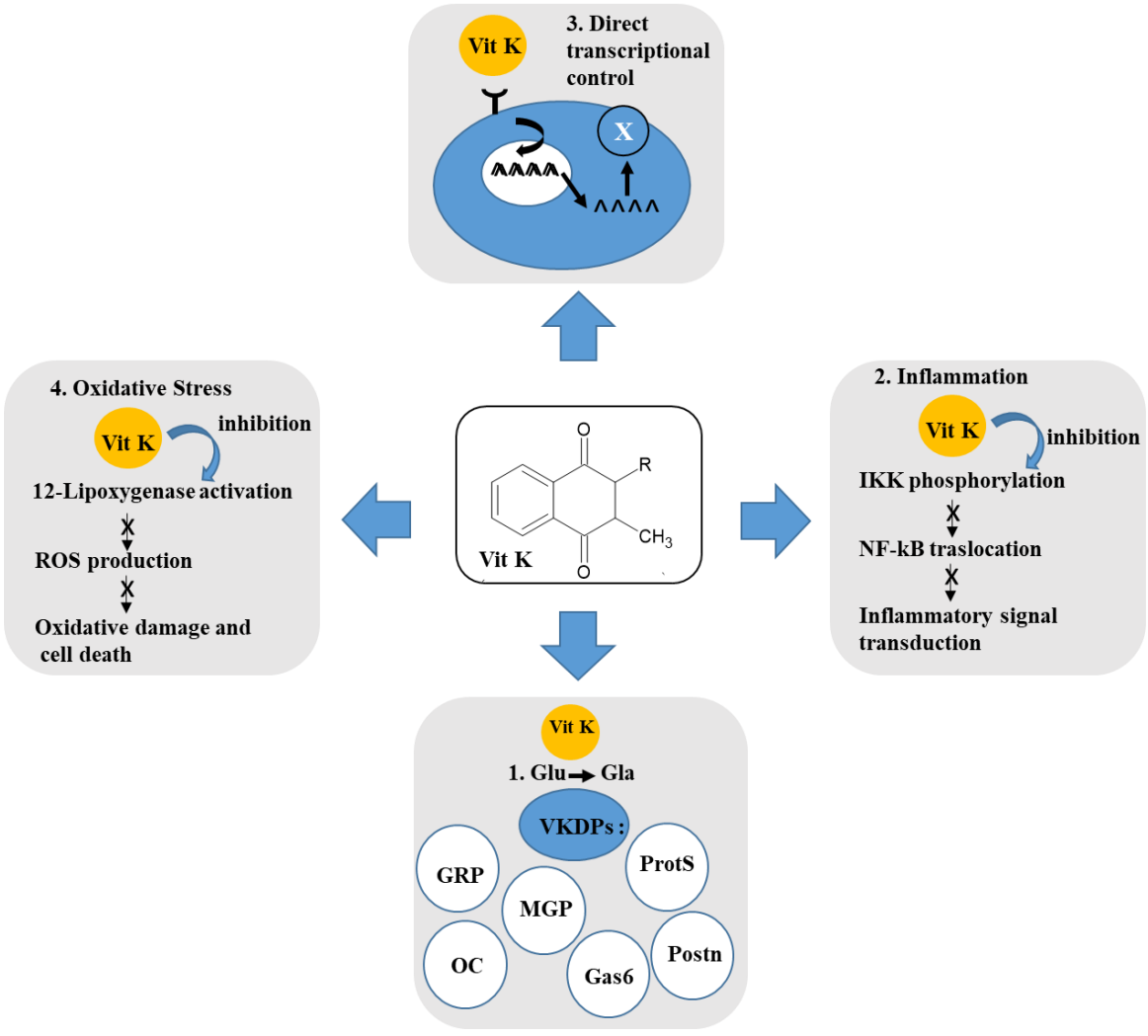

Figure 1. 7 Vitamin K in multiple molecular pathways: 1. Vitamin K may exert actions on skeletal tissues by acting as a co-factor in the γ-carboxylation of Glu to Gla residues of VKDPs (GRP, MGP, OC, ProtS, Gas6, Postn). 2. Vitamin K may act as an anti-inflammatory agent by suppressing the NF-κB signal transduction. 3. Vitamin K may affect cartilage and bone by modulation of downstream signaling pathways ultimately modifying gene expression. 4. Display a protective role by blocking the generation of ROS. Glu, glutamic acid, Gla, γ-carboxyglutamic acid, IKK, nuclear factor kB kinase, NF-kB, nuclear factor kB.

Recently, consequences of vitamin K deficit in human health and molecular aspects of

the protective role of vitamin K, and its involvement in the interaction between pathological calcification and inflammatory processes in aging and age-related diseases, have been reviewed (129). The health benefits of vitamin K are not only linked with blood homeostasis but closely linked to chronic low-grade inflammatory diseases such as cardiovascular disease, osteoarthritis, dementia, cognitive loss and mobility loss (129).

In relation to OA, clinical evidence of a preventive role of vitamin K1 was observed in some pre-clinic studies, with low plasma levels of vitamin K1 being associated with an increase of OA prevalence and OA progression (132-134). Other clinical studies have demonstrated an association between low vitamin K1 plasmatic levels and joint cartilage loss (135-136). Together, these results point out for the role of vitamin K in bone and cartilage health, specifically in preventing OA and its progression.

VKDPs are characterized by the presence of Gla residues as mentioned before, and 17 different human VKDPs have been identified, divided into hepatic and extrahepatic VKDPs. Hepatic VKDPs are synthesized in the liver and are essential for regulating blood coagulation, essentially through bonding of their Gla residues, calcium and negatively charged membrane phospholipids (137-138). The most relevant hepatic VKDPs are the coagulation factors II, VII, IX and X, and the anticoagulant proteins C, S and Z. Matrix Gla protein (MGP), osteocalcin (OC), Gla-rich protein (GRP), growth arrest-specific protein 6 (Gas6), proline-rich Gla proteins (PRGP1 and 2), transmembrane Gla proteins (TMG3), periostin (Postn) and the enzyme GGCX are the known extra-hepatic VKDPs. Extra-hepatic VKDPs have a protecting role in the bone and cardiovascular system, through management of several biological functions, such as bone homeostasis, ectopic calcification, cell differentiation and proliferation, inflammation, signal transduction and regulation of energy metabolism (139-141). Three of them have been specifically associated with calcification processes: OC, MGP and GRP.

OC was the first identified extrahepatic VKDP and is mainly synthesized by osteoblasts (138). OC is able of modulating the osteoblast and osteoclast activity and has been associated to the negative regulation of bone mineralization (139,143). OC can bind hydroxyapatite crystals, and interferes with the mineral maturation rate, while functions as a stabilizer and regulator of bone matrix (140). Moreover, it has been suggested that serum undercarboxylated OC (ucOC) has a role in regulating systemic glucose and energy metabolism (145-146). Osteocalcin has also been related with OA, in the sense that serum osteocalcin levels were elevated in OA patients and higher expression of osteocalcin in articular cartilage and subchondral bone has been noticed in human OA joints (143). Vitamin K deficiency was

associated to the presence of ucOC and serum hyaluronic acid, a marker for synovitis in OA. Further, ucOC was considered a biomarker for evaluating the pathophysiological condition of knee OA (144).

MGP is synthesized by chondrocytes and vascular smooth muscle cells (VSMCs), and plays a beneficial role in vascular calcification and various pathological processes. It is implicated in the regulation of endochondral calcification, in the control of mineral deposition, and low levels of MGP have been linked to pathological calcification. MGP was able of suppressing calcification of the joint and osteophyte formation (145), and to prevent calcification of vessel walls (146). This VKDP is also involved in the regulation of osteogenesis and chondrocyte maturation (147), and has shown to modulate angio- and tumorigenesis (152-154). OA chondrocytes produce mainly ucMGP, while chondrocytes from normal donors produce functional γ-carboxylated MGP and fetuin complexes (150). Fetuin-A is a circulating hepatic glycoprotein, considered a very important systemic inhibitor of soft-tissue calcification. Fetuin-A is capable of trapping mineral nuclei into calciprotein particles (CPP), inhibiting crystal growth and aggregation, while enabling the clearance of calcium crystals from extracellular fluids (156-157). MGP calcification inhibition is partially based on its direct calcium crystals binding ability through the Gla residues (153), but it was also proposed to occur via a fetuin-A-MGP complex present in chondrocyte-released matrix vesicles (MVs) in control conditions (150). Also, MGP helps to counterbalance the activity of BMP2 by binding to it and inhibiting its effects, avoiding osteoblast differentiation and soft tissue calcification (154). The interplay between MGP, vitamin K, and BMP2 highlights the importance of maintaining adequate vitamin K levels for proper bone and vascular health. In fact, the lack of functional MGP in animal models has been shown to originate similar processes as those occurring in OA (155), and it is most likely that insufficient functional MGP, associated with inadequate concentrations of vitamin K, potentially play a role in OA, contributing to abnormal mineralization (156). Elevated levels of dephosphorylated and undercarcoxylated MGP (dp-ucMGP) were found in individuals with higher propensity to have osteophytes, bone marrow lesions, subarticular cysts, and meniscal damage. Individuals with very low plasma K1 had cartilage deterioration and meniscal damage aggravation over time, although dp-ucMGP was not associated with progression of any OA features (135-136), supporting the possible role of vitamin K in OA, independent of its function in MGP carboxylation.

In addition to MGP and OC, GRP was recently associated with OA pathophysiology. GRP was first identified in sturgeon cartilaginous tissue and has an abundant Gla residues

content, 15 possible Gla residues in case of the human protein (157), contrasting with the 3 to 5 Gla residues present in OC and MGP, respectively. This characteristic confers GRP an unusually high capacity to bind calcium and calcium mineral. GRP is a circulating protein, expressed in soft tissues of rats and human. GRP accumulates in skin, vascular tissues, bone and cartilage of rats, and has been associated to sites of pathological calcification in human, including blood vessels and skin (163-165).

GRP as a global soft tissue calcification inhibitor

GRP has been identified as a modulator of calcium availability (158), and has demonstrated to have a crucial role in avoiding ectopic calcification. Like that, this protein has been related to ectopic calcification-associated pathologies, such as vascular calcification, cancer and OA. GRP is involved in the prevention of pathological calcification through multiple mechanisms. GRP is able to establish a direct connection with mineralized tissues by binding to hydroxyapatite crystals, the primary components of calcified tissues. Also, by binding to calcium ions, GRP limits their availability for crystal growth both in the circulation and at the tissue level. Like that, GRP acts as an inhibitor of crystal growth and maturation, thereby impeding the formation of larger and more mature calcific deposits (160).

Moreover, GRP has shown to be capable of regulating osteo/chondrogenic differentiation and phosphate-induced mineralisation of VSMCs, as it was involved in inhibiting BMP 2 expression and its 'downstream target small mother against decapentaplegic' (SMAD) in the respective signaling pathway. It was also demonstrated that γ-carboxylation of GRP (cGRP) is required for its interaction with BMP2 (164,166).

Furthermore, studies have indicated that GRP is associated with the mineralization capacity of extracellular vesicles (EVs). Bone matrix regulatory proteins, such as BMP2, BMP-4, osteopontin, MGP and OC, are expressed in calcifying vessels (162). In response to high level of extracellular calcium and phosphate, and an inefficiency calcification inhibition, VSMCs release EVs with high mineralization capability functioning as nucleation sites for mineral growth in the extracellular matrix (158), contributing to ectopic calcification. Low levels of GRP were found in calcifying VSMCs-derived EVs, supporting the notion that decreased levels of calcification inhibitors in EVs are associated with its increased calcification potential. By regulating EVs ability to promote calcification, GRP contribute to prevent ectopic mineralization. GRP is a constitutive component of circulating EVs and CPPs (163), and was found in a CPP complex with MGP and fetuin-A, known to stabilize minerals (163,169).

Moreover, higher levels of CPP with lower content of fetuin-A and GRP were associated with chronic kidney disease (CKD) stage 5 patients, when compared with healthy individuals (165). CPPs isolated from CKD stage 5 patients increased calcification of VSMCs while pre-incubation of these CPPs with γ-carboxylated GRP rescued VSMCs induced calcification. Also, *in vitro* results showed that the formation and maturation of basic calcium phosphate crystals was highly reduced in the presence of γ-carboxylated GRP, fetuin-A, and MGP, showing the role of GRP as an inhibitory agent to prevent calcification at systemic and tissue levels (168,171).

These mechanisms highlight the diverse role of GRP in inhibiting ectopic calcification. Through its direct connection to mineralized tissues, inhibition of crystal growth and maturation, reduction in vascular cell transdifferentiation, and association with EV-mediated mineralization, GRP plays a protective role against pathological calcification in various tissues.

GRP in osteoarthritis

GRP participates in several processes during physiological conditions, having a role in the chondrogenesis, stabilization of cartilage matrix and in inhibiting osteogenesis (172-173). In the context of OA, GRP interferes with several processes related with the articular cartilage degradation, bone remodelling, tissue inflammation and extracellular matrix mineralization (174-175).

GRP may prevent articular cartilage degradation in various ways, as recently reviewed by M. Stock (119): by blocking aggrecanolysis and the aggrecanase activity of ADAMTS-4 and -5, that is one of main process of cartilage destruction in OA (174-175), and by reducing chondrocyte apoptosis. It was observed that chondrocyte death is highly increased in GRP-deficient mice, reinforcing the protective role of GRP in this process (170), contributing to ECM homeostasis. GRP also contributes for avoiding cartilage damage by binding cartilage-associated collagen types II, IX, and XI with high affinity, sustaining the cohesion of the cartilage matrix and stimulating its mechanical rigidity (119). Consistently, a recent work from Okuyan *et al*. (171) demonstrated that intra-articular injections of GRP in the knee joints of rats with experimental OA ameliorated cartilage degeneration.

It is established that inflammation precedes the joint structure modification in OA (172). *In vitro* results revealed that treatment of articular chondrocytes and synoviocytes stimulated

with inflammatory interleukin-1β, with cGRP and ucGRP, inhibited inflammation as evidenced by lower levels of cytokines production and of inflammatory markers accumulation (173). These results indicate that γ-carboxylation is not essential for the anti-inflammatory activities of GRP, although evidence from preclinical studies have shown a predominance of the undercarboxylated forms of GRP in cartilage and synovial membrane from OA patients (178-179). Furthermore, a positive correlation was established between synovial fluid GRP levels in OA patients and radiographic outcomes and symptomatic severity of OA (175).

Overall, these results show that GRP is a secreted VDKP involved in ectopic calcification and protects articular cartilage under pathological conditions such as osteoarthritis and inflammatory arthritis. Additionally, and taking in consideration the outcomes of the biological activity of cGRP, particularly in the OA context, and the fact that it has been shown that vitamin K deficiency is a potential risk factor for knee OA (130), it is worthy to consider vitamin K supplementation as a convenient and inexpensive strategy to prevent or treat OA.

1.6.3 Marine compounds as a promising source of active anti-osteoarthritic compounds

Osteoarthritis is characterized by gradual loss of joint cartilage associated with inflammation, resulting in pain, stiffness and restricted movement. The high incidence of diseases in which inflammation is involved as a pathological entity and the association of adverse effects in many of the anti-inflammatory drugs commonly used in current medical practice, has guided research towards the search of new safer and more effective anti-inflammatory molecules. Since ancient times, products of marine origin have been explored as therapeutic alternatives for the treatment of numerous pathologies (176). Among these marine resources, algae, sponges, and invertebrates are known to produce a wide range of bioactive compounds, which may act as potential anti-inflammatory agents (177). However, despite the efforts, the latest data indicates that there is currently no active compound from marine sources established for the treatment of osteoarthritis (178).

Chondroitin sulfate is a sulfated glycosaminoglycan, a compound found in the cartilage of marine animals, including sharks, that may be bound to proteins and form an agrecan-type proteoglycan. This is an important structural component of cartilage, as it retains water and nutrients and provides resistance to compression and elasticity being also present in synovial fluid. Studies have shown that chondroitin sulphate can relieve pain and improve joint function

in patients with osteoarthritis, therefore slowing the progression of the disease (184-185). Chondroitin has been used as a dietary supplement for the treatment of osteoarthritis (181), and its effect is believed to combine anti-inflammatory and immunomodulatory activities, by stimulation of the synthesis of proteoglycans and hyaluronic acid, and inhibition of the synthesis of proteolytic enzymes and nitric oxide. *In vitro* studies have shown that chondroitin reduces NF-kB in IL-1β induced chondrocytes. As NF-kB is a transcription factor that plays a key role in the initiation of various proinflammatory genes involved in the pathogenesis of OA, its reduction can decrease the expression of various proinflammatory enzymes and molecules such as phospholipase A2, cyclooxygenase-2, IL-8, metalloproteinases, proteinases, and prostaglandin E2, preventing changes in the subchondral bone (182).

Cystoseira usneoides is a brown alga, commonly found in the Mediterranean Sea. Some studies have investigated the chemical composition of the brown alga *Cystoseira usneoides* and evaluated the potential anti-inflammatory, antioxidant and anticancer properties of *Cystoseira usneoides* extract (183). It was shown that many of the isolated compounds, including several meroterpenoids, shown significant cytotoxic effects against lung cancer cells with potential anticancer activities. In parallel, several meroditerpenoids exhibited significant antioxidant and anti-inflammatory activities, suggesting that *Cystoseira usneoides* may be a promising source of natural products with potential therapeutic applications in the treatment of oxidative stress and inflammatory diseases, such as osteoarthritis (183). Overall, there is limited research on the link between *Cystoseira usneoides* and osteoarthritis or inflammation, and more research is needed to fully understand the potential therapeutic applications of *Cystoseira usneoides* extracts.

As mentioned before, deficiency in vitamin K has been linked to various health conditions that involve abnormal calcification and inflammation, emphasizing the significance of vitamin K-dependent proteins and vitamin K itself in CID diseases, such as OA (131-132,189). While vitamin K is primarily used clinically for preventing blood clotting disorders, there is increasing interest in its potential as a health-promoting supplement due to evidence demonstrating its beneficial effects, namely its antioxidant and anti-inflammatory properties, in cognitive promotion, inhibition of tumor progression, and regulation of osteoblastic gene expression, without adverse reactions or known toxicity (123). Vitamin K is present in various marine organisms, including several species of macroalgae and microalgae, such as *Porphyra sp*. (*Rhodophyta*), *Sargassum muticum*, *Sargassum fusiforme*, *Undaria pinnatifida*, *Nannochloropsis in vivoioculata* (*Ochrophyta Tetraselmis suecica*, *Dunaliella salina*,

Desmodesmus asymmetricus, *Chlorella vulgaris*, *Chlamydomonas reinhardtii* (*Chlorophyta*), *Isochrysis galbana, Pavlova lutheri* (*Haptophyta*), and *Skeletonema costatum* (*Bacillariophyta*) (190-192), and certain cyanobacteria, such as *Anabaena cylindrica*, *Anabena variabilis*, *Spirulina sp*., and *Nostoc muscorum*, *Synechocytis sp. PCC 6803* (193-194). The biosynthesis of vitamin K1 is mainly associated with oxygenic photosynthetic organisms like plants, algae, and cyanobacteria. Conversely, the synthesis of menaquinones (MKs) is attributed to a limited number of bacteria. However, exceptions exist, as certain cyanobacteria and microalgae, such as cyanobacteria *Gloeobacter violaceus* and *Synechococcus sp. PCC 7002*, the diatom *Chaetoceros gracilis*, and the red algae *Cyanidium caldarium* (195-197) have been discovered to synthesize MK-4. A recent study examined seven microalgae species and identified the cyanobacteria Anabaena cylindrica as the richest source of the active E-isomer of vitamin K1, with a concentration of approximately six times higher than that found in parsley (186), a known dietary source of K1, and higher than any previously reported source of phylloquinone (191). Additionally, Spirulina sp., another cyanobacteria, and the marine green microalgae Tetraselmis suecica also exhibited a considerable concentration of vitamin K1 on a dry weight basis (192). Although both vitamin K1 and K2 are commercially available, there is a need for optimized production methods and more efficient formulations for each vitamer to meet increasing customer demands at affordable prices. Moreover, the global market for marine diet supplements and functional products is already well-established, and the exploration of new sources of vitamin K from aquatic organisms holds potential benefits for human health, as well as economic and environmental interests.

Chitosan is a biopolymer derived from chitin, mostly obtained from marine organisms such as shrimps, crabs, and lobsters, which possess chitin in their exoskeletons. The applications of chitosan and its derivatives in tissue engineering and medicine are extensive. Composed of glucosamine and N-acetylglucosamine units connected by β-1,4-glycosidic linkages, chitosan exhibits significant potential as a biomaterial for various purposes, including nanoparticles and *in vivo* scaffolds (VS) (193). Its advantageous properties, including biocompatibility, progressive degradability, non-toxicity, biological activity, anti-inflammatory effects, and antibacterial activity, make it an ideal candidate for drug delivery systems (194). Furthermore, studies have demonstrated the chondroprotective properties of chitosan by promoting chondrocyte proliferation, enhancing the expression of cartilage matrix components, and inhibiting inflammatory and catabolic mediators in OA models through intra-articular injection. Moreover, chitosan has demonstrated the ability to inhibit cartilage

degradation and inflammation in the synovial membrane (201-202), making it a potential synergistic partner for OA treatment.

These are just a few examples of marine compounds that may be promising in osteoarthritis treatment. Other compounds, including lectins, peptides and polyphenols, have also been identified from marine organisms and have shown potential anti-inflammatory bioactivity but further research is needed to fully understand the mechanisms of action and potential clinical applications of these compounds.

1.7 Main aim and thesis organization

Osteoarthritis (OA) is a prevalent joint disorder with considerable global impact, yet there are still significant gaps in the understanding of its occurrence and progression. Late diagnosis associated with limited treatment options, challenges the management of this degenerative condition. Therefore, research efforts in the field of OA are crucial to improve disease knowledge and promote solutions. Pathologic calcification is a prevalent feature observed in both vascular and articular diseases characterized by inflammation, degradation of the extracellular matrix, and mineral nucleation. Despite the need for novel therapeutic strategies in both diseases, the currently available pharmacological options are very limited. GRP, a VKDP with a strong affinity for calcium binding, has recently been demonstrated to possess anti-inflammatory and anti-mineralization properties in articular cells. It is suggested that GRP plays a significant role in the interconnection between inflammation and mineralization processes in OA. In order to explore the therapeutic potential of GRP in OA, in Chapter 2, we developed the encapsulation of GRP into chitosan-based nanoparticles, expecting to enhance its bioavailability and bioactivity, thereby facilitating its application in functional assays. To evaluate the therapeutic potential of new compounds and minimize the probability of incorrect preliminary therapeutic responses, we have developed an experimental design pipeline as described in Chapter 3. This pipeline involves a series of activity assessments, starting from a simpler cell-based model of osteoarthritis and progressing to a more complex co-culture model based on human cartilage, which closely mimics the *in vivo* scenario of OA. By mimicking the early stages of the disease, this approach enables the examination of potential drugs as mediators of inflammation and mineralization. In the search for new bioactive compounds, the utilization of marine natural products as a therapeutic approach for osteoarthritis is an emerging

field, as these products offer diverse biological activities. In our study, in Chapter 4, we investigated the utilization of the marine bioactive compound amentadione in the context of osteoarthritis treatment, using the experimental pipeline here developed. Finally, in Chapter 5, a comprehensive discussion is provided.

Chapter 2

Gla-rich protein (GRP): an anti-inflammatory agent with potential application in osteoarthritis?

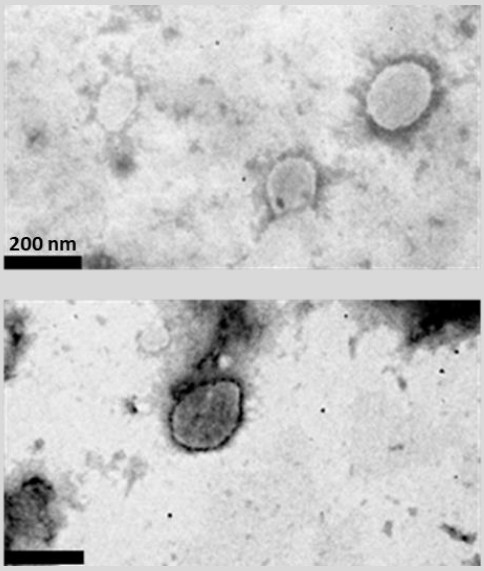

Abstract

Gla-rich protein (GRP) is a vitamin K dependent protein (VKDP) shown to act as a mineralizing inhibitor in chronic and degenerative calcification-related inflammatory diseases, such as osteoarthritis (OA). GRP has been previously suggested to act as a dual agent by modulating the interplay of calcification and inflammation in articular chondrocytes and synoviocytes. In this chapter, we continue to explore the role of GRP in the OA context, and further extend the investigation of GRP in the inflammatory response mechanism of immune cells, known to play a relevant role in OA. Furthermore, we aim to develop a novel chitosan-based nanoformulation of GRP with biocompatibility and chondroprotective properties, while resolving drawbacks related with low protein solubility. For this purpose, fluorescein labelled chitosan (FC)/ tripolyphosphate (TPP) nanoparticles (FCNP) and GRP-loaded FC/TPP nanoparticles (FCNG) were produced and characterized for further use in functional assays. The biological anti-inflammatory potential of FCNP and FCNG formulations were tested using previously established *in vitro* model assays including differentiated human THP-1 macrophage cells (THP-1 MoM) and primary articular chondrocytes and synoviocytes cells.

Our results demonstrated that treatments of LPS activated THP-1 MoM with purified γ-carboxylated and noncarboxylated GRP protein forms (cGRP and ucGRP, respectively) resulted in the downregulation of the inflammatory mediator TNFα, independently of the GRP γ-carboxylation status. Moreover, *in vitro* biological data demonstrated that encapsulated GRP mediate the inflammatory responses acting as an anti-inflammatory agent in macrophages and chondrocytes, by decreasing the accumulation of inflammatory agents TNFα and IL-6, respectively. This is a very promising outcome for the use of GRP nanoparticle formulation as a valid strategy to develop new therapeutic approaches for OA.

2.1 Introduction

Pathologic calcification and chronic inflammation are two synchronised events in several chronic diseases, such as atherosclerosis, chronic kidney disease (CKD) and OA, representing driving forces towards disease progression (131,203). In OA, pro-inflammatory cytokines and inflammatory mediators are overexpressed, contributing to the degradation of articular cartilage, with the accumulation of specific extracellular matrix (ECM) degradative enzymes,

such as metalloproteases (MMP) and aggrecanases (66,68). Increased ECM remodeling, in tandem with chondrocyte differentiation and apoptosis, are responsible for ECM disruption and gradual loss of articular cartilage. In turn, cartilage degradation potentiates pathologic calcification, aggravating the pro-inflammatory responses in a vicious cycle of inflammatory and calcifying stimuli and responses (118,204-205). In this context, it is of upmost importance the search for new active agents to treat OA, preferably capable of interfering with the interplay inflammation-calcification at different levels and targeting various players involved in this chronic disease. GRP is an endogenous VKDP that was previously shown to exhibited very promising results in the disease context of OA (173), with a potential role in the interplay between inflammation and mineralization processes. Indeed, the response of mineral and inflammatory stimulated articular chondrocytes and synoviocytes was modulated by GRP, with GRP acting in a concerted way in the two interlinked events of ectopic calcification and inflammation in OA. While cGRP inhibited ECM calcification, both GRP and GRP-coated basic calcium phosphate (BCP) crystals treatment led to the down-regulation of inflammatory cytokines and inflammation mediators, regardless of its carboxylation status (173).

Among the cell players in OA, the role of macrophages in the disease pathogenesis also deserves particular attention as activated macrophages were identified at early stages of OA, suggesting a primary role in the disease development (206-207) and *in vivo* tomography studies revealed 76 % of activated macrophages in OA affected joints linked to radiographic joint disease severity and symptoms (202). GRP has been detected in foam macrophages in calcific aortic valve disease (160), accumulating in osteoarthritic cartilage and co-localized with CD45 in osteoarthritic synovial membrane, characterized by lymphocytes and plasma cells infiltration (203). Overall, the role of GRP as an inhibitor of calcification and as an anti-inflammatory agent in cells involved in OA, indicated strong therapeutic potentialities (203). However, GRP was shown to have limited solubility at physiological pH (157), with possible implications in terms of bioavailability and bioactivity, limiting its use in therapeutics. The possibility of GRP encapsulation as a strategy to overcome these limitations, promote easy manipulation, storage stability and a more efficient cell delivery, while minimizing inflammatory responses, was therefore explored in this study.

In general, nanotechnological approaches are expected to improve the delivery of drugs through a controlled release manner and toward specific cell populations or anatomical compartments, such as the joint in OA, anticipating advantages by reducing side toxicities and improving long-term therapeutic efficacy (200). The incorporation of bioactive compounds into chitosan-based nanoparticles is a therapeutic strategy that has been previously explored, as

chitosan is a natural cationic and hydrophilic polysaccharide, biocompatible, nontoxic, with high bioavailability and chemical resistance (210-214). Improvement of absorption and bioavailability of drugs encapsulated into chitosan nanoparticles is expected as shown by several reported applications (206) in the biomedical field (207), and in particular in therapeutics as drug-delivery vehicle (217-218). Also, chitosan-based nanoparticles can be modified with specific ligands or antibodies, for specific cell targeting.

In this work the choice of chitosan to formulate GRP containing nanoparticles was also expected to add beneficial properties related with anti-inflammatory and cartilage repair abilities, based on the previously reported anti-inflammatory and chondroprotective properties of chitosan (219-220). N-acetyl-glucosamine and glucosamine, chitosan monomers, are natural components of cartilage, structural units of proteoglycans, with impact in the regeneration of damaged or inflamed tissues (221-222). Based on this, chitosan could represent a potential synergetic drug-partner in the OA drug delivery system (223-226).

In this chapter, we aimed to further investigate the role of GRP as an anti-inflammatory agent in stimulated macrophages and we describe the development of a well-characterized chitosan-based nanoformulation of non-carboxylated GRP (ucGRP) labelled with fluorescein. The OA therapeutic potential of these novel GRP nanoformulations was evaluated using *in vitro* cell models of inflammation and OA, including differentiated human THP-1 macrophage cells (THP-1 MoM) and primary articular chondrocyte and synoviocyte cells.

2.2 Experimental procedures

2.2.1 Chemicals

Deacetylated chitosan (CS) (low molecular weight, deacetylation degree 75-80 %), fluorescein sodium salt, sodium tripolyphosphate (TPP), and 1-ethyl-3-(3-dimethylaminopropyl) carbodiimide hydrochloride (EDAC) were obtained from ‘Sigma Aldrich’, Bovine serum albumin (BSA) was purchased from ‘nzytech’ and Triton X-100 was acquired from ‘plusone’.

2.2.2 Expression and purification of recombinant human GRP (ucGRP)

The expression of recombinant uncarboxylated human GRP (ucGRP) was performed in *E. coli* as previously described (157). Briefly, human GRP cDNA coding for the secreted GRP-F1

isoform cloned into pET151/D-TOPO vector (Champion pET Directional TOPO Expression kit, Invitrogen) was used to transform Escherichia coli BL21star (DE3). Induction was performed with 1 mM IPTG for 4h. Cells were then centrifuged, and the pellet resuspended in binding buffer (20 mM sodium phosphate, 0.5 M NaCl, 20 mM imidazole, pH 7.4). The resuspended cells were further sonicated for 3 minutes in 10 second pulses series at 60 volts. The resulting supernatant was loaded onto 1 mL HisTrap HP Column, for affinity chromatography purification, according to manufacturer's instructions, and recombinant protein was eluted with 20 mM sodium phosphate, 0.5 M NaCl, 500 mM imidazole, pH 7.4 (157). Final purification was performed by Reverse Phase-High Performance Liquid Chromatography (RP-HPLC). HisTrap eluted GRP-containing fractions were injected onto a Vydac C18 reverse-phase HPLC column (4.6 mm inner diameter and 25-cm length) equilibrated in 0.1 % trifluoroacetic acid in water and at a flow rate of 1 mL/min (initial conditions). The HPLC was run for 7 min at initial conditions, and then proteins were eluted from the column with a 1.5-h linear gradient to 0.1 % trifluoroacetic acid in 60 % acetonitrile. Fractions of 1 mL were collected and protein content was determined by spectrophotometry, as described in section 2.2.3. and stored at -80 ºC. GRP purity was evaluated by determining the protein profile by SDS-PAGE. The protein solution was then lyophilized, resuspended in 6 M guanidine-HCl and dialysed against distilled water, under agitation over 3 days, at 4 ºC, with 2-3 daily changes of medium. After dialysis, the content was quantified by spectrophotometry or by a specific sandwich ELISA for total GRP forms (GRP), as described in section 2.2.3, aliquoted and kept at -80 ºC.

2.2.3 GRP quantification

GRP content was estimated by spectrophotometry at 280 nm (NanoPhotometer® NP80), based on the general reference setting that a protein solution with an extinction coefficient (E) of 0.1 % (1 mg/mL) produces an absorbance of 1.0 at 280 nm (with a path length of 1 cm) (216), or quantified using a specific sandwich ELISA for total GRP forms (GRP) (163). In the experiments involving the preparation and use of the ucGRP nanoformulations (FCNG), GRP was quantified by ELISA.

2.2.4 Chitosan labelling with fluorescein (FC)

250 mg of chitosan (CS) were dissolved in 15 mL of an 1 % acetic acid aqueous, at room

temperature. Fluorescein (10 mg) was dissolved in 1 mL of ethanol 96 % and 7.5 mg of 1-ethyl-3-(3-dimethylaminopropyl) carbodiimide (EDAC) were dissolved in 4 mL of Milli-Q water. The fluorescein solution was carefully added to the chitosan solution under stirring, followed by the addition of the EDAC solution. The mixture was stirred overnight, at room temperature and UV protected. The mixture was then dialysed against water, with a molecular weight cut-off of 2000 Da (Sigma-Aldrich). The mixture was under agitation over 3 days and the water changed 2 to 3 times a day. The dialysis was stopped when the water appeared transparent and uncoloured. The resultant solution was lyophilized to afford a fluorescent yellow/orange solid. The process yield (PY) was calculated as follows:

PY (%) = CS weight / Total solids (CS + Fluorescein) weight × 100.

2.2.5 Preparation of nanoparticles CNP, CNG, FCNP and FCNG

Chitosan (CS)/TPP nanoparticles (CNP) were prepared by ionic complexation, by means of an electrostatic interaction of CS with TPP anions, in which the positively charged amino groups of CS interact with the negatively charged phosphate groups of TPP (217). Briefly, CS in 1 % of acetic acid (1 mg/mL, w/v, pH 2.7), was added to an aqueous solution of TPP (0.714 mg/mL, w/v), at room temperature, pH 8.9, to obtain a final theoretical CS/TPP ratio of 3.5/1, (w/w), pH 3. The nanoparticles were spontaneously formed on incorporation of 0.8 mL of the TPP solution into 2 mL of the CS solution, under magnetic stirring at room temperature. Nanoparticles were pelleted by centrifugation at 16,000 g, at 15 ºC, for 30 min. The supernatants were discarded and nanoparticles were resuspended in distilled water or in cell culture media for further use.

The same procedure was followed to prepare the ucGRP-loaded CS/TPP nanoparticles (CNG). TPP (0.8 mL of 0.714 mg/mL), was added to a 2 mL solution containing 1 µg of ucGRP (quantified by ELISA as described in section 2.2.3) and CS (1 mg/mL), to reach the theoretical FC/TPP ratio of 3.5/1 (w/w). The theoretical percentage of GRP present in the final nanoparticle formulation, considering that all protein is incorporated, is 0.05 % respectively to the CS content (w/w).

Fluorescein labelled chitosan (FC)/TPP nanoparticles (FCNP) were prepared following the same methodology. Briefly, aqueous TPP solutions (0.8 mL of 0.666 mg/mL and 0.714 mg/mL) were added to the acidic solution of FC (2 mL, 1 mg/mL), at room temperature, under magnetic stirring, to obtain ratios of 3.75/1 and 3.5/1 of FC/TPP (w/w), respectively. Nanoparticles were concentrated by centrifugation at 16,000 g, at 15 ºC, for 30 min. The

supernatants were discarded and nanoparticles were resuspended in water or in the appropriated cell culture media for further use.

The same procedure was followed to prepare the ucGRP-loaded FC/TPP nanoparticles (FCNG). A solution containing 1 µg of ucGRP in distilled water (quantified by ELISA as described in section 2.2.3), was added to the acidic solution of FC (1mg/mL) and a final 2 mL solution (pH 2.62) was allowed to react with the aqueous solutions of TPP (0.8 mL of 0.666 mg/mL and 0.714 mg/mL), to a final FC/TPP ratios of 3.75/1 and 3.5/1 (w/w), respectively. Considering that all ucGRP is incorporated, the percentage of ucGRP in the final formulation is 0.05 % relative to FC, taking in consideration the initial amounts of synthesis (further referred as FCNG). Additionally, based on the same methodology and assumptions, nanoparticles containing different % of ucGRP were prepared, 0.25 % (5 µg ucGRP, $FCNG_{0.25}$), and 0.375 % (7.5 µg of ucGRP, $FCNG_{0.375}$) (w/ w) of protein respective to the FC content.

2.2.6 Determination of nanoparticles synthetic yield

The nanoparticles production yield was calculated by gravimetry. Fixed volumes of aqueous nanoparticle suspensions were centrifuged (16000 × g, 30 min, 15 ºC) and sediments were freeze-dried over 24 h. The process yield (PY) was calculated as follows:

PY (%) = Nanoparticles weight / Total solids (FC + TPP) weight × 100, for FCNP

or

PY (%) = Nanoparticles weight / Total solids (FC + TPP + ucGRP) weight × 100, for FCNG.

2.2.7 Characterization of FCNP and FCNG nanoparticles

2.2.7.1 Physicochemical properties

FCNP and FCNG nanoparticles were characterised in terms of size, polydispersity index (PdI) and ζ-potential on freshly prepared samples, as described in 2.2.5, by photon correlation spectroscopy and laser Doppler anemometry, respectively, using a Zetasizer® NanoZS (Malvern Instruments, Malvern, UK). The characterisation was performed in an electrophoretic cell, in which a 20 µL aliquot of nanoparticles was diluted in 1 mL of ultrapure water. Size and polydispersity index were determined with a detection angle of 173 °, at 25 ºC, and ζ-potential was calculated from the mean electrophoretic mobility values. The measurements were

performed in triplicate. In addition, nanoparticles were also characterised regarding size and polydispersion index (PDI), after resuspension of nanoparticles in cell culture media (RPMI 1640, Lonza).

FCNP and FCNG particle concentrations and size distributions were also determined using the Nanoparticle Tracking Analysis (NTA) technique on the NanoSight NS300™ (Malvern Instruments, Worcestershire, UK) equipment. These analysis were performed by our collaborators from iBET-Instituto de Biologia Experimental e Tecnológica, and ITQB-Instituto de Tecnologia Química e Biológica António Xavier, Universidade Nova de Lisboa. The samples were initially solubilized in MilliQ water to a final volume of 2 mL, and then diluted with MilliQ water (1: 100). Each sample was analyzed 3 times (n=3) with independent dilutions. Capture settings (shutter and gain) were adjusted manually for each analysis and all steps were carried out at room temperature. Sample videos were analyzed with the NTA.

2.2.7.2 Morphology

The morphological analysis of the FCNP and FCNG nanoparticles was performed by transmission electron microscopy (TEM) (CM 12 Philips, Eindhoven, Netherlands), by our collaborators from Universidade Nova de Lisboa (Departamento de Química, Lisboa, Portugal) and Centro de Investigação Interdisciplinar Egas Moniz. The samples were freshly prepared as described in 2.2.4, resuspended in ultrapure water, stained with stained with 1.5 % aqueous uranyl acetate (w/v) and adsorbed onto copper grids with Formvar1 films. The morphological examination of nanoparticles was performed by transmission electron microscopy (TEM), in a JEOL 1200EX transmission electron microscope.

2.2.7.3 ucGRP association efficiency (AE)

The association efficiency (AE) of GRP in FCNG was calculated based on the quantification of ucGRP present in the supernatant by ELISA, after FCNG sedimentation by centrifugation (16,000× g, 30 min, 15 ◦C). representing the fraction of GRP not encapsulated, relative to the quantity of protein initially added, as follows:

$$AE\ (\%) = (\text{Total ucGRP amount} - \text{Free ucGRP amount}) / \text{Total ucGRP amount} \times 100$$

2.2.8 *In vitro* release studies

In vitro release studies of ucGRP from FCNG nanoparticles were performed after sedimentation (section 2.2.5). Nanoparticles were resuspended in 2 mL of RPMI (Lonza) and incubated at 37 ºC and 5 % of CO_2 atmosphere. At pre-determined time intervals, between 0 min and 48 h, samples were collected, centrifuged for 30 min, at 15 ºC and 16000 x g, and the ucGRP in the supernatant was quantified by ELISA (n=3) as described in section 2.2.3.

2.2.9 Cell culture maintenance

THP-1 cell line was kindly given by Dr. Nuno Santos (CBME, University of Algarve, Faro) and cells were cultured according to ATCC instructions in RPMI Growth Medium (RPMI 1640 with L-Glutamine (Lonza), 10 % heat-inactivated Fetal Bovine Serum (FBS, Invitrogen) and 1 % Pen-Strep P/S, Gibco). Differentiation into macrophagic THP-1 (THP-1 MoM) was achieved by culturing cells in 25 ng/mL PMA (Sigma) in complete RPMI, for 48h. Primary human fibroblast-like synoviocytes (ECACC, Sigma-Aldrich, St. Louis, MO, USA) and human articular chondrocytes (Lonza, Visp, Switzerland) used in this work were commercially acquired. Additionally, 3 sets of primary human fibroblast-like synoviocytes and human articular chondrocytes, derived from tissue explants, were used in this work and developed by collaborators as described (229,230). Synoviocytes and chondrocytes were cultured in Advanced Dulbecco's Modified Eagle's Medium (Adv DMEM) (Invitrogen, Carlsbad, CA, USA) supplemented with 10 % (v/v) of heat-inactivated FBS, 1 mM of L-Glutamine (L-Gln, Invitrogen) and 1 % (v/v) of P/S. All cell cultures were maintained at 37 °C in a humidified atmosphere containing 5 % CO_2, and experiments were performed on confluent synoviocytes and chondrocytes, and using an average of 1×10^6 cells /mL of THP-1 MoM.

2.2.10 Inflammatory assays

2.2.10.1 GRP inflammatory activity in LPS-stimulated THP-1 MoM cells

Purified and characterized fully γ-carboxylated GRP from sturgeon (cGRP) (157) and uncarboxylated recombinant human GRP produced in *E. Coli* (ucGRP) (section 2.2.2), quantified by spectrophotometry as described in 2.2.3, were used to evaluate their anti-inflammatory potential in THP-1 MoM cells. THP-1 cells were seeded in 96 well plates at a density of 2.5 $x10^5$ cells/well and differentiated as described above in 2.2.9. After

differentiation, media was removed and cells were treated for 24 h with 0.5, 0.75 and 1.5 μg/mL of cGRP and ucGRP, followed by treatments with 50 ng/mL of LPS for additional 24 h. Dexamethasone treated cells (2 μM) were used as positive control. At the appropriate time, cell culture media were collected, centrifuged at 13.000 rpm for 20 min at 4 ºC, and supernatants were immediately pipetted and anti-inflammatory activity analyzed using commercially available ELISA assays to measure TNFα (PreproTech) levels, according to the manufacturer's protocols. ELISA results were analyzed using a four parameter logistic curve fitting model in GraphPad Prism software.

2.2.10.2 Anti-inflammatory activity of ucGRP nanoformulations in LPS-stimulated THP-1 MoM cells

To evaluate the anti-inflammatory potential of ucGRP nanoformulations in THP-1 MoM, THP-1 cells were seeded at a density of $1x10^6$ cells/mL, differentiated as described in section 2.2.9, and supplemented with FCNP and FCNG nanoparticles resuspended in RPMI [$(11.7 \pm 4.5) \times 10^9$ particles/mL] (section 2.2.7), or 2 μM dexamethasone (DXM) during 2 h, 8 h and 24 h. Additionally, [$(11.7 \pm 4.5) \times 10^9$ particles/mL] of FCNG, $FCNG_{0.25}$ and $FCNG_{0.375}$, and 2 μM DXM were used as pre-treatment of THP-1 MoM during 24 h. After each pre-treatment period, cells were stimulated with 100 ng/mL LPS for an additional 24 h. At each time, cell media were collected for TNFα quantification as described above.

2.2.10.3 Inflammatory assays of FCNP and FCNG in articular cells

To evaluate the anti-inflammatory potential of FCNP and FCNG in articular cells, confluent human synoviocytes and chondrocytes were cultured in advanced DMEM or pre-treated with FCNG [$(11.7 \pm 4.5) \times 10^9$ particles/mL], FCNP [$(11.7 \pm 4.5) \times 10^9$ particles/mL] or 2 μM dexamethasone (DXM), during 24 h and then stimulated for further 24 h with IL-1β (10 ng /mL). Cell media were collected for IL-6 measurement using a specific ELISA (Peprotech) and following manufacturer's instructions.

For each biological assay, nanoparticle formulations were freshly prepared, immediately centrifuged (16000 × g, 30 min, 15 ºC) and the pellets resuspended in 2 mL of the appropriate cell culture medium. All nanoparticle suspensions were combined in a unique batch, and promptly used in the biological assays. The nanoparticles concentration was calculated based on NTA results, described in section 2.2.7.1.

2.2.11 Quantification of total GRP in THP-1 MoM cells and respective cell culture media, pre-treated with FCNP and FCNG

Total GRP from THP-1 MoM inflammatory assays pre-treated with FCNG [(11.7 ± 4.5) × 10^9 particles/mL] and FCNP [(11.7 ± 4.5) × 10^9 particles/mL], during 24 h, and stimulated with 100 ng/mL LPS for an additional 24 h, was determined by ELISA (220) on the cell culture media and in cells protein extracts. After collection, cell culture media were centrifuged at 13.000 rpm for 20 min at 4 ºC to remove cell debris, and THP-1 MoM protein extracts were obtained by extraction with RIPA buffer (50 mM Tris HCl pH 8, 150 mM NaCl, 1 % NP-40, 0.5 % sodium deoxycholate, 0.1 % SDS), for 1h at 4 ºC, with agitation, followed by a centrifugation at 16 000 xg for 15 min at 4 ˚C.

2.2.12 Cellular proliferation measurement

Cells were seeded in 96-well plates at 2 × 10^4 cells/well and cultured in their respective growth medium and cell culture conditions, and supplemented with cGRP (0.5µg/mL, 1 µg/mL and 1.5 µg/mL), ucGRP (0.5µg/mL, 1 µg/mL and 1.5 µg/mL), quantified by spectrophotometry (section 2.2.3), FCNP [(11.7 ± 4.5) × 10^9 particles/mL] and FCNG [(11.7 ± 4.5) × 10^9 particles/mL], quantified as described in 2.2.9. Cell viability was assessed at appropriate time points, using the CellTiter 96 cell proliferation assay (Promega, Madison, WI, USA), following manufacturer's instructions.

2.2.13 Sample preparation for Flow cytometry

FCNP and FCNG, freshly prepared as described in 2.2.5, were incubated with the purified polyclonal CTerm-GRP antibody (5 µg/mL [adapted from (159)]), diluted in distilled water, for 30 min in ice, followed by 2 washes with PBS (137 mM NaCl, 2.7 mM KCl, 10 mM sodium phosphate, 1.8 mM potassium phosphate) and incubation with fluorochrome ALEXA Fluor® 647 Donkey anti-rabbit IgG Antibody (Biolegend, 1µg/mL), during 1h, following the manufacture´s indications. Samples were washed and resuspended in PBS for acquisition in Flow Cytometer (FACS Calibur, BD Bioscience, Ca, USA).

FCNP and FCNG were incubated with THP-1 MoM (1x10^6 cells/mL) for 2h, as described in 2.2.11. Cells incubated with CNP and CNG were used as controls. Flow cytometry

protocol from ORIGENE was used for cell staining. Briefly, after dethatching, centrifuged cell pellets were blocked with a 0.5 % BSA solution, for 30 min, incubated with PE anti-mouse/human CD11b antibody (1 µg/mL, Biolegend), and fixed in 0.2 % PFA solution in PBS, overnight at 4 ºC. A permeabilization step with 0.1 % Triton in PBS, preceded the incubation with the purified polyclonal CTerm-GRP antibody (5 µg/mL [adapted from (159)]). At the end, pellets were treated with the fluorochrome (ALEXA Fluor® 647 Donkey anti-rabbit IgG Antibody, Biolegend, 1 µg/mL), and resuspended in PBS for acquisition in Flow Cytometer (FACS Calibur, BD Bioscience, Ca, USA). Samples were protected from UV light, along the protocol and kept in ice.

2.2.14 Flow cytometry data acquisition

Flow cytometry acquisitions were performed on a Becton Dickinson FACS Calibur (BD Biosciences) flow cytometer using the Cell Quest Pro software (version 6.0). The 488 nm argon laser combined with a 530/30 nm band pass filter was used to access the FITC fluorescence, while the same laser combined with 585/45 nm band pass filter was used to measure PE fluorescence. Alexa Fluor 647 fluorescence was accessed using the 633 nm laser combined with a 661/16 nm band pass filter. Compensation was performed using single stain controls and all gates were set based on Fluorescence Minus One (FMO) controls. For each sample 10,000 events were recorded. Flow cytometry data was analysed using FlowJo software (version 6.7).

2.3 Results

2.3.1 Effect of cGRP and ucGRP in the inflammatory response of differentiated THP-1 macrophages

Since macrophages are key players in the inflammatory events, particularly linked to ectopic calcification in chronic inflammatory diseases, such as OA (232,233,234), we decided to assess if c/ucGRP could have a direct effect on the LPS-stimulated immune response of THP-1-differentiated macrophage (THP-1 MoM) cells, and whether that effect was dependent of its γ-carboxylation state. Fully γ-carboxylated GRP purified from sturgeon (*A. Naccarii*) (cGRP) (157) and uncarboxylated recombinant human GRP (ucGRP), produced in *E. Coli* (159), were used in this study. THP1-macrophage cells viability was unaffected in the presence of LPS and ucGRP or cGRP at 1.5 µg/mL (**results not shown**). THP-1 MoM cells were treated with

increasing concentrations of cGRP/ucGRP, previously used in functional assays (164,178), or dexamethasone (DXM), followed by exposure to LPS.

Inflammatory responses were determined by measuring TNFα accumulation in cell media (**Figure 2.1**). Results revealed a significant increase of TNFα in the LPS stimulated cells, while cells treated with ucGRP resulted in a dose-dependent decrease of TNFα levels relative to LPS treated cells, with a maximum decrease at 1.5 μg/mL of ucGRP (**Figure 2.1**). Treatments with cGRP also shown decreased TNFα levels although to a less extent and independent of the concentrations used (**Figure 2.1**).

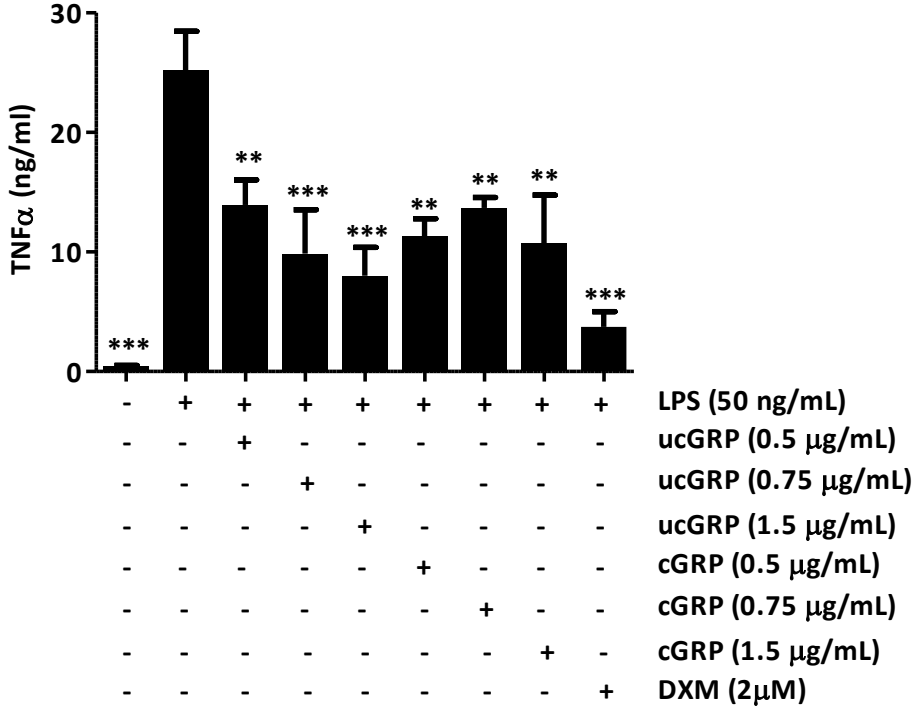

Figure 2.1 GRP reduces TNFα production in THP-1 MoM stimulated with LPS. Differentiated THP-1 MoM cells were treated with 0.5 μg/mL, 0.75 μg/mL and 1.5 μg/mL of purified cGRP and ucGRP proteins for 24 h, followed by exposure to 50 ng/ml LPS for additional 24 h. Cells treated with 2 μM dexamethasone (DXM) were used as a positive anti-inflammatory control, and non-stimulated cells as controls to LPS stimulation. Conditioned cell culture media were collected and used to determine TNFα accumulation by ELISA. Data are presented as means ± standard error of triplicates of two independent experiments (n=2), with triplicates. Ordinary one-way ANOVA was used and multiple comparisons were achieved with Dunnett's test. Statistical significance was defined as P< = 0.05 (*), P< = 0.01 (**) and P< = 0.001 (***).

2.3.2 Production and characterization of fluorescein labelled chitosan /TPP nanoparticles (FCNP) and fluorescein labelled chitosan /TPP nanoparticles containing ucGRP (FCNG)

Based on the anti-inflammatory activity of ucGRP in THP-1 MoM cells and taking in consideration the drawbacks related with low protein solubility in physiological conditions, a nano-formulation of ucGRP using fluorescent chitosan-based nanoparticles was developed. The encapsulation of ucGRP using this nano-formulation is expected to not only increase its bioactivity and bioavailability, but will also represent an advantage for bioimaging studies due to their unique optical properties. For that, low molecular weight chitosan was FITC- labelled. The chemical addition of the fluorescein carboxylic acid groups to the primary amine groups of the D-glucosamine residues of chitosan, mediated by 1-ethyl-3-(3-dimethylaminopropyl) carbodiimide hydrochloride (EDAC), yielded 84.5 % of the polymer (FC). Different mass ratios of FC to the polyanion sodium tripolyphosphate (TPP), with and without ucGRP (FCNG and FCNP, respectively), were initially combined to yield the nanoparticles preparation by ionic gelation. Nanoparticles production yield ranged from 12.1 ± 4.7 % for FCNP and of 15.1 ± 6.7 %, for FCNG, and significantly decreased with increasing FC-TPP ratio, both in the absence and presence of GRP (**Table 2.1**). Although the yield range for the nanoparticles production was low, the FC-TPP mass ratio of 3.5/1 was applied to prepare FCNG and FCNP nanoparticles (**Table 2.1**).

Table 2.1 Production yield of different FCNP and FCNG formulations, using variable ratios of FC/TPP/ucGRP. Results are demonstrative of 10 independent preparations for each component combination (n=10).

Nanoparticle	CS/ TPP/ucGRP (w/w/w)	Production Yield (%)
FCNP	3.5 / 1 / 0	12.1 ± 4.7
	3.75 / 1 / 0	8.9 ± 5
FCNG	3.5 / 1 / 1.75 E-3	15.1 ± 6.7
	3.75 / 1 / 1.75 E-3	6.2 ± 2.5

In relation to distribution of particle sizes, NTA analysis revealed that both FCNP and FCNG were present in 100 % between 0 and 400 nm. The content of FCNP and FCNG at 200 nm was 92.8 ± 9.3 % and 90 ± 4.7 %, respectively (**Figure 2.2**). The size distributions for FCNP and FCNG were predominantly unimodal, with a prominent peak at 88 ± 24 nm for FCNP and

107 ± 34 nm for FCNG. However, FCNP exhibited a slightly broader distribution compared to FCNG (**Figure 2.2**).

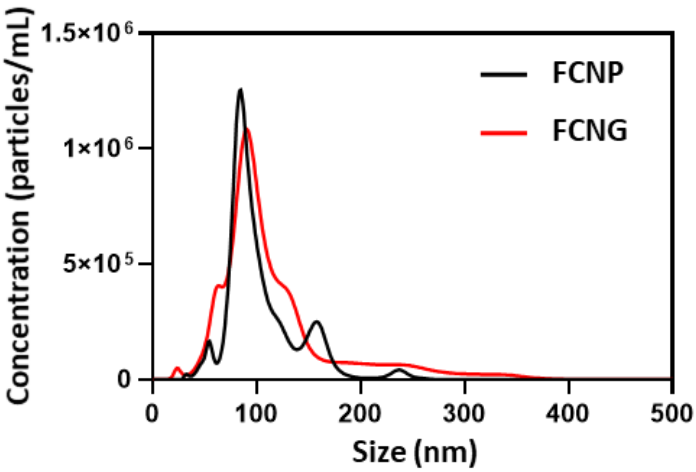

Figure 2.2 NTA analysis provided a representative assessment of FCNP and FCNG, displaying the particle concentration based on size (224).

The total particle concentration, as determined by NTA, was consistent between FCNP ((8.8 ± 3.6) × 10^9 particles/mL) and FCNG ((14.5 ± 3.4) × 10^9 particles/mL), showing no statistically significant differences. The polydispersity index (PDI) was 0.33 ± 0.07 for FCNP and 0.39 ± 0.06 for FCNG (**Table 2.2**). Both FCNP and FCNG exhibited positive zeta potentials, with FCNP showing a higher value of 37 ± 2 mV compared to FCNG's 28 ± 7 mV (**Table 2.2**). None of the measured parameters showed statistically significant differences between FCNP and FCNG. Levels of ucGRP were measured by ELISA in the supernatant after FCNG sedimentation, representing the fraction of ucGRP not encapsulated, and compared with the initial amount of protein added (**Figure 2.3**). The results revealed that most of the ucGRP used for the FCNG nanoparticles synthesis was incorporated, confirming a high degree of protein encapsulation with an AE of 99.8 ± 0.1 (**Table 2.2**).

Table 2.2 Production yields and physicochemical characteristics of nanoparticles: production yield, polydispersion index (PDI), zeta potential (results are demonstrative of at least 6 independent preparations, n≥ 6), size variation, particles concentration and ucGRP (0.05 % relatively to FC content) association efficacy (AE) (n=4). Data are shown as mean ± SD.

Sample	Production Yield (%)	PDI*	Zeta Potential* (mV)	Range Size** (relative amount, %)		Particles Concentration** (particles/mL)	AE*** (%)
				0 – 180 nm	180 – 400 nm		
FCNP	17.1 ± 3.8	0.33 ± 0.07	37 ± 2	94.7 ± 1.4	5.2 ± 1.1	(8.8 ± 3.6) E+9	n/a
FCNG	15.1 ± 6.7	0.39 ± 0.06	28 ± 7	77.9 ± 0.8	21.1 ± 1.1	(14.5 ± 3.4) E+9	99.8 ± 0.1

* Data obtained from DLS analysis; ** Data obtained from NTA analysis; *** Data obtained from Elisa, specific for GRP.

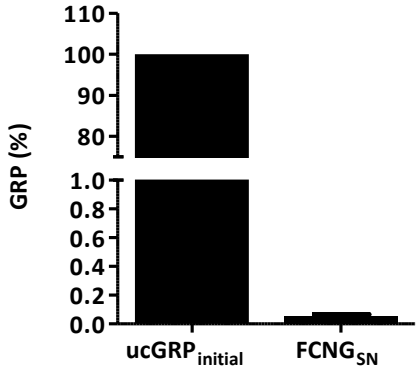

Figure 2.3 Percentage of ucGRP present in the nanoparticles formulations (FCNG): % of GRP detected by ELISA (**section 2.2.3**) in the supernatants of the ucGRP-loaded nanoparticles synthesis ($FCNG_{SN}$), relatively to the initially available ucGRP ($ucGRP_{initial}$). Data is representative of six independent experiments (n=6), with triplicates (224).

Ultrastructural analyses of FCNP (**a, Figure 2.4**) and FCNG (**b, Figure 2.4**), by transmission electron microscopy (TEM) revealed a population of small nanoparticles with spherical morphology, mostly varying from 100 to 250 nm, for both nanoformulations.

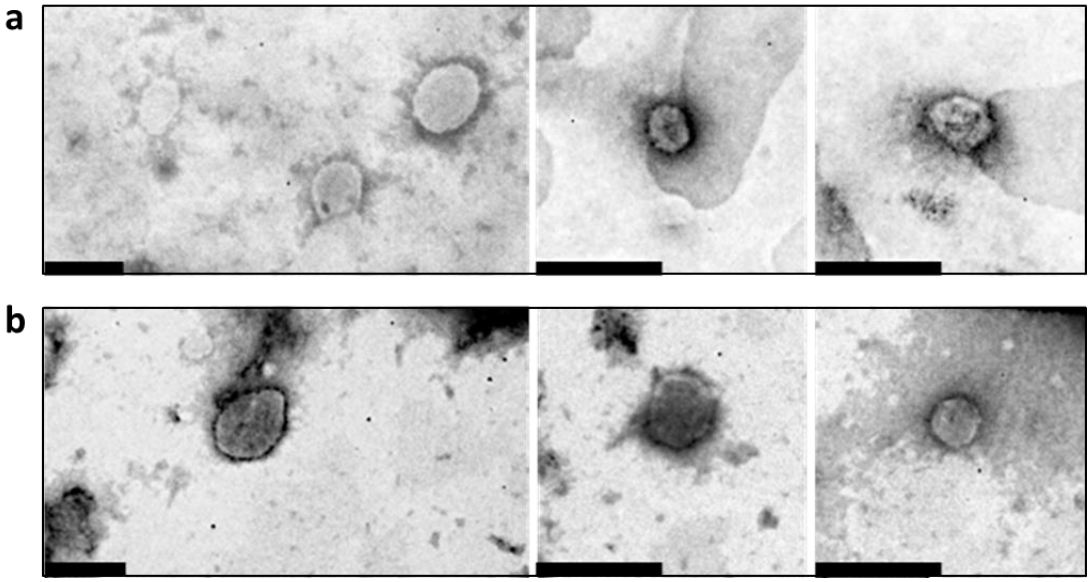

Figure 2.4 Ultrastructural nanoparticle characterization by transmission electron microscopy (TEM): morphology of FC based nanoparticles (a) FCNP and (b) FCNG. Scale bar of 200 nm (224).

FCNP and FCNG flow cytometry analysis showed that 98.3 % of FCNP events analysed were positive for FITC, indicating that almost all nanoparticles were FC labelled (**a, Figure 2.5**). FCNG stained with Alexa 647 for GRP detection showed that 39 % of the initial population was positive for FITC and Alexa 647, indicating the presence of GRP in the FC-based nanoparticles formulation (**b, Figure 2.5**).

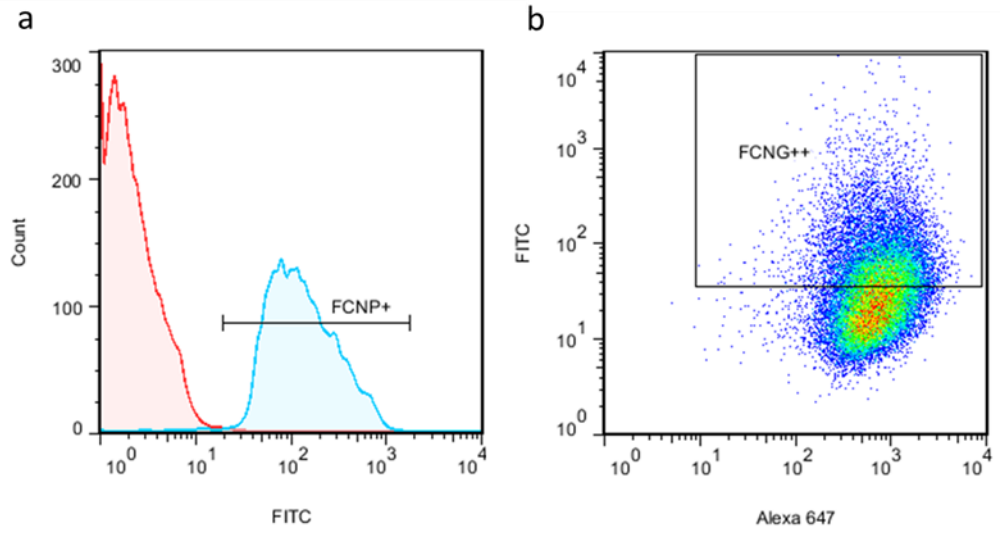

Figure 2.5 Chitosan-based nanoparticles analysis by flow cytometry. (a) Histogram overlay plot showing unstained control of nanoparticles of chitosan (CNP) in red and nanoparticles of fluorescein-labelled chitosan (FCNP) in blue. 98.3 % of FCNP events are positive for FITC, exhibiting higher fluorescence intensity (FCNP+). (b) Dot plot showing nanoparticles of

fluorescein-labelled chitosan with ucGRP (FCNG). The FCNG were stained with Alexa 647 for ucGRP protein detection. The gate FCNG++ is double positive for FITC and Alexa 647, representing 39.7 % of the initial population (excluding the debris).

In order to explore the stability of the nanoparticles containing ucGRP in cell culture media for application in biological cell assays, the rate of ucGRP release from FCNG nanoparticles over a time frame of 48 h was assessed. The protein release profile of FCNG was investigated mimicking the *in vitro* assays environment, by resuspending FCNG, (11.7 ± 4.5) × 10^9 particles/mL as determined by NTA, in RPMI cell culture media, at 37 ºC and 5 % of CO_2 atmosphere, during different periods, 0 min, 15 min, 30 min, 150 min, 24 h and 48 h. Results of ucGRP levels released to the cell culture media, measured by ELISA, demonstrated that the protein release rate remains between 10-15 % after 48h (**Figure 2.6).**

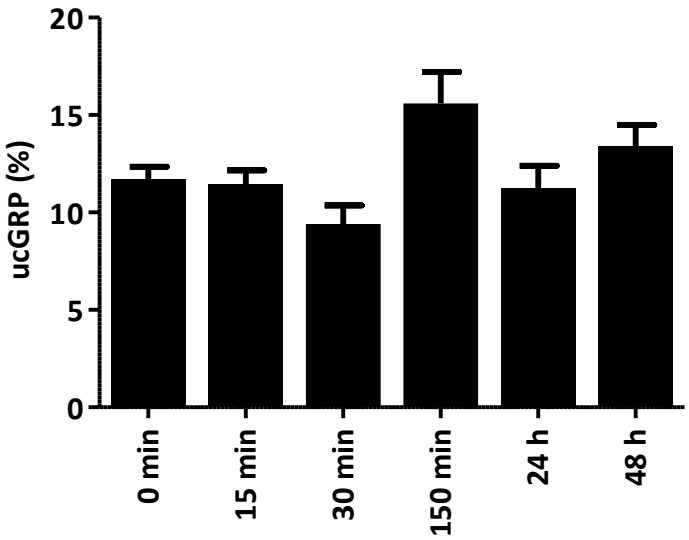

Figure 2.6 GRP releasing assay. Levels of ucGRP released from FCNG to cell culture media (RPMI) were measured by ELISA, at different times: 0 min, 15 min, 30 min, 150 min, 24 h and 48h. Data are representative of three independent experiences (n=3) and are statistically non-significant (224).

2.3.3 THP-1 MoM cellular uptake of FCNP and FCNG

To evaluate THP-1 MoM binding/uptake of the prepared nanoparticles, flow cytometry studies were performed using a triple stained system, designed and optimized to simultaneously detect the fluorescein-based nanoparticles through FITC, GRP through ALEXA647, and through PE for the extracellular CD11b membrane labelling (**Figure 2.7**).

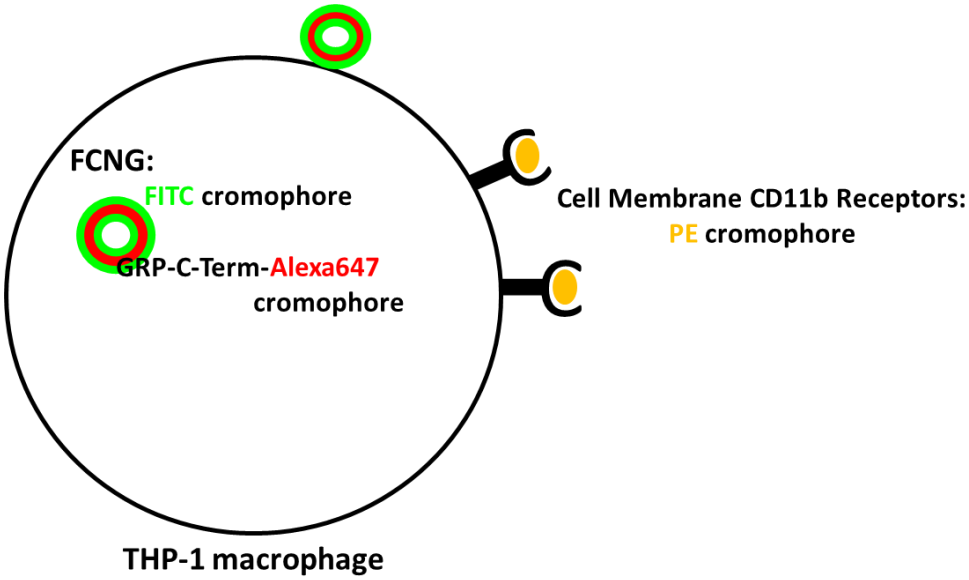

Figure 2.7 Schematic experimental design for the cytometry analysis of THP-1 MoM treated with FCNG. Triple stained system for detection of fluorescein (FITC), GRP (Alexa647), and CD11 (PE) in THP-1 MoM population.

The presence of the fluorescent nanoparticles in THP-1 MoM exposed to FCNP and FCNG for 2h was evaluated. The process of phagocytosis by macrophages can occur from 30 min to several hours, depending on the size and surface properties of the particle, and 2h is a time previously considered for macrophage nanoparticles uptake (236-237). At 2h of incubation, two conjoint positive signals for the presence of fluorescein (FITC) and for cell membrane labelling (PE) were detected. Analysis showed that 67.1 % of the cells exposed to FCNP, and 73.7 % of the cell population exposed to FCNG, were positive for FC labelling (**Figure 2.8**).

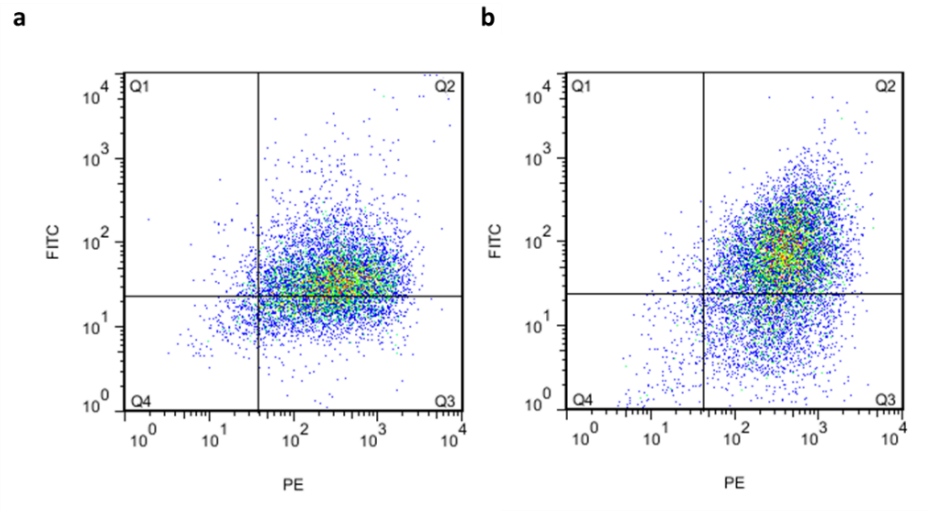

Figure 2.8 THP-1 binding/uptake of FCNP and FCNG nanoparticles by flow cytometry. Dot plots show THP-1 MoM exposed for 2h to (a) FCNP and (b) FCNG. The Q2 quadrant represents cells that have fluorescein-labelled nanoparticles and the THP-1 MoM marker (both FITC and PE positive). Q2 is 67.1 % for FCNP and 73.7 % for FCNG (224).

The presence of FCNG was further confirmed by the high intensity fluorescence for the 3 different fluorophores, corresponding to fluorescein (FITC), cell membrane labelling (PE) and GRP (ALEXA 647). The first plot shows the debris exclusion in the side scatter (SSC) vs. the forward scatter (FSC) (**a, Figure 2.9**). In plot **b**, 73.7 % of the population was double positive, positive for FITC and PE, indicating that fluorescein-labelled nanoparticles and the THP-1 MoM marker were gated. Plot **c** shows the selection of the population of interest, FCNG++, which represents THP-1 MoM cells with fluorescein-labelled nanoparticles containing GRP labelled with Alexa 647 (73.3 % are triple positive for FITC, PE and Alexa 647) (**c, Figure 2.9**).

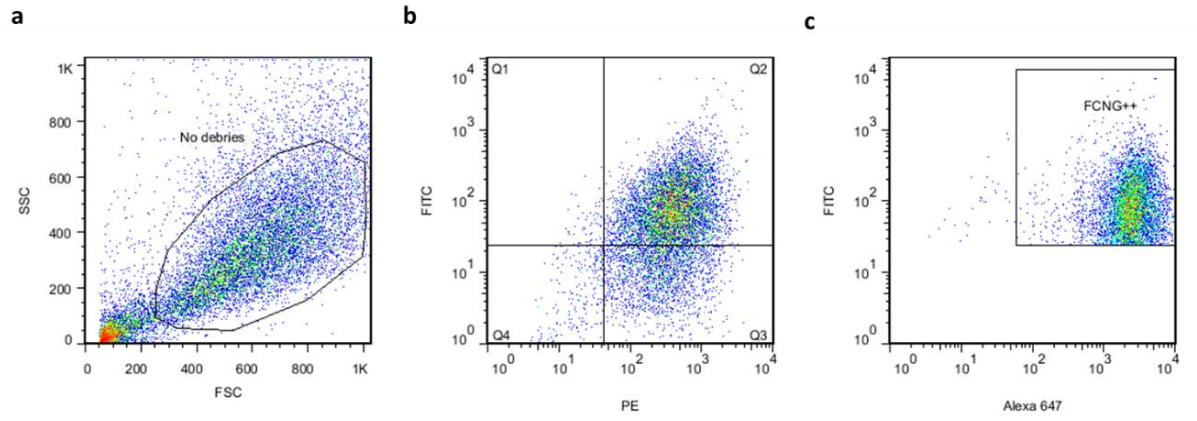

Figure 2.9 Flow cytometry gating strategy. Population of interest was first (a) gated on a forward scatter (FSC)/side scatter (SSC) plot to remove cell debris and then (b) gated on Q2, which represents cells that are positive for fluorescein-labelled nanoparticles and positive for THP-1 MoM marker (73.7 % are double positive for FITC and PE). These were then further (c) gated for the subset of interest, FCNG++, that represents THP-1 MoM cells with fluorescein-labelled nanoparticles containing GRP (73.3 % are triple positive for FITC, PE and Alexa 647) (224).

2.3.4 Effect of fluorescein labelled chitosan/TPP nanoparticles (FCNP) and fluorescein labelled chitosan /TPP nanoparticles containing ucGRP (FCNG) in the inflammatory response of THP-1 MoM and articular cells

The capacity of nanoparticles containing ucGRP to modulate the inflammatory response of stimulated THP-1 MoM and articular chondrocytes and synoviocytes was further evaluated.

2.3.4.1 Inhibition of LPS-induced inflammatory response by FCNG and FCNP on THP-1 MoM cells

To evaluate the anti-inflammatory potential of encapsulated ucGRP (FCNG) in the inflammatory processes occurring in OA, a first functional evaluation was performed on THP-1 MoM cells. LPS-stimulated THP-1 MoM cells were pre-treated with FCNP and FCNG for 2h, 8h and 24h, followed by 24h LPS stimulation. The effect of DXM was also analysed as a positive anti-inflammatory control. Cell viability of THP-1 MoM exposed to $(11.7 \pm 4.5) \times 10^9$ particles/mL of FCNG and FCNP, was assessed by the MTS cell proliferation assay, and no toxicity was observed in the concentrations tested (**Figure 2.10**).

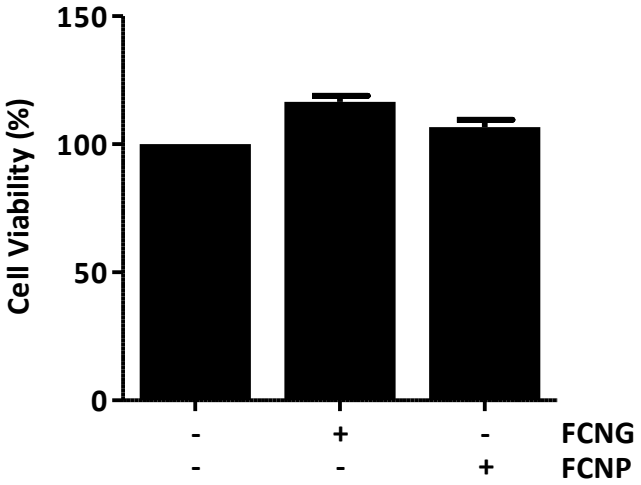

Figure 2.10 Cell viability of THP-1 macrophages treated with FCNP and FCNG. Effect of $(11.7 \pm 4.5) \times 10^9$ particles/mL FCNG and FCNP in THP-1 MoM after 24h of exposure assessed by the MTS cell proliferation assay (224).

The anti-inflammatory effect of FCNG was analyzed at different time points by measuring levels of TNFα released into the cell culture media. The results show decreased TNFα levels in FCNG-treated cells at all-time points tested, with the highest effect at 8h and prolonged until 24h of pre-treatment (**Figure 2.11**). An anti-inflammatory effect of the FCNP was also observed, although restricted to the 2h of nanoparticles pre-treatment, at the inflammation peak response (**Figure 2.11**).

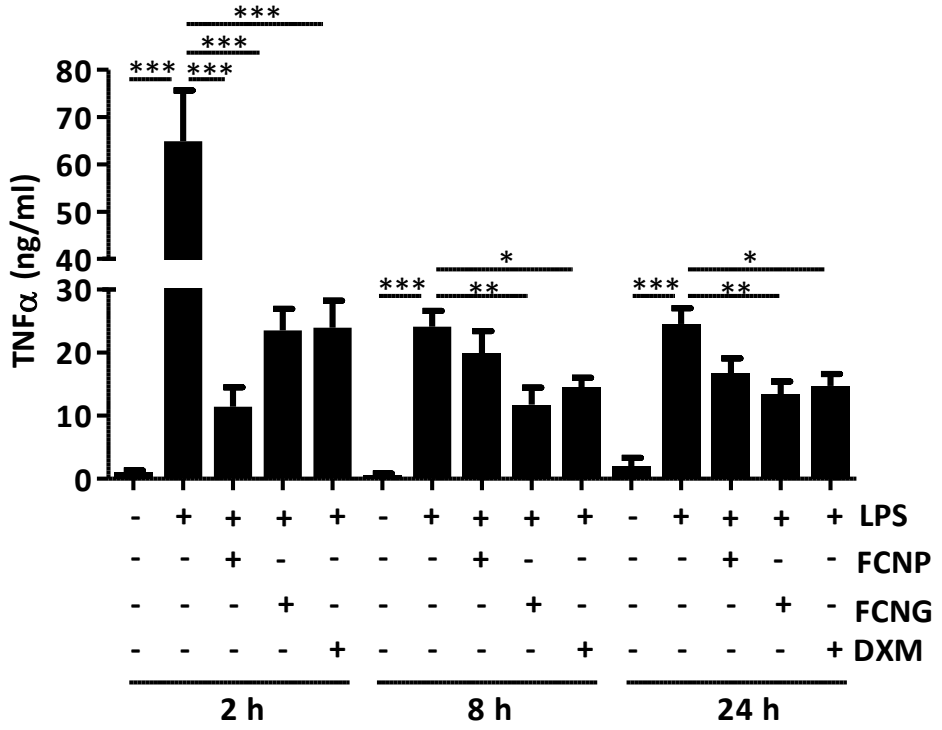

Figure 2.11 Anti-inflammatory effect of FCNP and FCNG in LPS-stimulated THP-1 macrophages. Evaluation of inflammatory marker TNFα was performed in the cell culture media of THP-1- MoM, previously treated for 2h, 8h or 24h with $(11.7 \pm 4.5) \times 10^9$ particles/mL FCNP or FCNG, and then stimulated with LPS (100 ng/mL) for further 24h. Dexametasone (DXM, 2 μM) was used as a positive anti-inflammatory control and non-stimulated cells as controls to LPS stimulation. Data are representative of three independent experiments (n=3), with triplicates. Two-way Anova and multiple comparisons were achieved with the Dunnett's test, and statistics presented were performed relatively to the LPS-stimulated condition. Both graphs show mean ± SD. Statistical significance was defined as $p \leq 0.05$ (*), $p \leq 0.005$ (**) and $p \leq 0.0005$ (***)(224).

2.3.4.2 Relation between FCNG treatments and GRP levels in THP-1 MoM cells

In order to explore the relation between levels of GRP and the anti-inflammatory activity observed in THP-1 MoM, GRP content was measured intracellularly and extracellularly in THP-1 MoM, cultured in LPS-induced inflammation and non-stimulated conditions, treated with $(11.7 \pm 4.5) \times 10^9$ particles/mL of FCNG and FCNP for 24h, or left untreated as controls. Results indicate higher levels of endogenous GRP in THP-1 MoM cells stimulated with LPS when compared to non-inflamed cells. Importantly, higher intracellular levels of GRP were observed in cells pre-treated with FCNG, either with or without LPS- stimulation, relatively to the control untreated cells and to LPS stimulated cells. An equivalent increase of GRP levels

was observed in the respective culture media of THP-1 MoM cells treated with FCNG (**b, Figure 2.12**). Cells pre-treated with FCNP did not present any significant increase in intracellular or extracellular GRP levels, relatively to untreated or LPS stimulated cells (**a, Figure 2.12**). These results indicate that treatments with FCNG are able to increase intracellular and extracellular GRP levels, suggesting nanoparticle cell internalization, in accordance with the data obtained by flow cytometry. The increase of GRP in the cell culture media of FCNG treated THP-1 MoM cells might be either resultant of a direct release from FCNG particles or as result of FCNG internalization by THP-1 MoM cells and further extracellular release. Overall, these results support the hypothesis that the anti-inflammatory activity of FCNG in THP-1 MoM cells is mediated by increased GRP levels.

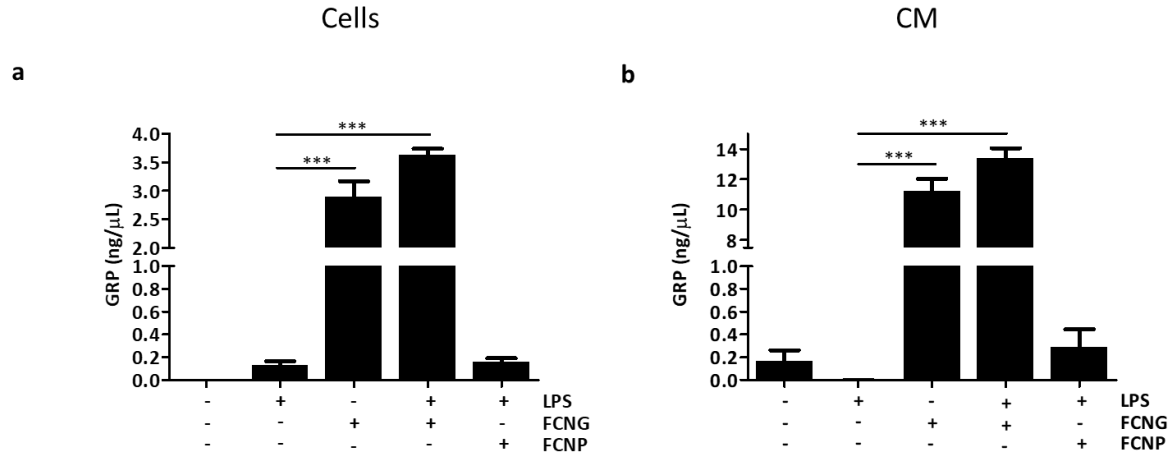

Figure 2.12 Evaluation of the GRP content in THP-1 MoM treated with FCNG and FCNP, under inflammatory or control conditions. Levels of total GRP were measured in the cell extracts (a) and culture media (b) of THP-1 MoM untreated cells, or pre-treated for 24 h with $(11.7 \pm 4.5) \times 10^9$ particles/mL of FCNG or FCNP, with or without further stimulation with LPS (100 ng/mL) for 24 h. Data are result of one experiment, with triplicates. Two-way Anova and multiple comparisons were achieved with the Dunnett's test. Statistical significance was defined as $p \leq 0.0005$ (***) (224).

Overall, these results are indicative that the anti-inflammatory effect of FCNG previously observed is mediated not only by increased extracellular GRP levels from the exogenously added GRP nanoparticles, but also by the increased intracellular GRP levels, most probably resulting from FCNG uptake by THP1-MoM cells.

2.3.4.3 Effect of GRP content in the formulation of FCNG on the anti-inflammatory response of THP-1 MoM

Additionally, FCNGs were produced with increasing concentrations of GRP, theoretically containing 0.05 % (FCNG), 0.25 % ($FCNG_{0.25}$), and 0.375 % ($FCNG_{0.375}$) (w/w) of GRP respective to the FC content considering that all protein used for nanoparticles production was effectively loaded, with similar dry weight yielding. In contrast to the distributions primarily unimodal observed for FCNP and FCNG formulations, the nanoparticle distribution for FCNG0.25 and FCMG0.375 displayed multiple peaks with different relative intensities, spanning up to 180 nm (**Table 2.3**). The concentration of total particles remained consistent across all preparations, including FCNP and FCNGs, with no statistically significant differences (Table 1). The relative levels of GRP measured in the supernatant, representing the fraction of non-encapsulated GRP, relative to the initial protein used in the synthesis, suggest that most of the ucGRP was incorporated, indicating a high degree of protein encapsulation and therefore a high association efficiency (AE), ranging from 97.8 ±1.81 in $FCNG_{0.25}$ to 99.9 ±0.05 in $FCNG_{0.375}$ (**Table 2.3**). The zeta potential was also assessed, with no significant variations (**Table 2.3**).

Table 2.3 Production yields and physicochemical characteristics of nanoparticles containing different percentage of ucGRP (FCNG, $FCNG_{0.25}$ and $FCNG_{0.375}$): production yield, polydispersion index (PDI), zeta potential, size variation, particles concentration and ucGRP association efficacy (AE). Data are shown as result of at least 6 independent preparations for yield determination, and at least 3 independent preparations for AE. Values are presented as mean ± SD.

Sample	Production Yield (%)	PDI*	Zeta Potential* (mV)	Range Size** (relative amount, %)		Particles Concentration** (particles/mL)	AE*** (%)
				0 – 180 nm	180 – 400 nm		
FCNG	15.1 ± 6.7	0.39 ± 0.06	38.1 ± 7.3	77.9 ± 0.8	21.1 ± 1.1	(14.5 ± 3.4) E+9	99.8 ± 0.1
$FCNG_{0.25}$	17.1 ± 3.8	0.37 ± 0.08	44.7 ± 7.1	85 ± 7.2	14.6 ± 8	(14.6 ± 1.6) E+9	97.8 ± 1.8
$FCNG_{0.375}$	15.6 ± 3.4	0.39 ± 0.07	40.2 ± 2.3	90.6 ± 2.3	9.25 ± 2.1	(12.4 ± 1.06) E+9	99.9 ± 0.05

* Data obtained from DLS analysis; ** Data obtained from NTA analysis; *** Data obtained from Elisa, specific for GRP.

Considering the previous results showing that FCNG remained active on modulating the inflammatory response of THP-1 MoM, by decreasing the levels of TNFα, after 24h of pre-

treatment followed by 24h of LPS exposure (**Figure 2.13)**, similar experimental conditions were followed to evaluate the anti-inflammatory activity of (11.7 ± 4.5) × 10^9 particles/mL of FCNG, $FCNG_{0.25}$ and $FCNG_{0.375}$. Measurements of TNFα in the cell culture media showed a decrease of TNFα accumulation similar for all concentrations of ucGRP in the nanoparticles formulations, 0.05 % (FCNG), 0.25 % ($FCNG_{0.25}$), and 0.375 % ($FCNG_{0.375}$) (w/w). These results indicate that increased levels of GRP available for nanoparticle formulations, with a high protein association efficacy rate, did not promote significant results in terms of anti-inflammatory effect (**Figure 2.13**).

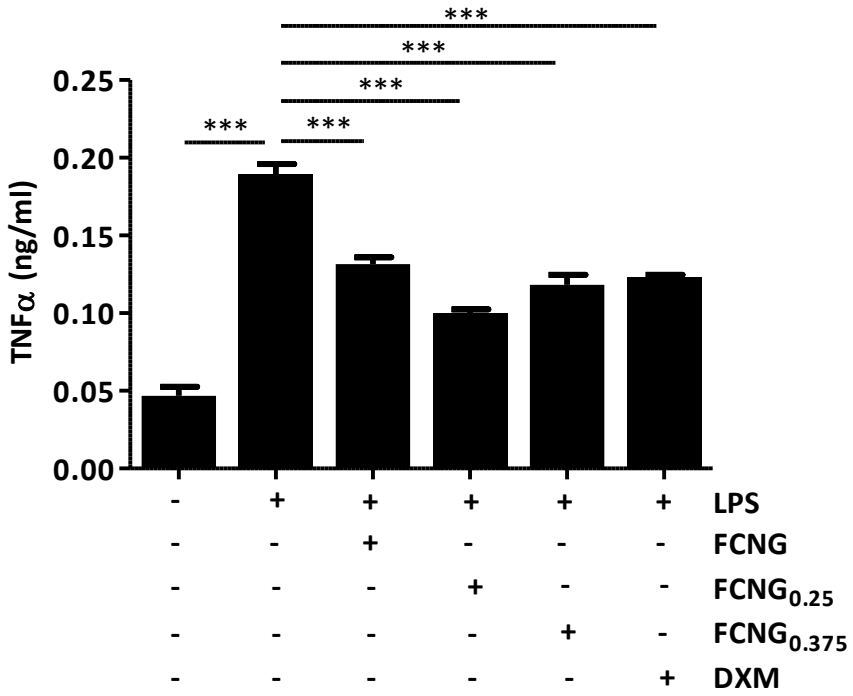

Figure 2.13 Anti-inflammatory effect of different FCNG formulations, in LPS-stimulated macrophages. ELISA for the evaluation of inflammatory marker TNFα levels in the cell culture media of THP-1 MoM, pre-treated for 24 h with (11.7 ± 4.5) × 10^9 particles/mL of FCNG loaded with different ucGRP contents, 0.05 % (FCNG), 0.25 % ($FCNG_{0.25}$), and 0.375 % ($FCNG_{0.375}$) (w/ w), and then stimulated with LPS (100 ng/mL) for further 24h. Data resulted from two independent experiments (n=2), with duplicates. Dexametasone (DXM, 2 μM) was used as a positive anti-inflammatory control. Two-way Anova and multiple comparisons were achieved with the Dunnett's test. Both graphs show mean ± SD. Statistical significance was defined as $p \leq 0.0005$ (***).

2.3.4.4 Evaluation of the anti-inflammatory potential of ucGRP-loaded nanoparticles (FCNG) on the inflammatory response of articular synoviocytes and chondrocytes

The results of anti-inflammatory activity of FCNG obtained in THP-1 MoM cells led us to further test the activity of the GRP nanoformulation on a previously established articular OA cell system, consisting of human chondrocytes and synoviocytes primary cell cultures. Based on previous results, the nanoformulation used in the following *in vitro* cell assays was FCNG, containing the lowest percentage of ucGRP used in the nanoparticle formulation (0.05 %, w/w, of protein in relation with FC content). Human synoviocytes and chondrocytes were pre-treated with FCNP and FCNG, followed by IL-1β stimulation, to simulate an inflammatory OA scenario (227). Cell viability was assessed by the MTS cell proliferation assay, and the results indicate no cell cytotoxicity of FCNP or FCNG in either chondrocytes or synoviocytes (**Figure 2.14**).

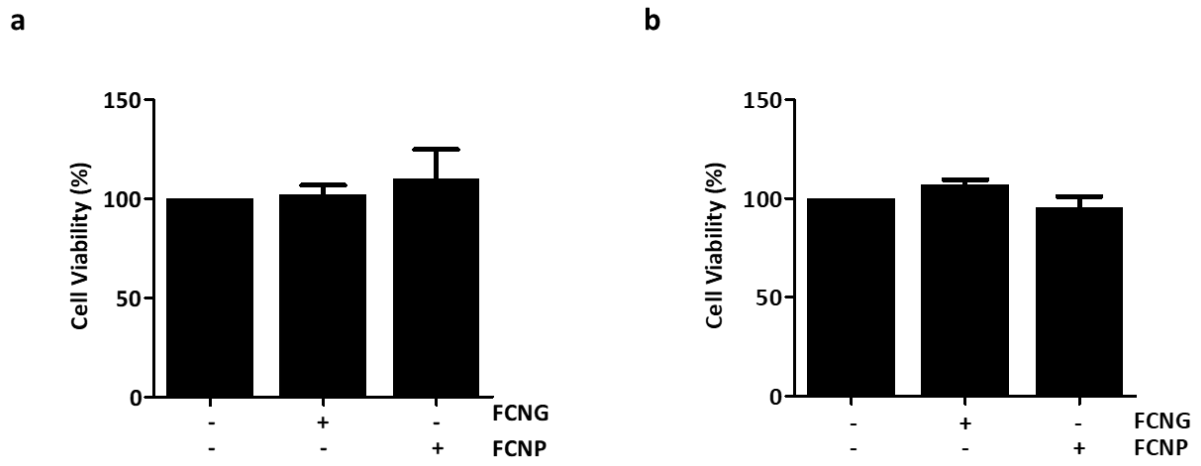

Figure 2.14 Cytotoxic effect of 24 h of exposure of (a) synoviocytes and (b) chondrocytes to FCNG and FCNP [(11.7 ± 4.5) × 10^9 particles/mL]. Data resulted from two independent experiments (n=2), with triplicates (224).

The effect of FCNG and FCNP nanoparticles was assessed by measuring the levels of the inflammatory marker IL-6 released to cell culture media. In chondrocytes, an anti-inflammatory response of the FCNP and FCNG was observed, with a reduction in the accumulation of IL-6, with higher expression in the culture media of cells pre-treated with FCNG (**a, Figure 2.15**). FCNP and FCNG pre-treatment of synoviocytes, did not interfere with the inflammatory response of the IL-1β stimulated cells (**b, Figure 2.15**). These results indicate increased anti-inflammatory functional activity of FCNG in chondrocytes in relation to

synoviocytes, at least in the experimental conditions tested.

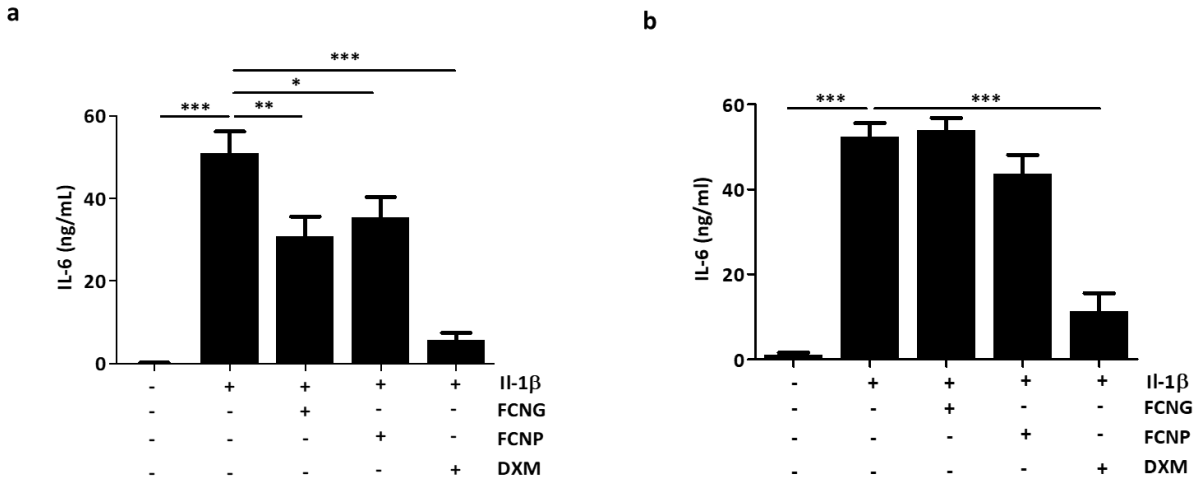

Figure 2.15 Anti-inflammatory effect of FCNP and FCNG nanoparticles, in stimulated synoviocytes and chondrocytes. ELISA of the inflammatory marker IL-6 present in the cell culture media of (a) chondrocytes and (b) synoviocytes pre-treated for 24 h with (11.7 ± 4.5) × 10^9 particles/mL of FCNG or FCNP, or dexametasone (DXM, 2 μM)) and then stimulated with IL-1β (10 ng/mL) for further 24 h. Data resulted from at least three independent experiments (n=3), with triplicates. DXM was used as a positive anti-inflammatory control. Two-way Anova and multiple comparisons were achieved with the Dunnett's test. Graphs show mean ± SD Statistical significance was defined as $p \leq 0.05$ (*), $p \leq 0.005$ (**) and $p \leq 0.0005$ (***) (224).

2.4 Discussion

In this chapter, the capacity of GRP in regulating inflammation, one of the two major and interlinked molecular processes affecting OA progression along with mineralization, was addressed in immune cells, more specifically in LPS activated THP-1 MoM. GRP demonstrated to be able of modulating the inflammatory response of immune cells, independently of its degree of γ-carboxylation. Moreover, the process of ucGRP encapsulation as a drug-delivery strategy, using biocompatible chitosan-based nanoparticles as the drug vehicle, was for the first time investigated. The anti-inflammatory profile of the novel nanoformulation containing ucGRP was evaluated and results indicated that FCNG were capable of manipulate the inflammatory response in activated macrophages, and also in human cultured chondrocytes, demonstrating an effective delivery of the protein and the retention of GRP anti-inflammatory activity. Although the specific mechanism of action of FCNG in different cell-specific inflammatory conditions remains unknown, the overall reduction of pro-inflammatory mediators suggests promising therapeutic potential for FCNG in chronic inflammatory diseases (CIDs).

It is well established that GRP acts as a calcification inhibitor with a dependence on GRP γ-carboxylation (159), and previous studies demonstrated that although both forms of protein, cGRP and ucGRP, had mineral binding capacity, only cGRP was able to reduce mineralization in articular chondrocytes and synoviocytes, under mineral stimuli (173). Additionally, results showed that GRP was also involved in osteoarthritic inflammatory processes, acting as an anti-inflammatory agent in both articular cells, but interestingly, this activity seemed to be independent of GRP γ-carboxylation status, indicating a possible parallel mechanism of action (173). This duality in the mode of action of GRP in the OA context and its relation with GRP carboxylation status previously explored in both chondrocytes and synoviocytes, was here investigated in immune human macrophages, an important cell type involved in OA. Macrophages are described to play a significant role in modulating joint inflammation in OA, by maintaining tissue homeostasis and protecting the host from infection. However, in case of chronic inflammation, macrophages start producing molecules responsible for cartilage degeneration (228). In fact, accumulation of macrophages in the synovial lining layer (240-241), and the implication of macrophages in OA pathogenesis has been demonstrated, as consequence of their contribution to matrix degradation and calcification through secreted inflammatory mediators, growth factors and proteinases (231).

In the present work, GRP was able to interfere with the inflammatory mechanism response as an anti-inflammatory agent in LPS THP-1 stimulated macrophages by reduction of the inflammatory marker TNFα. This result was in line with data aiming to explore the capacity of immune cells for expression and carboxylation of GRP, and its association with inflammatory responses, that revealed the presence of GRP in immune monocytes and macrophages (203), and indicated that GRP behaved as an endogenous anti-inflammatory agent in LPS and hydroxyapatite (HA) stimulated THP-1 MoM (203).

Additionally, GRP γ-carboxylation, demonstrated as essential for its anti-mineralization effect, was not required for the observed GRP anti-inflammatory activity in THP-1 MoM, in agreement with parallel results for chondrocytes and synoviocytes (173). Both treatments with ucGRP and cGRP resulted in a decrease of the inflammatory response. Nevertheless, it was noticed a less extended effect and independent of the concentrations for the cGRP treatment (203). These results reinforce that the mechanism of action of GRP acting as anti-calcifying or anti-inflammatory agent, seem to be independent. It is important to strengthen that independently of targeting distinct disease pathways, GRP will continuously have an impact in the relation inflammation-calcification. Indeed, by avoiding calcification, cGRP contributes to avoid chondrocyte differentiation towards a mineralizing and hypertrophyc phenotype (76),

circumventing ECM disruption and consequently reducing the probability of inflammatory events. In a similar way, by avoiding inflammatory pathways, ucGRP will contribute to cartilage homeostasis, preventing ectopic calcification potentiation.

Despite the potential therapeutic profile of GRP in OA, GRP was shown to have limited solubility at neutral pH (157) with possible implications in terms of bioavailability, limiting its use in therapeutics. The possibility of protein encapsulation as a strategy to overcome the GRP solubility issue was therefore explored in this study. Considering the former results, showing that γ-carboxylation is not required for GRP anti-inflammatory activity, biosynthetic ucGRP was chosen to be encapsulated. The integration of bioactive compounds into chitosan-based nanoparticles is a therapeutic strategy already explored and in use, as chitosan is a biocompatible, nontoxic, with high bioavailability and chemical resistant polymer (211-213,243). Low molecular weight chitosan was selected to prepare ucGRP containing chitosan-based nanoparticles, as the nanoscaled size of chitosan particles have significant correlation with its molecular weight (217).

Fluorescent labelling of nanoparticles is an important approach that allows the monitoring of populations distribution and accumulation, and an intra and extra cellular particle tracking, representing a very useful biomedical and pharmacological tool (235). The synthetic approach implemented, via ionic gelation methodology (217), was based in positively charge chitosan and ucGRP by acidification of the respective solutions, reacting with anionic TPP. Anionic TPP is one of the most used cross-linker in the preparation of chitosan nanoparticles because it is a small and non-toxic cross-linking agent, able of establishing strong binding with positive amine groups of chitosan (220,225,245). The ratio TPP/CS was the recommended for the formation of nanometer-sized particle suspensions (237), avoiding aggregation and consequent precipitation through chitosan chain crosslinking in the presence of higher concentrations of the anionic TPP. Indeed, PDI values for both FCNP and FCNG formulations were within an acceptable range for biomedical or pharmaceutical applications (up to 0.5). The nanoparticles generated in this study revealed their nanoscale dimensions, ranging from 120 to 150 nm, which aligns with the majority of previous reports on CS-based nanoparticles produced using similar methods, with sizes ranging from 40 to 250 nm (246-248). In this study, fluorescein-labeled CS was used to produce FCNP and FCNG formulations, which may exhibit different sizes compared to unlabeled CS-based nanoparticles. However, it has been demonstrated that similar fluorescein labeling does not interfere with the properties of CS nanoparticles (244,249).

ucGRP was successfully encapsulated in FC-based nanoparticles with an association

efficiency of approximately 99 % for all ucGRP/FC contents, in concordance with previous reports showing the higher loading efficiency of this incorporation method (246,248), and justified in part by the low % of ucGRP to be uploaded relatively to the FC content. These results are indicative of a non-saturation point of protein loading, meaning that higher content of GRP may be uploaded into this nanoformulation, if needed. Moreover, FCNG's broader particle distribution indicates a range of particles slightly differing in size, which might reflect different quantities of ucGRP molecules encapsulated. Although a considerable increase of the amount of protein for nanoparticle incorporation was made available, it did not lead to significant changes in the production yields, apparently not contributing to a more efficient ionic gelation protocol, although a more complete study is needed to afford further conclusions. Despite the high association efficiency of ucGRP, the mean size of FCNG nanoparticles was found to be comparable to that of FCNP, which was anticipated due to the small molecular weight of the protein. The slight size increase of FCNG relatively to unloaded FCNP, might reflect the fact that positively charged GRP could compete with the ionic interactions between the FC NH_3^+ groups and the TPP phosphate moieties, allowing less FC/TPP strong bonding and therefore slightly larger particles. The cationic surface charge of loaded FCNG was not significantly different from the FCNP surface charge, though a slight decrease tendency is observed, but still in the acceptable range for stable colloidal dispersions (241).

TEM images revealed that nanoparticles, FCNP and FCNG, are apparently spherical and with similar morphology. The populations observed were heterogeneous in terms of size, in agreement with data available of similar chitosan-based nanoparticles, and explained by different factors known to influence nanoparticles size, such as chitosan concentrations and molecular weight, the degree of CS acetylation, and the CS/TPP molar ratio, as mentioned before (246,251). Flow cytometry confirmed the effective presence of ucGRP in the FCNG formulation, and FCNP and FCNG cellular uptake, by THP-1 MoM. While our current data doesn't provide specific differentiation between intracellular and surface-located FCNG, CS and FCNPs are recognized for their effective internalization by cells. This process is primarily facilitated by nonspecific electrostatic forces that increase the paracellular permeability, opening tight junctions. Additionally, it involves adsorptive endocytosis, partly mediated by clathrin-mediated mechanisms, and in the case of macrophages, phagocytosis (213,246,248,249,252). The use of complementary techniques, such as fluorescence microscopy could improve the analysis of protein-particle interactions. By incorporating immunofluorescence targeting GRP, it becomes possible to visualize the protein and determine its relative localization in relation to the nanoparticle.

ucGRP releasing studies from FCNG revealed that approximately 15 % of ucGRP was released from the nanoparticles at the nanoparticles pellet resuspension time, probably correspondent to the desorption of GRP from nanoparticle surface. That release rate was kept almost constant throughout 48h, reflecting a sustained protein release. The hydrogel structure of FC nanoparticles is dynamic and dependent on pH, and at a close to neutral pH (pH of cell culture media used for releasing and biological studies), it is expected that the chitosan hydrogel matrix remained stable, preventing a burst release of ucGRP and allowing a slow delivery of the drug, as it is desired for functional purposes. This observation provides some insight into the extended anti-inflammatory effect of FCNG. In fact, GRP nanoformulations demonstrated maximum anti-inflammatory response during the peak of cell stimulation, that remained effective for a continuous 24-hour period. This observation could be attributed to the higher concentration of GRP present, as elevated levels of GRP were detected in both THP-1 MoM cells and their culture media, irrespective of LPS stimulation. Interestingly, the cells treated with FCNG demonstrated a more significant increase in GRP levels compared to the basal (endogenous GRP) and also to the LPS-stimulated conditions (203), both intracellularly and extracellularly. This suggests effective internalization of GRP and preservation of its anti-inflammatory activity, either through FCNG cell incorporation and subsequent GRP release or through extracellular protein release from the nanoformulation. Additionally, the elevated GRP levels may also be attributed to a self-upregulation effect of GRP, wherein the endogenous GRP is increased. However, further studies are required to confirm this possibility.

IL-6 and TNF-α are the main cytokines associated with inflammation, and correlated to the progression of knee cartilage loss and with OA severity (253-255). Higher levels of IL-6 were found in the synovial fluid of patients with symptomatic cartilage lesions and of OA donors, when compared to healthy individuals. Osteoarthritic chondrocytes produce higher concentrations of IL-6 during regeneration (254-255), and the activity of IL-6 was directly related with cytokines and growth factors present during OA, such as IL-1β, TGF-β, and prostaglandins (247). Importantly, up-regulation of IL-6 showed the detrimental potential of calcification in OA, and increased levels of IL-6 and BCP were associated with cartilage degradation through the induction of matrix-degrading enzymes activity in chondrocytes (247), feeding the vicious cycle of inflammation-calcification and leading to the disease progression. IL-1β stimulation of primary articular chondrocytes and synoviocytes has been used previously to mimic OA (173). It is expected that IL-1β treatment could reflect part of the inflammatory process, particularly with impact on IL-6 accumulation. IL-1β concentrations have been used in *in vitro* studies in concentrations ranging from 5 to 100 ng/mL, though with a similar

inflammatory outcome (227), and in this study 10 ng/mL were used.

Our findings demonstrate the anti-inflammatory properties of FC based nanoparticles across the stimulated *in vitro* cell systems of THP-1 MoM and chondrocytes, strengthening the beneficial utilization of the CS excipient, as it not only meets the necessary requirements for GRP delivery but also provides an additional therapeutic effect. This is not surprising, as chitosan has been shown to reduce the production of inflammatory and catabolic mediators by OA chondrocytes and tended to stimulate the synthesis of cartilage matrix components. In fact, its N-acetyl-glucosamine and glucosamine monomers, natural components of cartilage, have been proven to be chondroprotective (220,226,257) representing an advantage to the OA drug delivery system, as a potential synergetic drug-partner. In this study, FCNG exhibited their functionality through their immunomodulatory activity, by effectively reducing pro-inflammatory cytokines and inflammation mediators in *in vitro* THP1-MoM and chondrocyte cell systems. This was evidenced by the decreased of TNFα and IL-6 levels after cell stimulation, that clearly indicate the preserved anti-inflammatory activity of GRP (ucGRP) already reported (178,209), in the FCNG formulation.

Overall, in this chapter we investigated encapsulated ucGRP as a possible therapeutic agent in OA, with the possibility of improving the protein bioavailability and activity stability, by the development of chitosan-based nanoparticles. Cell treatment with FCNG resulted in the decrease of the inflammatory responses of stimulated THP1-MoM and chondrocyte cell systems, with indication of GRP activity preservation through an effective protein delivery system, probably through a particle cell internalization process. It was shown that successfully encapsulated uncarboxylated GRP contributed to control the levels of inflammatory mediators, such as TNFα in activated THP-1 MoM and IL-6 in stimulated chondrocytes. Although the mechanism of action of FCNG has not been explored, it can be anticipated that the established anti-inflammatory effect of GRP released from the formulation, eventually potentiated by chitosan itself, might represent a feasible strategy to attenuate cartilage damage through dropping inflammation and like that protecting against early OA.

2.5 Acknowledgements

We acknowledge Dr. Joana Magalhães and Dr. Francisco Blanco, from Unidad de Medicina Regenerativa, Grupo de Investigación en Reumatología (GIR), Instituto de Investigación Biomédica de A Coruña (INIBIC), Complejo Hospitalario Universitario de A Coruña

(CHUAC), and Centro de Investigación Biomédica en Red (CIBER), Madrid for the primary cell cultures of synoviocytes and chondrocytes, that were used in part of this work.

We kindly acknowledge Prof. Ana Grenha and her research group, from Centro de Ciências do Mar (CCMAR), Universidade do Algarve, in particular to PhD Jorge Pontes, for the excellent support in the nanoencapsulation procedures and for all the knowhow shared in this field.

We express our gratitude to Dr. Maria dos Anjos Macedo and to Prof. António A. de Matos, from Universidade Nova de Lisboa (Departamento de Química, Lisboa, Portugal) and Centro de Investigação Interdisciplinar Egas Moniz, Egas Moniz-Cooperativa de Ensino Superior, responsible for the TEM studies and respective analysis.

We are grateful to Dr. Ana S. Moreira and Dr. Tiago Q. Faria, from iBET-Instituto de Biologia Experimental e Tecnológica, and ITQB-Instituto de Tecnologia Química e Biológica António Xavier, Universidade Nova de Lisboa, for the NTA studies.

Acknowledges to Dr. Maurícia Vinhas for all the support in the execution of the Flow Cytometry assays and their interpretation and lay-out, from Algarve Biomedical Center Research Institute (ABC-RI), Universidade do Algarve.

Part of the work presented in this chapter represents our published results in Viegas *et al*. (224).

Chapter 3

Development of a screening biological pipeline model for the study of osteoarthritis

© Nuna Araújo

Abstract

In this chapter, we developed a novel osteoarthritis (OA) preclinical drug development pipeline designed to evaluate the anti-inflammatory and anti-mineralizing activities of potential OA preventive or modifying compounds, and to achieve a deeper knowledge in the interplay between inflammation and mineralization processes in OA. After an initial screening using THP-1 macrophages, the testing workflow was based on *in vitro* synoviocytes and chondrocyte primary cell cultures, followed by human cartilage explants assays and a new 3D co-culture model, combining human cartilage with synoviocytes, representing a close to *in vivo* OA scenario, under inflammatory interleukin-1β (IL-1β) or mineral hydroxyapatite (HAP) stimulation. A combination of gene expression analysis, measurement of cytokine/chemokine production levels, and histopathological characterization of cartilage tissues, showed that the proposed OA models respond to both stimuli. Overall, the 3D OA model mimicking early OA disease stages, allow new insights into the disease mechanisms, and promote the evaluation of potential novel agents as modulators of OA progression and their potential use in therapeutic or prophylaxis.

3.1 Introduction

The inexistence of OA effective treatments and the failure of many potentially efficacious drugs when reaching clinical trials are the main contributors to the critical health situation of OA. The process of drug development is time consuming and costly, with most drugs failing in clinical trials, mainly due to preclinical assays limitations that may compromise information about safety and efficacy (249). So, it is imperative to simultaneously invest more efforts in preclinical models, creating new approaches to improve and accelerate drug development pipeline, and search for new drug targets to fight this multifactorial disease affecting the whole joint (250).

It is well accepted that to date, no single ideal experimental OA model exists, and preclinical animal models, differing from the human context rarely translate to the clinic scenario (117). New approaches may include the development of preclinical set-ups integrating simple, rapid and effective screening assays using the advantages of 2D cell culture systems to select the most promising drug candidates, which would be further tested in more complex disease models, closer resembling the pathologic context of OA.

A major constrain in the discovery of new disease-modifying osteoarthritis drugs (DMOADs) with important clinical benefit, as well as in the search for new drug targets, has been the lack of reliable models able to simulate the physiologic OA scenario. Monolayer cell culture approaches have been widely used to study specific molecular aspects of OA pathophysiology, and although they present several advantages such as an easy manipulation and controlled investigational conditions, these are limited by the lack of a physiologic context (97,238,260). The limited interactions with biological surroundings and the requirement of being cultured and growing in a planar flat plate, alter the cell morphology and leads to cell polarization, with impact in several signaling pathways (227). Additionally, chondrocytes and synoviocytes have been considered as the OA cell model, subestimating the contribution of the other cell types involved in the articular joint (252). It is therefore understandable that to create a more complete and reliable model for the study of OA, the diversity of articular joint tissues should be considered and investigated as a whole entity. In that sense, 2D co-cultures using transwell plate models represent an improvement over monolayer systems, as it allows the study of cell exchanges, through the investigation of secretory mediators present in the cell culture media. Nonetheless, some limitations are unavoidable such as the inability to explore direct cell-cell connections or the essential cell-ECM interaction. A wide range of three-dimensional human tissue systems, taking into consideration cell–cell and cell–extracellular matrix interactions have been developed to overcome some of the limitations of conventional 2D cell culture systems. Explant-based models derived directly from *in vivo* tissue maintain cells in their 3D context, allowing the investigation of a variety of factors through multiple treatments, representing an upgrade over 2D models. Even though, human tissue sources are limited and are still not demonstrative of the OA heterogeneity (97,261). *In vivo* models were used and optimised to mimic idiopathic primary OA and secondary OA, and are required to assess drug efficacy before entering clinical trials and the drug approval process. Preclinical animal models represent a more complete and a biologically more complex system, but are not totally representative of the human physiopathology, frequently leading to the failure of therapeutic responses in a later stage of the drug validation process (238,262).

In vitro OA models usually include the use of IL-1β or TNF-α to induce an OA inflammatory phenotype (239,263). After stimulation, the biological potential of the drug under screening is evaluated by the ability of attenuating the increased catabolic factors [IL-1β, TNF-α, NO, PGE2, Cyclooxygenase 2 (COX-2), MMP3, MMP13, ADAMTS-4 and ADAMTS-5] or promoting anabolic mediators (Insulin-like growth factor 1 (IGF-I), TGF-β, BMPs, Cartilage-derived morphogenetic proteins (CDMPs), and IL-4], thus its ability of

preventing inflammation and preserving the articular cartilage integrity (259,264).

In OA, inflammation plays an important role by interplaying with calcification in a cycle of extracellular matrix (ECM) degradation, apoptosis and mineral deposition, contributing to local tissue damage and failed tissue repair, resulting in cartilage loss and progressive joint deterioration (84,265). The interplay between calcification and inflammation is a well-established promotor of OA progression, and the crosstalk between the two events should be further explored in preclinical studies. In this chapter the development of a preclinical pipeline for drug activity assessment is described This pipeline allows the evaluation of the anti-mineralizing and anti-inflammatory activity of new drugs in OA, contributing to better understand this interplay in the disease's physiopathology. The testing workflow culminates with a 3D OA co-culture system includes cartilage *ex vivo* explants and synoviocytes to allow new insights into the mechanism of the disease and provide a closer-to-*in vivo* OA scenario useful for preclinical evaluation of novel therapeutic agents.

3.2 Experimental procedures

3.2.1 Biological material and sample processing

Primary human chondrocytes and synoviocytes were commercially acquired (chondrocytes, Lonza, Visp, Switzerland; synoviocytes, ECACC, Sigma-Aldrich, St. Louis, MO, USA) and obtained from human tissue explants using well-defined methodology (229, 266). THP-1 cell line was kindly given by Dr. Nuno Santos (CBME, University of Algarve, Faro) and all cell types were cultured following the same guidelines as indicated in Experimental Section of Chapter 2.

3.2.2 Inflammatory assays in monolayer cells

THP-1 macrophage cells (THP-1 MoM) (1×10^6 cells/mL) were cultured in 500 µL of complete RPMI, using 24-well plates, and treated with 100 ng/mL of lipopolysaccharides (LPS, 100 ng/mL) for 24 h, 48 h and 96 h, or synthetic hydroxyapatite nanocrystals (HAP) (Sigma) (250 µg/mL, 500 µg/mL or 750 µg/mL) for 72 h, respectively. Confluent chondrocytes and synoviocytes were cultured in 1 mL of Advanced DMEM, using 12-well plates, and further treated with 10 ng/mL of interleukin-1β (IL-1β) for 3 h and 6 h, or with 750 µg/mL HAP for

6h. As controls, cells were cultured with respective media without any treatment. At determined time points, cell culture media were collected for ELISA analysis and cells harvested for RNA extraction.

3.2.3 Cell proliferation

THP-1 MoM seeded in 96-well plates at 2×10^5 cells/well, and confluent chondrocytes and synoviocytes, were cultured in their respective growth media and supplemented with different concentrations of HAP. Cell viability was determined at appropriate time points using the CellTiter 96 cell proliferation assay (Promega, Madison, WI, USA), following manufacturer's instructions.

3.2.4 Cartilage collection and tissue explants preparation

Knee articular cartilage was obtained from osteoarticular cuts performed on the femoral and tibial sides, from eight patients (4 male and 4 females, aged 71,5 ± 5,9 years) who had undergone arthroplasty surgeries at Hospital Particular do Algarve (Faro, Portugal). This study was approved by the ethics committee of the hospital, and written informed consent was obtained from all the participants. All principles of the Declaration of Helsinki of 1975, as revised in 2000, were followed. Macroscopically normal full-depth cartilage slices were removed in sterile conditions using a scalpel, collected in complete Advanced DMEM media, and incubated for 24 h, at 37 ºC, in a humidified atmosphere containing 5 % CO_2, for tissue equilibration before preparation of tissue explants. After equilibration, 2 mm diameter and 1,71 ± 0,70 mm thickness cartilage explants, were obtained using a 2 mm biopsy punch (Integra-Miltex). Samples of the initial cartilage explant tissues were fixed in 4 % PFA for histological evaluation.

3.2.5 Cartilage explant assays

Cartilage explants (8-10 per well) were plated in a 12 well plate and cultured at 37 °C, in a humidified atmosphere containing 5 % CO_2, in 1 mL of complete Advanced DMEM media and underwent distinct treatments. Explant mineralization treatments were performed with HAP (750 μg/mL) for 72 h. Inflammatory explant assay treatments were performed with either IL-1β (10 ng/mL) or THP-1 MoM conditioned media (MCM), during 24 h, 48 h or 72 h. MCM

was obtained by stimulating THP-1 MoM with LPS (100 ng/mL) for 24 h, 48 h and 96 h. Based on the concentration of TNFα in the THP-1 MoM conditioned media, MCM after 96 h of culture was selected for further use in the explant inflammatory assays. As controls, cartilage explants were cultured without treatment. At the end of each experiment, cartilage explants were collected, washed twice with PBS, immediately processed for RNA extraction as described below, and the cell culture media collected for ELISA analysis.

3.2.6 Co-culture assays

Cartilage explants (10 per well) were plated in a 12 well plate and co-cultured with synoviocytes in a transwell system (6.5 mm insert diameter, 3.0 μm polyester membrane, Corning Incorporated Life Sciences), in 1.8 mL of complete Advanced DMEM, at 37 °C, in a humidified atmosphere containing 5 % CO_2. Co-cultures were supplemented with IL-1β (10 ng/mL) during 24 h, or HAP (750 μg/mL) during 72 h. Cartilage explants were collected as described above for RNA extraction, and cell media collected for ELISA analysis. As controls, explants and synoviocytes were cultured without treatment. At the end of each experiment, cartilage explants were collected, washed twice with PBS, immediately processed for RNA extraction as described below, and the cell culture media collected for ELISA analysis.

For the mineralization assays, co-cultures were supplemented with $CaCl_2$ to a final calcium concentration of 5.4 mM for 2 weeks, with media changed every 3 days. Cartilage explants were washed twice with PBS, and either collected in 4 % PFA for histological analysis or lyophilized and weighted for calcium quantification. Dried tissues were completely digested with nitric acid (65 %), and calcium content was measured by O-cresolphthalein complexone chemistry using a colorimetric assay (Calcium assay CA-590, Randox, Co. Antrim, UK) according to manufacturer's recommendations, and normalized to cartilage explants dry weight.

3.2.7 RNA extraction, cDNA amplification and quantitative real-time PCR (qPCR)

Cartilage tissue was immediately snap-frozen and manually grounded to powder in liquid nitrogen. Cells and tissue lysis was performed in a proportion of 1 mL of 4 M guanidine thiocyanate solution per 10^7 cells or 100 mg cartilage tissue, thoroughly mixed and passed 10

times through a 22G needle. Total RNA was further extracted as described by Chomczynski and Sacchi (257). Briefly, homogenates were sequentially mixed with 2 M sodium citrate pH 4, phenol pH 4.2 and chloroform/isoamyl alcohol. After centrifugation, total RNA present in the aqueous phase was precipitated with isopropanol, redissolved in 4 M guanidine thiocyanate solution, reprecipitated in isopropanol, washed with 75 % ethanol and resuspended in water (Sigma). RNA concentration was determined by spectrophotometry at 260 nm (Nanodrop 1000, Thermo Scientific). RNA was then treated with RQ1 RNase-free DNase (Promega, Madison, WI, USA) and reverse-transcribed using the qScipt cDNA SuperMix (Quanta bio) according to manufacturer's recommendations.

Quantitative real-time PCR reactions were performed using the CFX connect, Real time System (Bio-Rad, Richmond, CA, USA), SoFast Eva Green Supermix (Bio-Rad), 300 nM of forward and reverse gene-specific primers for genes of interest (**Table 3.1**), and a 1:5 cDNA dilution. The following PCR conditions were used: initial denaturation/enzyme activation step at 95 °C for 13 min, 50 cycles of amplification (one cycle is 15 s at 95 °C and 30 s at 68 °C). Fluorescence was measured at the end of each extension cycle in the FAM-490 channel. Levels of gene expression were calculated using the comparative ΔΔCt method and normalized using gene expression levels of glyceraldehyde-3-phosphate dehydrogenase (GAPDH), with the iQ5 software (BioRad).

Table 3.1 Gene-specific primers used for gene expression analysis by qPCR.

Gene	Primer Designation	Sequence (5´ to 3')
GAPDH	GAPDH_F	AAGGTGAAGGTCGGAGTCAACGGA
	GAPDH_R	TCGCTCCTGGAAGATGGTGATGGG
COX-2	COX-2_F	TGGTCTGGTGCCTGGTCTGATGATGT
	COX-2_R	GCCTGCTTGTCTGGAACAACTGCTCA
NF-kB	NF-kB_F	GCAATCATCCACCTTCATTCTCAACTT
	NF-kB_R	CCTCCACCACATCTTCCTGCTTAG
Col10	Col10_F	AGCTGCCAAGGCACCATCTCCA
	Col10_R	AGTGGGCCTTTTATGCCTGTGGGC
MMP3	MMP3_F	CGTGGCAGTTTGCTCAGCCTATCC
	MMP3_R	GCACTTCGGGATGCCAGGAAAGGT
Runx2	Runx2_F	TCCGCAGGTCACTACCAGCCACC
	Runx2_R	GGTGTCACTGTGCTGAAGAGGCTGT
IL-6	IL-6_F	AAGCAGCAAAGAGGCACTGGCAGAA
	IL-6_R	CTGCACAGCTCTGGCTTGTTCCTCAC

3.2.8 ELISA analysis

At the appropriated times, the cell culture media were collected and treated as described in section 2.2.10.1, and supernatants used for the quantification of TNFα (Peprotech), IL-6 (Peprotech) and MMP3 (Life Technologies), using commercially available ELISA kits and following the manufacture's protocols.

3.2.9 Histological evaluation

Paraffin-embedded cartilage tissue sections were processed at the Histopathology Department of Centro Hospitalar e Universitário do Algarve (CHUA, Faro) and used for histological assessment. Cartilage grading of initial tissue samples was conducted based on modified criteria originally established by Mankin *et al* (258), and the specimens were analyzed for tissue abnormalities in terms of structure, cellularity and extracellular matrix staining, using hematoxylin-eosin (HE, Bio-Optica, Italy), safranin-O (SO)/Fast Green (Sigma-Aldrich,

Germany) and toluidine blue (Merck, Germany) staining (268-269) . Four tissue sections from each sample were analyzed. Further histological evaluation of experimental cartilage sections was based on HE and alcian blue staining, following the manufacturer's specifications (Atom Scientific). Mineral deposition was identified by von Kossa staining as described (261).

3.2.10 Statistical analysis

Each independent experiment (n) was performed with different primary cell culture batches and cartilage from distinct patients. Replicates within an individual experiment were performed using the same batch of cells and cartilage from a single patient. Data are presented as mean ± standard deviation (SD). Multiple t tests were used for comparison between two groups. For more than two groups significance was determined using one-way analysis of variance (ANOVA) with comparison between groups by Dunnett test. Statistical significance was defined as $p \leq 0.05$ (*), $p \leq 0.005$ (**) and $p \leq 0.0005$ (***).

3.3 Results

3.3.1 Establishing an *in vitro* OA cell system consisting of macrophages, chondrocytes and synoviocytes

With the aim to create a novel OA preclinical drug development pipeline designed to mimic the pathological mineralization and inflammation features associated with OA, and evaluate the anti-mineralizing and anti-inflammatory activity of potential novel drugs, monolayer cultures were implemented as a first screening for drug activity. Cell cultures are known to be easily manipulated, allowing preliminary investigation of the critical pathological mechanisms, as well as the evaluation of the drug effect on the cell phenotype. An *in vitro* cell system involving the more relevant cells involved in OA, macrophages and the two main articular joint cell types, was developed. Inflammatory IL-1β stimuli know to trigger inflammation in OA, and the mineralizing agent HAP associated with OA pathogenesis, were applied to the cell systems, following previously optimized conditions (173).

THP-1 MoM were included in this pipeline as a first screening test for anti-inflammatory compounds. Cells were treated with a range of HAP concentrations, from 250 µg/mL to 750 µg/mL, to evaluate its capacity of inducing inflammatory responses, using

bacterial endotoxins LPS as a positive control. This dose-dependence study was performed also to explore the suitable HAP concentration to afford an acceptable inflammatory response that could be further used in the biological assays. The levels of TNFα produced when using 750 µg/mL HAP, were similar and close to the levels obtained after LPS induction, indicating that HAP stimuli promoted the expected inflammatory response. Also, treatment with 750 µg/mL HAP showed the higher accumulation of TNFα and was selected for further use in all assays (**a, Figure 3.1**). HAP showed no toxicity in the concentrations tested (**b, Figure 3.1**).

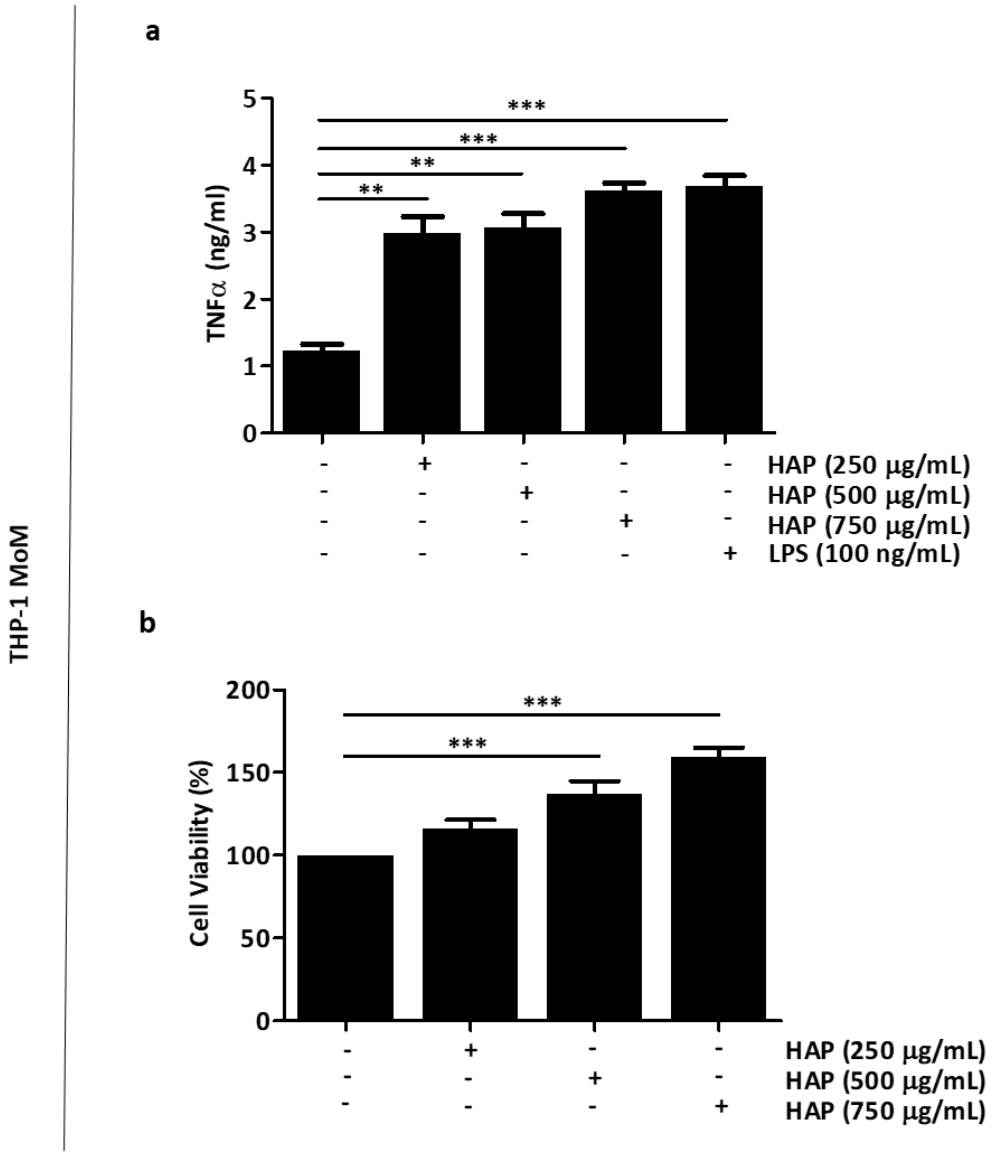

Figure 3.1 Inflammatory response of THP-1 MoM stimulated with different doses of HAP and cell viability of THP-1 exposed to different HAP concentrations. (a) Levels of TNFα in cell culture media of THP-1 MoM treated with different concentrations of HAP for 72 h. Data are presented as means of two independent experiments (b) Viability of THP-1 macrophage cells, exposed to different concentrations of HAP for 72 h. All graphs show mean ±SD. One-way Anova and multiple comparisons were achieved with the Dunnett's test. Statistical significance

was defined as $p \leq 0.005$ (**) and $p \leq 0.0005$ (***).

The inflammatory response was further evaluated in activated articular primary cells. Gene expression profiling of inflammation and known OA-related markers, namely COX-2 and NF-kB were assessed, and overexpression of both genes was observed under IL-1β stimulation, with its peak occurring at 6 h for chondrocytes (**a-b, Figure 3.2**) and at 3 h of stimulation for synoviocytes (**d-e, Figure 3.2**). Accumulation of IL-6 in chondrocytes and synoviocytes was observed under IL-1β activation relatively to untreated cells (**c-f, Figure 3.2**).

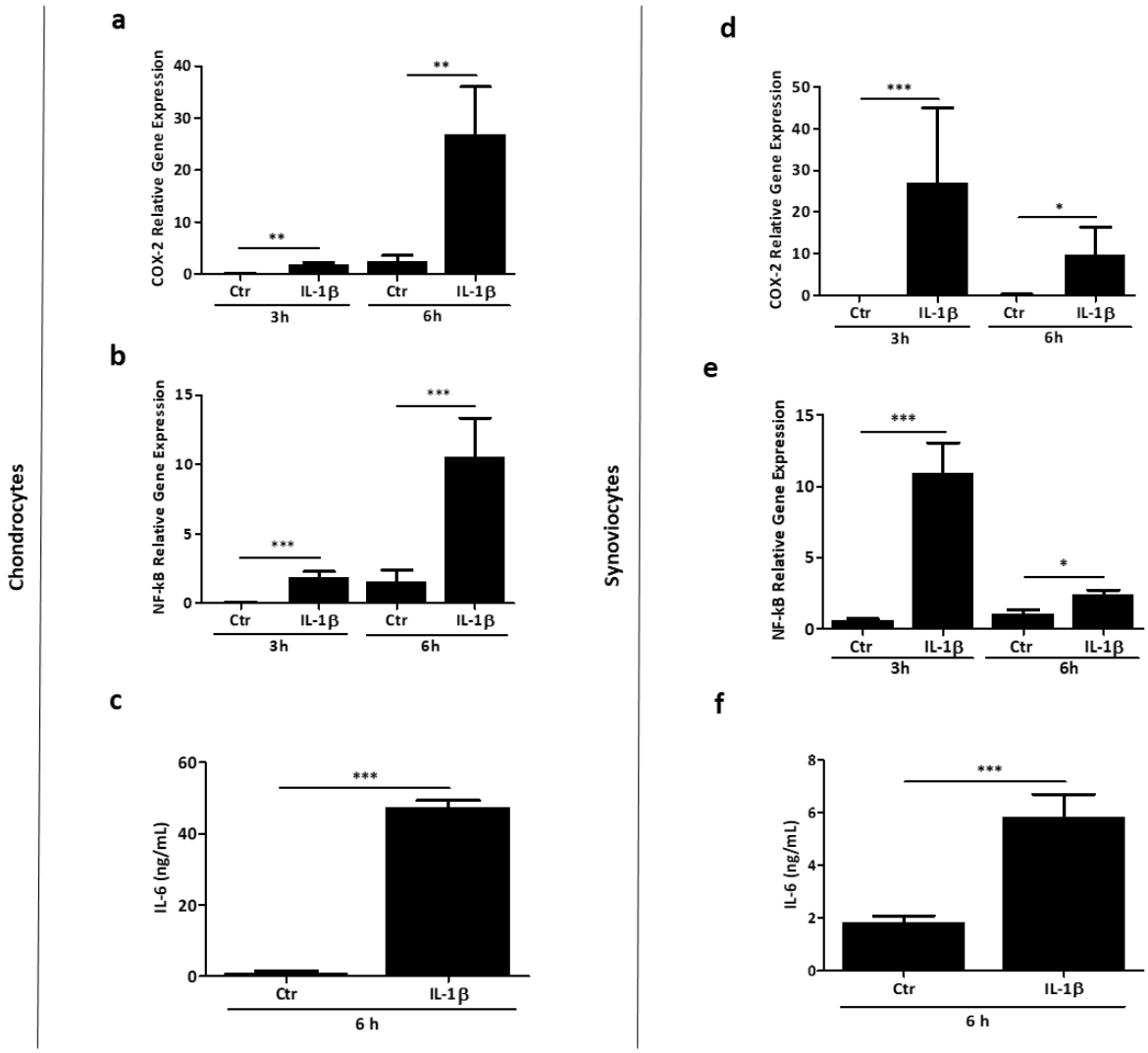

Figure 3.2 Levels and relative gene expression of inflammatory markers in articular primary cells stimulated with IL-1β. Relative gene expression of COX-2 and NF-kB were determined by qPCR, at 3h and 6h post IL-1β stimulation in (a, b) chondrocytes and (d, e) synoviocytes. (c, f) Levels of IL-6 in cell culture media at 6h post IL-1β stimulation in (c) chondrocytes and (f) synoviocytes. Data are presented as means of three independent experiments. All graphs show mean ±SD. Multiple t tests were used for comparison between two groups and One-way Anova and multiple comparisons were achieved with the Dunnett's test. Statistical significance

was defined as $p \leq 0.05$ (*), $p \leq 0.005$ (**) and $p \leq 0.0005$ (***).

HAP stimulation of chondrocytes and synociocytes for 6 h, resulted in an increase in COX-2 expression in both cell types (**a, c, Figure 3.3**). Cell proliferation assays were performed to confirm that HAP did not affect chondrocytes or synociocytes viability, and no cytotoxicity was found in the conditions tested (**b, d, Figure 3.3**).

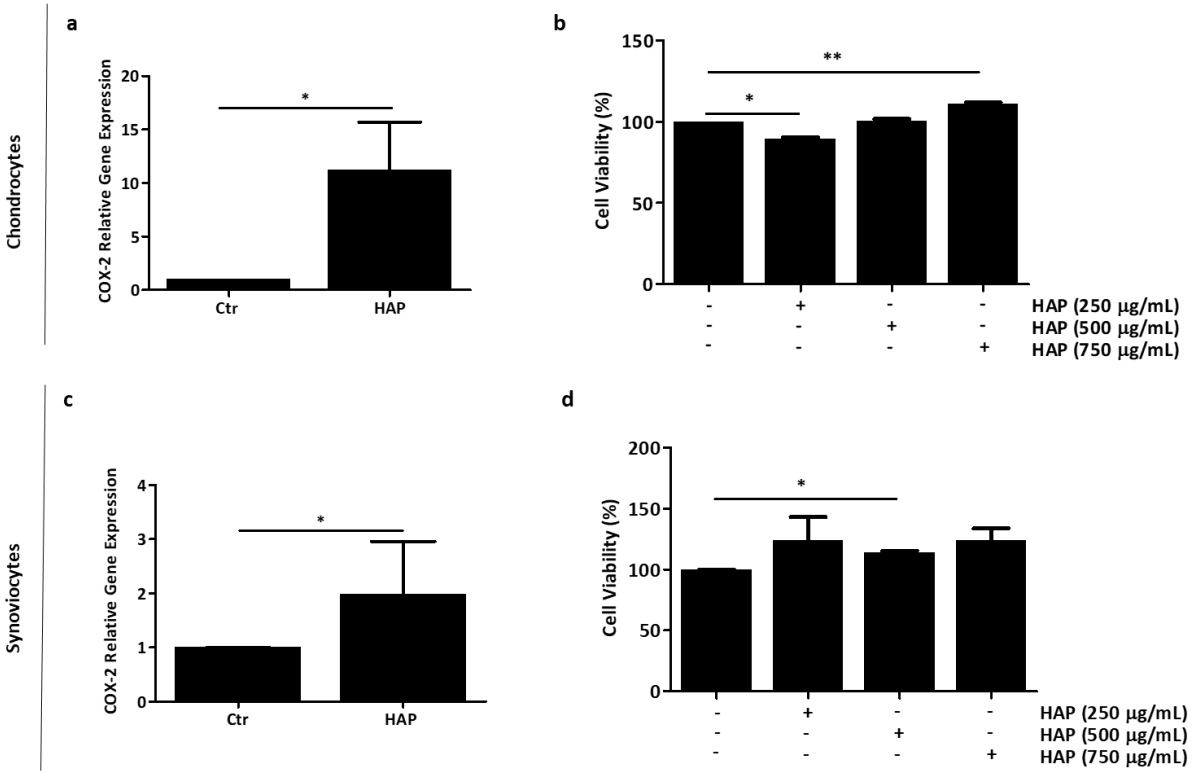

Figure 3.3 Inflammatory responses of articular primary cells stimulated with HAP. Relative gene expression of COX-2 was determined, at 6h post HAP (750 µg/mL) stimulation in (a) chondrocytes and (c) synoviocytes. Viability of (b) chondrocytes and (d) synoviocytes, exposed to different concentrations of HAP. Data are presented as means of two independent experiments, with triplicates. All graphs show mean ±SD. Multiple t tests were used for comparison between two groups and One-way Anova and multiple comparisons were achieved with the Dunnett's test. Statistical significance was defined as $p \leq 0.05$ (*) and $p \leq 0.005$ (**).

Overall, the primary articular cell systems shown to be responsive to the inflammatory and mineralizing stimuli, with inflammatory feedback translated into an increase of expression and accumulation of specific pathologic OA markers.

3.3.2 Setting up an *ex vivo* human cartilage based assay

Since cartilage is the main affected tissue in OA, and chondrocytes the unique cell type constitutive of cartilage, cartilage tissue explants were selected as an experimental OA model to evaluate the *ex vivo* response in the bioactivity testing pipeline. Human cartilage explants used in all experimental conditions were classified as normal- to early-OA tissues through the modified Mankin score (258). Histological analysis revealed a smooth surface, a normal and uniform structural organization, and a normal to slight reduction in matrix staining, with Mankin total score ranging from 1 to 4 in the 1/13 modified Mankin scale (**Table 3.2**).

Table 3.2 Modified Mankin score used for histological evaluation of human cartilage explants, using hematoxylin-eosin (HE), Safradin-O (SO) and Fast Green as staining (268-269).

ID Sample	**Mankin Score**			**Mankin Total Score**
	Structure	**Cellularity**	**Matrix Staining**	
1	0	0	1	1
2	1	0	2	3
3	1	0	2	4
4	0	1	4	4
5	0	0	1	1
6	0	0	4	4
7	2	0	1	3
8	2	0	2	4

Ectopic mineralization is a known trigger of several joint alterations, closely linked to inflammation and cell differentiation, ultimately leading to cartilage degradation. Based on this, cartilage explants responses were first assessed under HAP stimulation (**Figure 3.4**).

The results showed that HAP treatment significantly upregulated collagen-10 (Col10), runt-related transcription factor-2 (Runx2), matrix metalloproteinase-3 (MMP3) and COX-2 gene expression, relative to controls (**a, Figure 3.4**), with simultaneous increased accumulation of MMP3 and IL-6 (**b, Figure 3.4**).

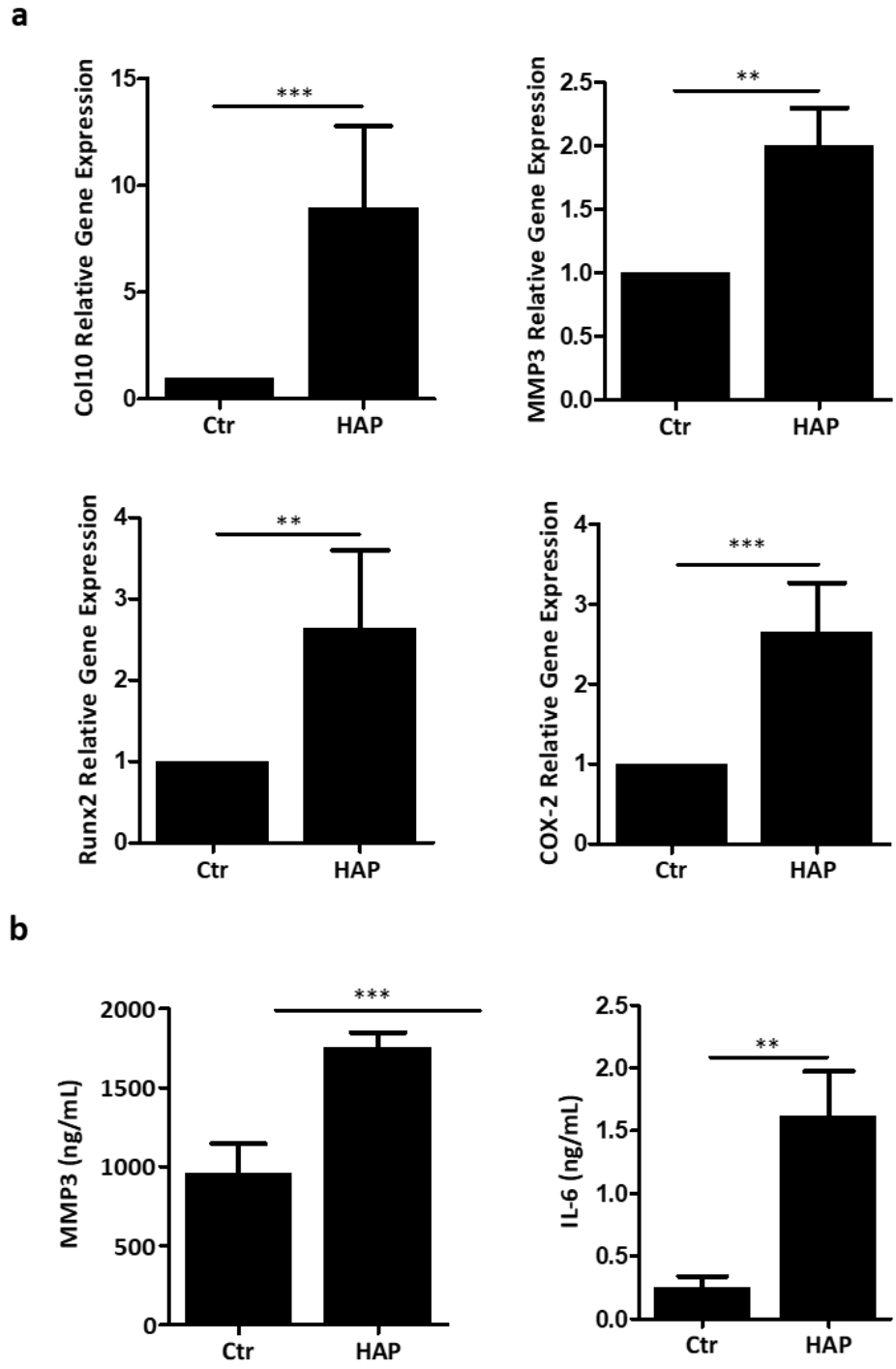

Figure 3.4 Hydroxyapatite (HAP) induce an upregulation of OA-related factors in cartilage *ex vivo* explants. Human cartilage explants were cultured in the presence of HAP or in control conditions (Ctr) for 72h. (a) Relative expression of Col10, MMP3, Runx2 and COX-2 marker genes at 72h post stimulation with HAP (750 µg/mL). (b) Levels of MMP3 and IL-6 in cell culture media were determined at 72h after stimulation with HAP (750 µg/mL). Data are presented as means of four independent experiences. All graphs show mean ± SD. Statistical significance was assessed using Student's t test, $p \leq 0.05$ (*), $p \leq 0.005$ (**) and $p \leq 0.0005$ (***).

In order to explore the inflammatory potential of culture media from monocytes and activated macrophages to trigger an inflammatory response in the *ex vivo* explant system, a first experiment was performed to evaluate the levels of TNFα accumulated in the conditioned media of THP-1 monocytes cultured during 14 days in control conditions, and of THP-1 MoM stimulated with LPS (100 ng/mL) and collected at different times, from 24h to 96h (**Table 3.3**).

Table 3.3 Levels of TNFα accumulated in the conditioned medium of THP-1 MoM stimulated with LPS, (24 h, 48 h and 96 h) (MCM) and THP-1 monocytes cultured in control conditions for 14 days (CM).

CM / MCM	TNFα (ng/mL)
THP-1 (14 days)	0.34 ± 0.009
THP-1 MoM (24 h)	1.12 ± 0.005
THP-1 MoM (48 h)	0.89 ± 0.012
THP-1 MoM (96 h)	1.49 ± 0.004

The highest levels of TNFα were found in the condition media of THP-1 MoM (MCM) after 96 h of LPS activation (**Table 3.3**) and selected to use in inflammatory assays and compared with IL-1β stimulation (**Figure 3.5**).

Gene expression of inflammation and ECM degradation markers were assessed to evaluate the cartilage explant system response to inflammatory stimulation with IL-1β and MCM (96 h). Overall, the study demonstrated that IL-1β activation generates higher expression levels of the analysed genes, in the interval of 24 h to 48 h (**Figure 3.5**). MCM (96h) produced a weaker effect, with higher impact in COX-2 and NF-kB expression between 24 h to 48 h (**Figure 3.5**).

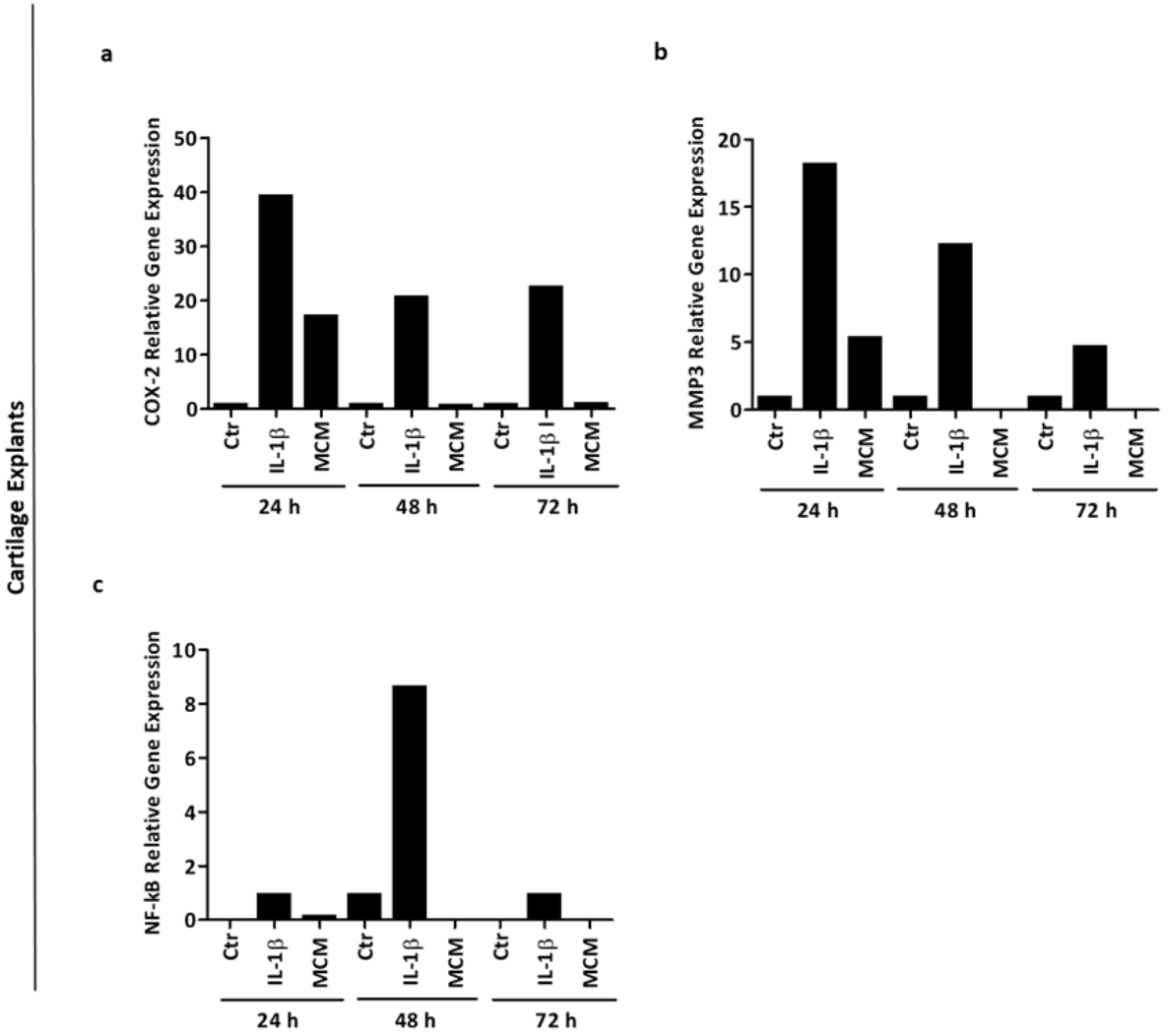

Figure 3.5 Inflammatory response of human cartilage explants exposed to IL-1β and THP-1 MoM conditioned culture media (MCM). Relative expression of (a) COX-2, (b) MMP3 and (c) NF-kB marker genes, treated with IL-1β (10 ng/mL) or MCM (96 h) at 24, 48 and 72h. Data are presented as one representative experiment, with triplicates.

3.3.3 Establishment of an *in vitro* co-culture model suitable for the study of OA, mimicking mineralization and inflammation events

Since in the joint environment, cartilage and synovial membrane are known to be involved in a complex crosstalk affecting cartilage integrity and driving OA progression, an *in vitro* co-culture model was developed to include in the preclinical testing workflow, representing a close to *in-vivo* OA model. Human cartilage explants were co-cultured with primary human synoviocytes and treated with IL-1β and HAP to simulate inflammatory and mineralizing conditions, respectively.

Increased gene expression of COX-2, IL-6 and MMP3 in the cartilage explants treated with IL-1β (10ng/mL), clearly indicated an induction of inflammatory reactions and ECM degradation at cartilage tissue level (**a, Figure 3.6**).

In order to analyse the effect of IL-1β at tissue level, cartilage explants treated in this co-culture system with two concentrations of IL-1β (10 and 100 ng/mL) were analysed by Alcian blue staining, and the results demonstrated a dose-dependent degradation of the ECM with a progressive loss of proteoglycans in the superficial zone and chondrocyte hypertrophy in the middle and deep zones (**b, Figure 3.6**).

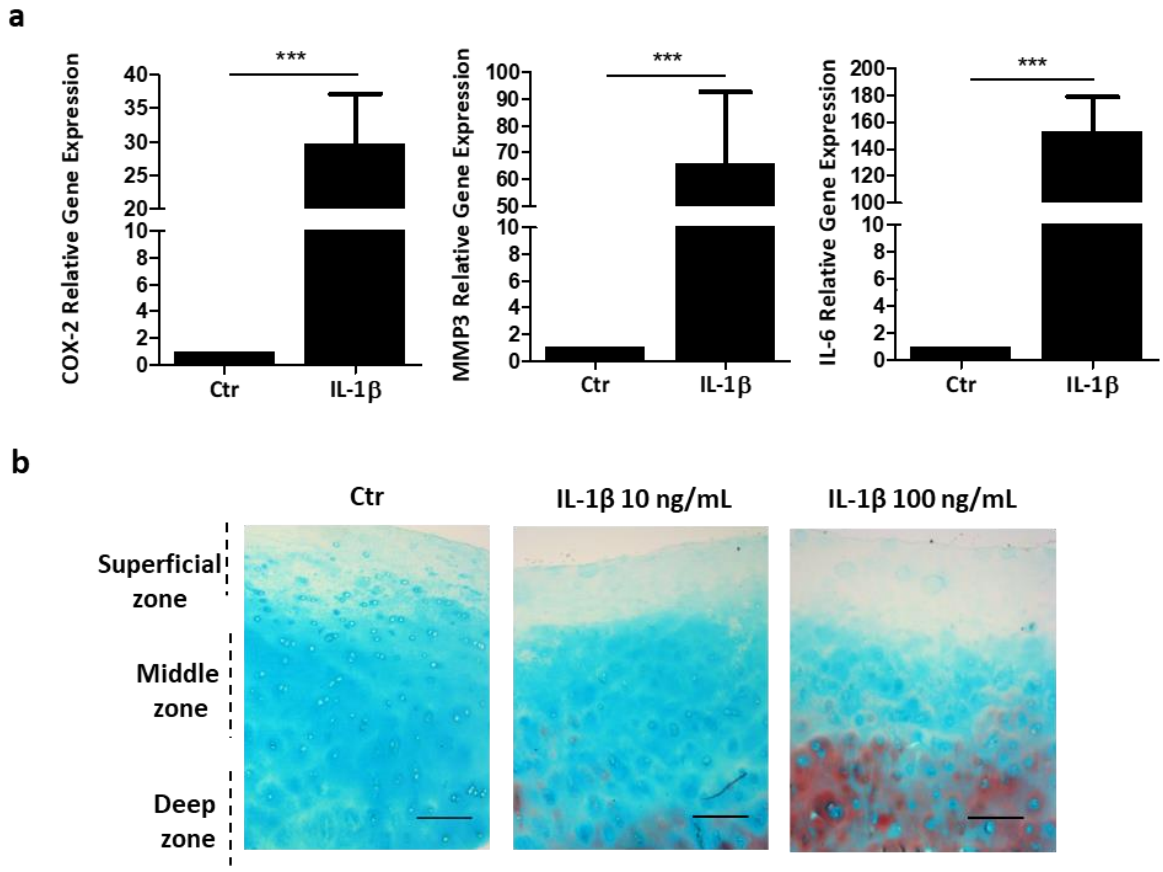

Figure 3.6 Cytokine stimulation of cartilage explants co-cultured with synoviocytes emulates phenotypic and molecular cartilage alterations occurring in OA. Human cartilage explants were co-cultured with human synoviocytes and stimulated with IL-1β. (a) Gene expression analysis of cartilage tissue of COX-2, MMP3 and IL-6 after 24h of stimulation with IL-1β (10 ng/mL). Data are presented as means of four independent experiences for COX-2 and MMP3, and two independent experiments for IL-6. (b) Representative Alcian Blue staining of cartilage tissue after 1 week of stimulation with 10 ng/mL and 100 ng/mL of IL-1β; scale bar represents 100 µm. Histological assessment of articular cartilage was based in distinct cartilage zones: superficial, middle and deep zone (258).

In addition, since HAP was shown to activate ECM calcification and degradation, cell differentiation and inflammatory pathways in the cartilage explants, the effective mineral deposition and the histomorphological features of cartilage tissue from the co-culture system was evaluated after treatment in mineralization conditions with $CaCl_2$ for 2 weeks. Increased calcium levels of the cartilage explant under mineralizing conditions (MM) were confirmed by calcium quantification (**a, Figure 3.7**), and von Kossa staining revealed the presence of large deposits of mineralized material in the vicinity of chondrocyte clusters (**b, Figure 3.7**).

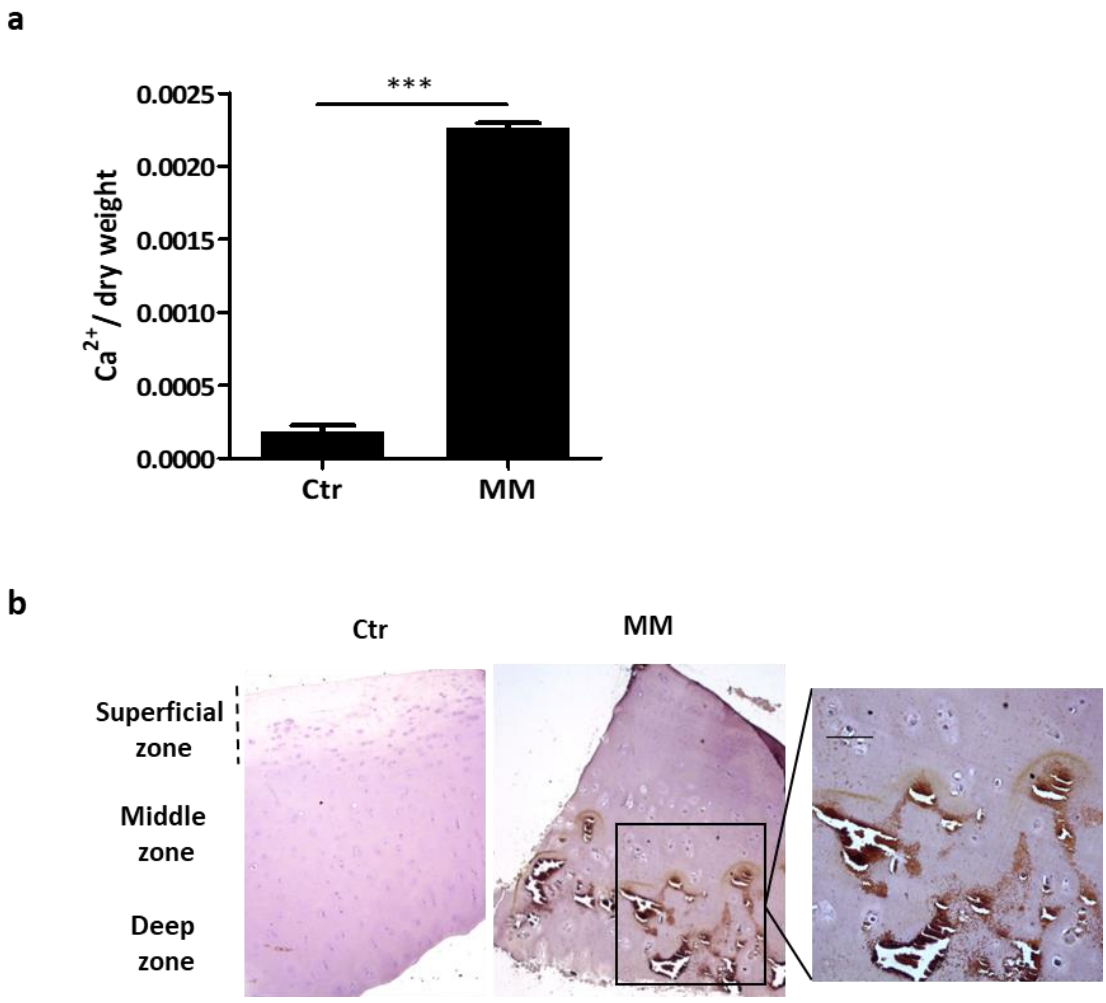

Figure 3.7 Mineral deposition and histomorphological features of cartilage explants co-cultured with synoviocytes under mineralization conditions, with $CaCl_2$. (a) Calcium quantification of cartilage tissue normalized to tissue dry weight after 2 weeks in control (Ctr) and mineralizing conditions (MM) with 5.4 mM $CaCl_2$. (b) Representative von Kossa/hematoxylin co-staining of cartilage tissue after 2 weeks in Ctr and MM conditions; scale bar represents 100 µm Control (Ctr) corresponds to co-cultures in non-supplemented media. Multiple t tests were performed, and statistical significance was defined as $p \leq 0.005$ (**) and $p \leq 0.0005$ (***). All graphs show mean ± SD.

In the co-culture system treated with HAP, higher levels of MMP3 and IL-6 were observed in the cell culture media (**Figure 3.8**).

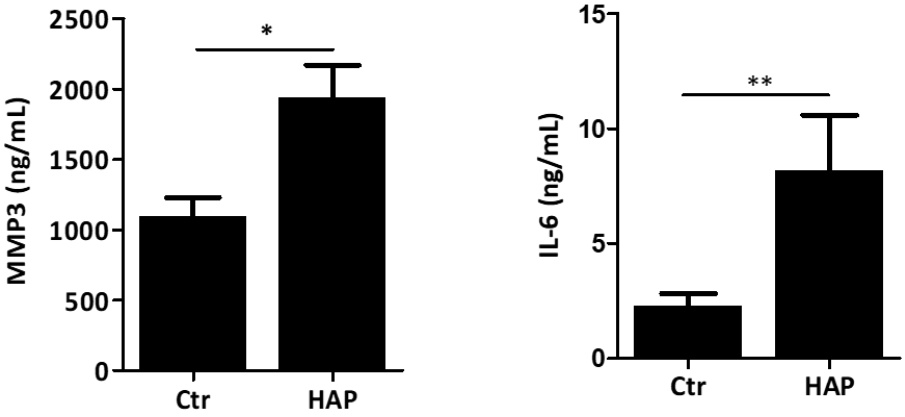

Figure 3.8 The impact of mineral treatment in cartilage explants co-cultured with synoviocytes, at the molecular and tissue levels. Human cartilage explants were co-cultured with human synoviocytes and stimulated with mineralizing conditions. Levels of MMP3 and IL-6 in the co-culture media after treatment with HAP (750 μg/mL) for 72h. Data are presented as means of three independent experiences. Control (Ctr) corresponds to co-cultures in non-supplemented media. Multiple t tests were performed, and statistical significance was defined as $p \leq 0.005$ (**) and $p \leq 0.0005$ (***). All graphs show mean ± SD.

3.4 Discussion

The main aim in this chapter was to establish a novel OA preclinical drug development pipeline as a useful tool for the screening of potential new OA drugs. The system is designed to be capable of evaluating the anti-mineralizing and anti-inflammatory activity of new potential drugs, and will be useful to support a better understanding of OA physiopathology. The screening pipeline was built up based on the knowledge of systems already available for the disease study. The complexity of the experimental pipeline model was progressively increased starting from a monolayer cell model until the establishment of an OA co-culture model. This 3D OA model integrate the contribution of synovial membrane cells and human cartilage tissue, with the combinatorial activity of mineralization and inflammatory processes, known as driving forces for OA progression.

Cell cultures are known to be easily manipulated, facilitating the multiple screening of potential drugs, and allowing preliminary investigation of the mechanisms critical to disease pathology, as well as the evaluation of the effects on cell phenotype. In this project an *in vitro* monolayer cell model system, including the more relevant cells involved in OA development

and progression, macrophage-like cells (THP-1 MoM), chondrocytes and synoviocytes, was selected as the first approach for bioactivity assessment, using knowledge and experimental conditions previously established by the group (173).

In OA, inflammation and calcification are the two major molecular processes occurring in the disease and leading to its progression. Inflammation interplays with calcification leading to extracellular matrix (ECM) degradation, apoptosis, mineral deposition and altered responses to inflammatory cytokines and mediators of inflammation. One important aspect included in the developed screening pipeline was to consider exploring and evaluate the response of candidate drugs in the crosstalk between the two events.

The synoviocyte and chondrocyte OA cell system, previously developed by our group, was shown to represent a useful first screening for OA relevant activities, such as inflammation and calcification. Inflammatory IL-1β stimuli, known to trigger inflammation in OA, and the mineralizing agent HAP, associated with cartilage calcification and OA pathogenesis, were applied to the cell systems to induce OA-like changes, following the conditions already optimized (173). Our results confirmed that the primary articular cell systems were able to respond to the IL1-β inflammatory and HAP mineralizing stimuli, with an inflammatory feedback translated into an increase of expression and accumulation of specific pathologic OA markers as COX-2, NF-kB and IL-6.

Complex and interconnected molecular events of cartilage homeostasis disruption associated to inflammation known to fuel cartilage degradation, are recognized as crucial for disease development and important targets for therapeutic approaches (262). Cartilage degradation is associated with chondrocytes differentiation leading to apoptosis and deposition of a mineralized extracellular matrix, which in turn contributes to loss of ECM integrity and inflammation (66,68). In fact, although the pathways involved in the crosstalk between inflammation and cartilage degradation are still not completely clarified, mineralizing and inflammatory events occur in a close related manner during OA progression (173). To further explore this features a human explant cartilage model using cartilage tissue classified as normal to early-OA according with the Mankin scale, was included to follow the 2D cell systems in the workflow, allowing the study of cell interactions and also including the variable cell-ECM in the analysis. The results obtained in this explant model confirmed that treatment with IL-1β or HAP nanocrystals were able to induce cartilage catabolic processes and inflammation by upregulating known markers of cartilage degradation and cell differentiation.

Based on the results obtained with the explant model a more complex *ex vivo* 3D OA co-culture model, combining human cartilage explants and synoviocytes and better mimicking the

articular context was developed. This 3D OA co-culture model was included in the final step of the pipeline to mimic early OA disease stages and should represent a powerful tool for the evaluation of potential active compounds in a preclinical stage of drug development.

Importantly this co-culture model will allow testing the activity of potential novel therapeutics in the context of inflammatory and mineralization conditions which are well-known players in the OA pathogenesis. In this last decade, calcium phosphate crystals have been consistently associated with the early stage of OA and have a pathogenic role in the development and rapid progression to end-stage OA (118,204). Basic calcium phosphate (BCPs) crystals have been found in the synovial fluid and membrane, and cartilage from OA patients (263), and have been associated with the activation of macrophages, synovial fibroblasts and articular cells, resulting in increased cell proliferation and production of pro-inflammatory cytokines and MMPs (76,273). An active inflammatory response to BCP was previously observed in macrophages, human chondrocytes and synoviocytes, by the production of pro-inflammatory cytokines TNFα, IL-1β, and IL-8 (256,274) or through up-regulation of COX-2 and MMP13 gene expression (266). Also, synoviocytes were shown to produce a mineralized ECM (173), contributing to increased BCP levels in the ECM, and consequently potentiating a tandem inflammatory response. In concordance, our results show an inflammatory response to HAP stimulation in all tested OA models, similar to those obtained with the classical inflammatory cytokine IL-1β. Of particular relevance, at cartilage level, treatment with hydroxyapatite induced overexpression of Col10 and Runx2, indicative of triggered chondrocyte differentiation towards hypertrophy and calcification, while the deposition of mineralized material co-localized with chondrocyte clusters, in a clearly disrupted ECM, confirmed cartilage calcification and degradation.

In addition, up-regulation of COX-2 and IL-6, widely known to be associated with joint inflammation, and MMP3, a major responsible for ECM degradation, clearly showed the detrimental potential of calcification in OA. This is in line with recent data showing that BCP upregulate IL-6 in *in vivo* murine OA models, which in turn induced the expression of genes involved in calcification, promoting BCP formation and potentiating a vicious cycle (247). Increased levels of BCP and IL-6 were associated with cartilage degradation through the induction of matrix-degrading enzymes activity in chondrocytes (247). In another study, calcium-phosphate complexes were shown to induce MMP3 and MMP13, which in turn, promoted the release of calcium and phosphate through degradation of the ECM calcified cartilage, in a positive loop (267).

Additionally, the effect of IL-1β on cartilage is known to reflect not only the catabolic effect of matrix metalloproteinases (MMPs) and aggrecanases upregulation, but also the downregulation of chondrogenic extracellular matrix synthesis (266). MMP3 is known to mediate the integrity of various constituents of the ECM, such as collagens (types II, III, IV, V, VII, IX, X), fibronectin, elastin, proteoglycans, directly or through the activation of other pro-MMPs and pro-TNFα, in OA (268) Our results showed that IL-1β induced an overexpression of MMP3, and loss of proteoglycans associated with hypertrophic chondrocyte differentiation, in the upper and middle zones of the articular cartilage (269) as well as hypocellularity, both features representative of an early stage OA grading (270). Overall, our results clearly demonstrated the potentialities of our developed 3D co-culture OA model to study the interplay between cartilage degradation and inflammation, of critical value in drug development for potential anti-osteoarthritic compounds.

3.5 Acknowledgements

Sincere gratitude to the Departamento de Ortopedia do Hospital Particular do Algarve - Gambelas (Faro, Portugal) for their collaboration, which made the collection of human biological material for this study possible. In particular, a profound appreciation to Doctor Acácio Ramos, who played a crucial role in collecting the control and osteoarthritic biological samples, as well as providing valuable clinical information about the subjects. Doctor Acácio Ramos showed great interest in this project and was always available to address any questions related to osteoarthritis medical aspects. Thanks also to Dr. Maria M. Carvalho, Dr. Henrique Cruz and Dr. João Paulo Sousa, from the same medical team for their availability and collaboration in this study.

Acknowledges to Dr. Joana Magalhães and Dr. Francisco Blanco, from Unidad de Medicina Regenerativa, Grupo de Investigación en Reumatología (GIR), Instituto de Investigación Biomédica de A Coruña (INIBIC), Complejo Hospitalario Universitario de A Coruña (CHUAC), and Centro de Investigación Biomédica en Red (CIBER), Madrid for the primary cell cultures of synoviocytes and chondrocytes. A special thanks to Dr. Joana Magalhães for her appreciated help in the evaluation of the human cartilage explants collected and used in this study. We would like to thank Dr. Joana Magalhães for all the support and participation during this PhD, with very useful advices and encouragement.

Furthermore, we would like to acknowledge the support of Doctor José Enriquez and

technician Alexandra Teixeira from Centro Hospitalar do Algarve (Departamento de Anatomia Patológica, Faro, Portugal). Their assistance has been of immense value. We are grateful to Doctor José Enriquez, the head of the department, for allowing this collaboration and providing expertise in analysing several histological characterization results. We also thank Alexandra Teixeira for her contributions in tissue paraffin embedding and some of the tissue sectioning in this chapter.

Part of the work presented in this chapter represents our published results in Araujo, N. *et al*. (271).

Chapter 4

Amentadione as a potential anti-osteoarthritic agent

Abstract

Osteoarthritis (OA) remains a prevalent chronic disease without effective prevention and treatment. In this chapter, purified marine meroterpenoids from the brown algae *Cystoseira sp* previously demonstrating anti-inflammatory activity, were evaluated as OA modulators, by using the novel OA preclinical drug development pipeline designed to evaluate the anti-inflammatory and anti-mineralizing activities of potential OA-protective compounds, as depicted in chapter 3. Succinctly, the workflow is based on an *in vitro* OA cell system consisting of macrophages, chondrocytes and synoviocytes followed by an *ex vivo* human cartilage-based assay and a new *in vitro* OA co-culture model, combining cartilage explants with synoviocytes. Since inflammation and mineralization play an important role in the genesis of OA, the model was designed to mimic early disease stages and to evaluate the activity of compounds using a combined approach with interleukin-1β (IL-1β) or hydroxyapatite (HAP) stimulation.

Using the workflow pipeline, the anti-inflammatory activity of purified meroditerpenoides Cystodione G (Cyd G), 11-Hydroxyamentadione (Cyd K), Cystone C (Cy C) and amentadione (YP) was screened in THP-1 macrophages by a combination of gene expression analysis and measurement of inflammatory mediators. One of the most promising compounds amentadione (YP), was selected to proceed in the preclinical pipeline to further evaluate its anti-osteoarthritic potential. YP counteracted inflammatory responses by downregulation of COX-2 and IL-6, improved cartilage homeostasis by downregulation of MMP3 and the chondrocytes hypertrophic differentiation factors Col10 and Runx2. Importantly, YP downregulated NF-κB gene expression and decreased phosphorylated IkBα/total IkBα ratio in chondrocytes.

These results strongly suggest YP as a cartilage protective factor by inhibiting inflammatory, mineralizing, catabolic and differentiation processes during OA development, through inhibition of NF-κB signaling pathways, with high therapeutic potential.

4.1 Introduction

OA has been defined as a “whole joint” and multifactorial disease, characterized by synovial inflammation, progressive loss of articular cartilage and remodeling of the underlying bone (249). Although OA physiopathology is still not completely understood, chronic inflammation is known to play a critical role in disease development and progression, with accumulating

evidence supporting the association between OA pathology and different markers of inflammation (250). OA cartilage and synovium overexpress cytokines and pro-inflammatory mediators that stimulate the accumulation of proteolytic enzymes, aggrecanases and matrix metalloproteinases (MMPs) responsible for the extracellular matrix (ECM) degradation, and for mediating detrimental effects through innate immunity signals (281-282). In particular, MMP3 is known to mediate the integrity of various constituents of the ECM, such as collagens (types II, III, IV, V, VII, IX, X), fibronectin, elastin, proteoglycans, directly or through the activation of other pro-MMPs and pro-TNFα, in OA (268). This molecular condition together with chondrocyte differentiation into a hypertrophic phenotype, result in loss of the ability to restore the ECM with consequent cartilage degradation. Basic calcium phosphate (BCP) deposition in the cartilage and synovial membrane is closely associated with OA inflammation and contributes to local tissue damage and failed tissue repair, further intensifying hyaline articular cartilage loss and progressive joint deterioration (118,204-205).

Current osteoarthritis prevention and treatment are still very limited and unsatisfactory, with therapeutics focused mainly on drugs which improve pain or symptoms, such as topic and oral nonsteroidal anti-inflammatory drugs, acetaminophen, and opioids (35). Although there are some advances in the design of new molecules to target cartilage repair and bone, or to treat inflammation and pain, at present, no effective OA drugs have yet been approved (274), making the search for new potential molecules a priority to overcome the growing burden of OA.

In the search of effective drugs that might prevent or slow down the development of the disease, natural products derived from plants and marine organisms, remain a source of new molecular entities for the treatment of chronic inflammatory related diseases, including osteoarthritis (284-285) Dietary supplements, of natural and synthetic origin, representing a nutritional and health benefit, were already related with OA human clinical trials. Although most were associated with OA pain relief, some were shown to modify the inflammatory OA process, by balancing anabolic and catabolic joint events, and promoting the synthesis of structural articulation precursors (286-288).

Among natural products, those containing phenolic rings, such as the flavonoids and some meroterpenoids, are usually provided of interesting biological activities, and have been shown to modulate cytokines such as TNFα, IL-1β and IL-6, with a crucial role in chronic inflammatory and autoimmune diseases (279). Some terpenoids based drugs are already available in the pharmaceutical market such as artemisinin and paclitaxel (Taxol®), acting as antimalarial and anticancer drugs, respectively (280).

In recent years, a series of meroterpenoids isolated from the brown alga *Cystoseira*

usneoides have been shown to exhibit anti-inflammatory and antioxidant activities, by reducing the secretion of pro-inflammatory cytokines and downregulating the expressions of COX-2 and iNOS enzymes in THP-1 activated macrophages (281) (188,292-293). Among those, YP, Cyd G, Cyd K and Cy C (**Figure 4.1**) showed radical-scavenging activity and demonstrated a significant role in reducing the production of TNFα in LPS-stimulated THP-1 human macrophages (183). These results led us to further investigate the anti-inflammatory action of this pure marine compounds and their potential as novel cartilage protective agents in an OA context. For that we usedthe the OA preclinical pipeline consisting of an *in vitro* 2D-cell based system followed by an *ex vivo* explant-based and co-culture OA models, as described in Chapter 3. Our aim was to evaluate the potential protective effect of YP, Cyd G, Cyd K and Cy C in the interplay between mineralization and inflammatory processes involved in OA development and progression.

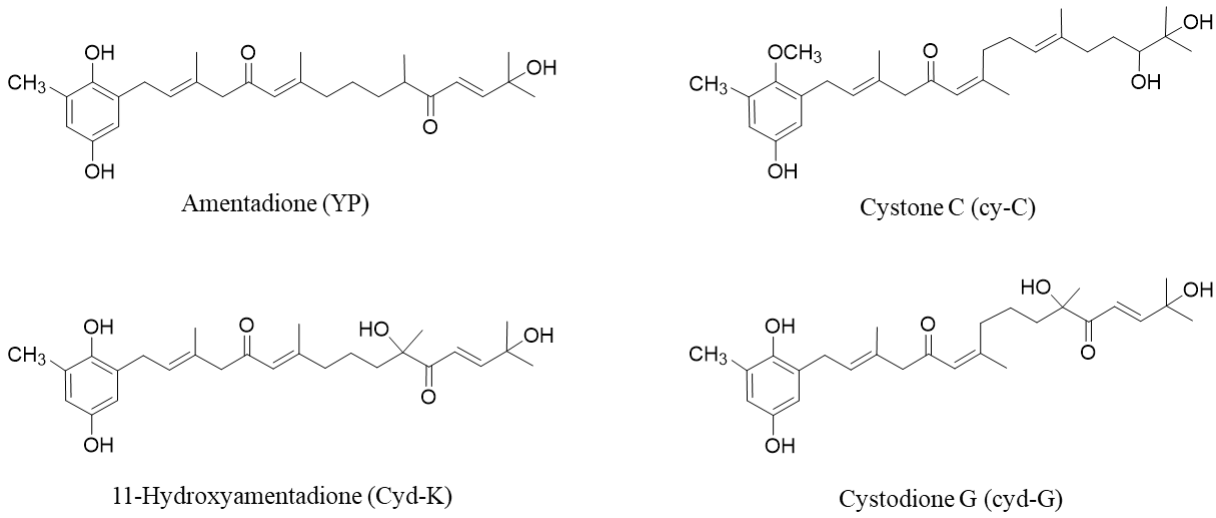

Figure 4.1 Meroditerpenoids isolated from the brown alga *Cystoseira usneoides* (183)

4.2 Experimental procedures

4.2.1 Cystodione G (Cyd G), 11-Hydroxyamentadione (Cyd K), Cystone C (Cy C) and amentadione (YP)

Purified meroditerpenoids Cyd G, Cyd K, Cy C and YP isolated from the brown alga *Cystoseira usneoides* collected off the coast of Tarifa (Spain) (183) were kindly provided by Eva Zubía, from Faculty of Marine and Environmental Sciences, University of Cadiz, Spain.

4.2.2. Cell culture

THP-1 monocytes were acquired, cultured and differentiated in THP-1 macrophages (THP-1 MoM) as described in the Experimental Section of Chapter 2. Primary human chondrocytes and synoviocytes were acquired and cultured as described in the Experimental Section of Chapter 3.

4.2.3 Cartilage collection and tissue explants preparation

Knee articular cartilage was obtained from osteoarticular cuts performed on the femoral and tibial sides, from eight patients (4 males and 4 females, aged 71,5 ± 5,9 years) and maintained in the appropriated culture conditions as detailed in the Experimental Section of Chapter 3.

4.2.4 Cell proliferation

THP-1 MoM cells seeded in 96-well plates at 2×10^5 cells/well, and confluent chondrocytes and synoviocytes, were cultured in their respective growth media and supplemented with different concentrations of Cyd G, Cyd K, Cy C, YP and HAP. Cell viability was determined at appropriate time points using the CellTiter 96 cell proliferation assay (Promega, Madison, WI, USA), following manufacturer's instructions.

4.2.5 Inflammatory assays in monolayer cells

THP-1 MoM (1×10^6 cells/mL) were cultured in 24-well plates, in 500 µL of complete RPMI supplemented with 10 µM of YP, Cyd G, Cyd K, Cy C or dexamethasone (DXM, 2µM) for 2 h and further stimulated with lipopolysaccharides (LPS, 100 ng/mL) or synthetic hydroxyapatite nanocrystals (HAP, 750 µg/mL), for additional 24 h or 72 h, respectively.

THP-1 MoM (1×10^6 cells/mL) were cultured in 500 µL of complete RPMI supplemented with different amentadione (YP) concentrations (2.5, 5 and 10 µM) in dose-dependent experiments, and with 10 µM YP in subsequent experiments, or with 2 µM DXM, during 24 h. After, 100 ng/mL of LPS or HAP (750 µg/mL) were added to the culture media for another 24 h or 72 h, respectively.

Confluent chondrocytes and synoviocytes were cultured in 12-well plates, in 1 mL of Adv DMEM supplemented with 10 µM of YP or 2 µM of DXM during 24 h, and further treated

with: 10 ng/mL of interleukin-1β (IL-1β) for 3 h and 6 h, or for 30 min in the assay for pIKBα content analysis; 750 µg/mL HAP for 6 h. Control cells were cultured with respective media without any treatment. At determined time points, cell culture media were collected for ELISA analysis and cells harvested for RNA extraction.

4.2.6 Cartilage explants assays

Cartilage explants (10 per well) were plated in a 12 well plate and co-cultured with synoviocytes in a transwell system as described in the Experimental section of Chapter 3, and then treated with HAP (750 µg/mL) for further 72 h. As controls, explants were cultured without treatment. At the end of each experiment, cartilage explants were collected, washed twice with PBS, immediately processed for RNA extraction as described below, and the cell culture media collected for ELISA assays.

4.2.7 Co-culture assays

Cartilage explants (10 per well) were plated in a 12 well plate and co-cultured with synoviocytes in a transwell system as described in Chapter 3.

To evaluate the effect of YP, co-cultures were supplemented with 10 µM of YP or 2 µM DXM for 24 h, followed by treatment with IL-1β (10 ng/mL) during 24 h, or HAP (750 µg/mL) during 72 h. Cartilage explants were collected as described above for RNA extraction, and cell media collected for ELISA analysis.

4.2.8. RNA extraction, cDNA amplification and quantitative real-time PCR (qPCR)

Cartilage tissue and cells were processed as described in Chapter 3, section 3.2.7. Total RNA was further extracted as described by Chomczynski and Sacchi (257) and as depicted in section Chapter 3, section 3.2.7. RNA concentration was determined by spectrophotometry at 260 nm (Nanodrop 1000, Thermo Scientific). RNA was then treated with RQ1 RNase-free DNase (Promega, Madison, WI, USA) and reverse-transcribed using the qScipt cDNA SuperMix (Quanta bio) according to manufacturer's recommendations.

Quantitative real-time PCR reactions were performed using the CFX connect, Real time System (Bio-Rad, Richmond, CA, USA), SoFast Eva Green Supermix (Bio-Rad, Richmond,

CA, USA), 300 nM of forward and reverse gene-specific primers for genes of interest (**Table 3.1**), and a 1:5 cDNA dilution, following the same procedure described in Chapter 3. The PCR conditions used are the same as depicted in Chapter 3, section 3.2.7 and fluorescence was measured at the end of each extension cycle in the FAM-490 channel. Levels of gene expression were calculated using the comparative ΔΔCt method, and normalized using gene expression levels of glyceraldehyde-3-phosphate dehydrogenase (GAPDH), with the iQ5 software (BioRad).

4.2.9. ELISA assays

The cell culture media were treated as described in section 2.2.10.1 and used for the quantification of TNFα (Peprotech), IL-6 (Peprotech) and MMP3 (Life Technologies) following the manufacture's protocols.

4.2.10. Histological evaluation

Paraffin-embedded cartilage tissue sections were processed at the Histopathology Department of Centro Hospitalar e Universitário do Algarve (CHUA, Faro) and used for histological assessment. Cartilage grading of initial tissue samples was conducted based on modified criteria originally established by Mankin *et al* (255) and the specimens were analysed as described in the Experimental Section of Chapter 3.

4.2.11. Protein extraction and quantification

Total protein from chondrocyte inflammatory assays and YP treatments was obtained by extraction with RIPA buffer (50 mM Tris HCl pH 8, 150 mM NaCl, 1 % NP-40, 0.5 % sodium deoxycholate, 0.1 % SDS) for 1h, at 4 ˚C, with agitation, followed by a centrifugation at 16 000 xg for 15 min at 4 ˚C. Protein concentration was assessed using Micro BCA kit (Thermo Scientific), according to the manufacturer's instructions.

4.2.12. Electrophoresis and Western blot

Aliquots of 20 µg of total protein extracts were size separated in a 4–12 % (w/v) gradient polyacrylamide precast gel containing 0.1 % (w/v) of sodium dodecyl sulphate (SDS) (NuPage, Invitrogen, Carlsbad, CA, USA) and transferred onto a nitrocellulose membrane (Biorad,

Richmond, CA, USA). Detection of pIKBα and GAPDH was performed through overnight (O/N) incubation with the pIKBα pSer32 ABfinity Rabbit Monoclonal antibody (2.5 µg/µL, Thermo Fisher, USA) and anti-GAPDH polyclonal antibody (1:500, Santa Cruz Biotechnology). Detection was achieved using Goat anti-rabbit IgG horseradish peroxidase-conjugated secondary antibody and Western Lightning Plus-ECL (PerkinElmer Inc., Waltham, MA, USA). Image acquisition was obtained using an IQ LAS 4000 mini biomolecular imager.

4.2.13. Determination of total and phosphorylated IkBα

Total IkBα and phosphorylated IkBα (pIkBα) were determined in chondrocyte cell lysates, using the InstantOne ELISA assay kit (Invitrogen) according to the manufacturer's protocol.

4.2.14. Statistical analysis

Each independent experiment (n) was performed with different primary cell culture batches and cartilage from distinct patients. Replicates within an individual experiment were performed using the same batch of cells and cartilage from a single patient. Data are presented as mean ± standard deviation (SD). Multiple t tests were used for comparison between two groups. For more than two groups significance was determined using one-way analysis of variance (ANOVA) with comparison between groups by Dunnett test. Statistical significance was defined as $p \leq 0.05$ (*), $p \leq 0.005$ (**) and $p \leq 0.0005$ (***)

4.3 Results

4.3.1. Anti-inflammatory activity of Cystodione G (Cyd G), 11-Hydroxyamentadione (Cyd K), Cystone C (Cy C) and amentadione (YP) in THP-1 MoM

To evaluate the anti-inflammatory potential of meroditerpenoids YP, Cyd G, Cyd K and Cy C (**Figure 4.1**) in the mineralization and inflammatory processes involved in OA development and progression, a first screening was performed on THP-1 MoM.

The inflammatory response of THP-1 MoM induced by lipopolysaccharide (LPS) was measured by the accumulation of the inflammatory marker TNFα. The results suggest a decrease in the inflammatory response by pre-treatment of the cell system with all compounds

tested, in a similar manner (**Figure 4.2**).

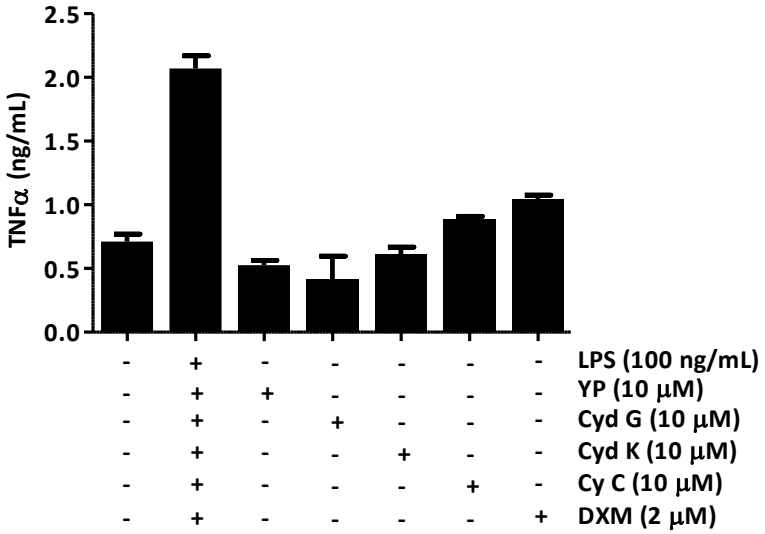

Figure 4.2 YP, Cyd G, Cyd K and Cy C reduce the inflammatory response of THP-1 macrophages (THP-1 MoM) stimulated with LPS. Levels of TNFα in cell culture media of THP-1 MoM pre-treated with different concentrations of YP, Cyd G, Cyd K and Cy C for 2 h, followed by exposure to 100 ng/ml LPS for additional 24h, determined by ELISA. Culture media of non-treated cells was used as control, and cells treated with 2 μM dexamethasone (DXM) were used as a positive anti-inflammatory control for LPS-stimulated THP-1 MoM experiment. Data are presented as duplicates of a representative experiment.

Furthermore, a similar trend was noticed in the attenuation of TNFα production levels in hydroxyapatite (HAP)-stimulated THP-1 MoM cells, by pre-treatment with YP, Cyd G, and Cyd K, but not by Cy C (**Figure 4.3**).

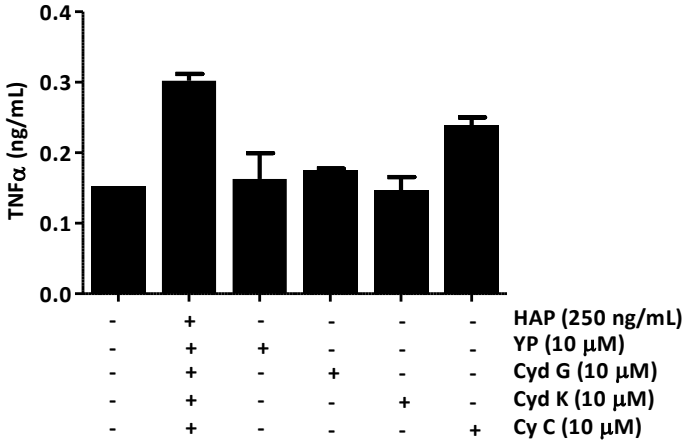

Figure 4.3 YP, Cyd G, Cyd K and Cy C reduce the inflammatory response of THP-1 macrophages (THP-1 MoM) stimulated with hydroxyapatite (HAP). Levels of TNFα in cell culture media of THP-1 MoM pre-treated with different concentrations of YP, Cyd G, Cyd K and Cy C for 2 h, followed by exposure to 250 μg/mL HAP for 72 h, determined by ELISA. Culture media of non-treated cells was used as control condition. Data are presented as duplicates of a representative experiment.

Cell proliferation assays were performed to confirm that in the conditions tested, YP, Cyd G, Cyd K and Cy C did not affect THP-1 MoM cell viability (**Figure 4.4**).

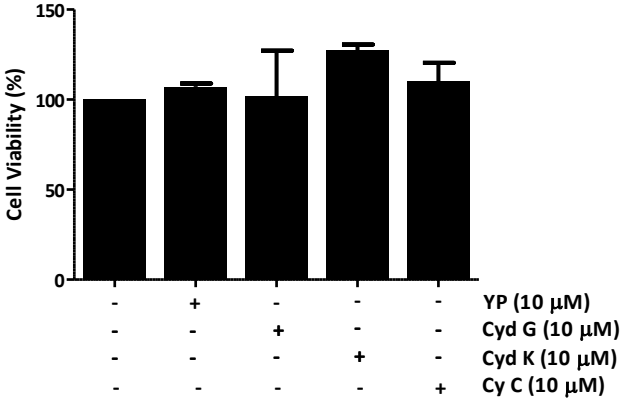

Figure 4.4 Viability of THP-1 macrophage cells (THP-1 MoM) exposed to 10 μM of YP, Cyd G, Cyd K and Cy C for 24 h. Cell culture media of non-treated cells was used as control. Graph shows mean ±SD.

Overall, the initial screening activity results indicated YP, Cyd G and Cyd K as most promising compounds to be further explored as anti-inflammatory candidates in OA.

4.3.2. YP acts as an anti-inflammatory agent in the articular OA cell system model

The indication of YP anti-inflammatory activity in THP-1 MoM cells as previously reported (188,291), led us to study the capacity of such terpenoid to manipulate the inflammation in an OA scenario. In order to evaluate the effects of YP on TNFα levels, a YP dose-dependent experiment was conducted using THP-1 MoM cells stimulated with LPS. The pre-treatment of cells with YP resulted in a consistent and gradual reduction of TNFα levels (**a, Figure 4.5**), and the concentration of 10μM of YP was selected for further biological assays. Results reported in Chapter 3, concerning a dose dependent study of HAP stimulation of THP-1 MoM cells (**Figure 3.1, Chapter 3**), showed that 750 μg/mL, the highest concentration of HAP tested, afforded the highest stimulation response. Based on that, 750 μg/mL of HAP was further used to stimulate THP-1 MoM, the time of YP pre-treatment was increased to 24 h and the TNFα levels evaluated. Under these conditions, YP showed to efficiently reduce the inflammatory response by decreasing TNFα levels (**b, Figure 4.5**).

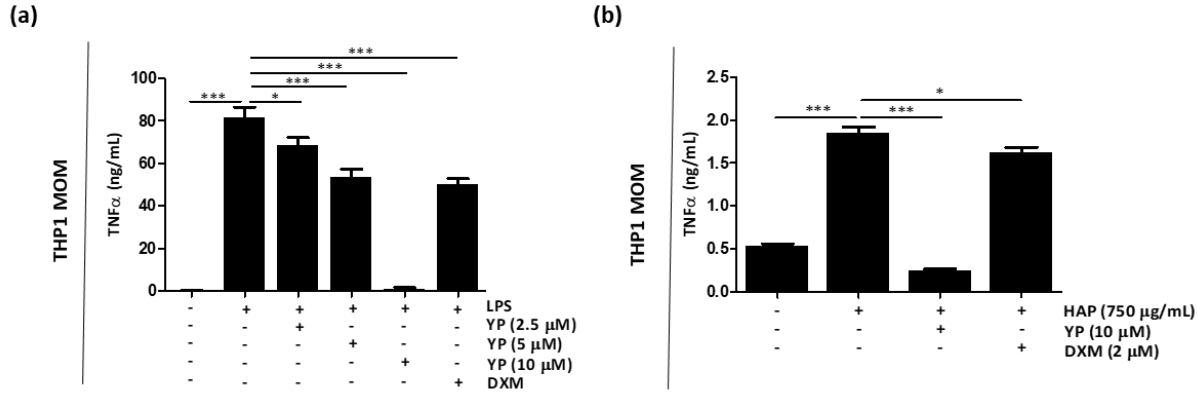

Figure 4.5 YP reduces the inflammatory response of THP-1 macrophages (THP-1 MoM) stimulated with LPS (a) and hydroxyapatite (HAP) (b). Levels of TNFα in cell culture media of THP-1 MoM pre-treated with different concentrations of YP for 24 h, followed by exposure to 100 ng/ml LPS for additional 24h (a) and to 750 μg/mL HAP for 72 h (b), determined by ELISA. Control (Ctr) corresponds to culture media of non-treated cells, and cells treated with 2 μM dexamethasone (DXM) were used as a positive anti-inflammatory control. Data are presented as means of at least three independent experiments. All graphs show mean ±SD. One-way Anova and multiple comparisons were achieved with the Dunnett's test. Statistical significance was defined as $p \leq 0.05$ (*), $p \leq 0.005$ (**) and $p \leq 0.0005$ (***).

Cell proliferation assays were performed to confirm that different concentrations of tested YP did not affect THP-1 MoM cell viability (**Figure 4.6**).

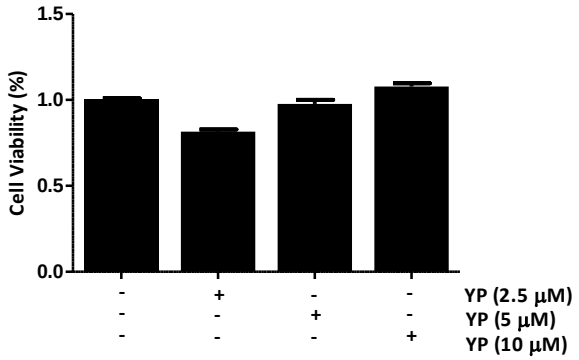

Figure 4.6 Viability of THP-1 macrophage cells (THP-1 MoM) exposed to different concentrations of amentadione (YP) for 24 h. Cell culture media of non-treated cells. Was used as control. Graph shows mean ±SD.

Based on these results, YP was further tested on the previously established articular OA cell system, and described in Chapter 3, consisting of human chondrocytes and synoviocytes primary cell cultures (173). Human synoviocytes and chondrocytes primary cells were pre-treated with YP for 24h, followed by IL-1β (**Figure 4.7**) and HAP (**Figure 4.8**) stimulation. The effect of YP was determined by measuring gene expression of the inflammatory marker cyclo-oxygenase-2 (COX-2) and levels of IL-6 released into the cell culture media. Pre-treatment with YP followed by IL-1β stimulation resulted in a significant downregulation of COX-2 and decreased levels of IL-6 in both type of cells, relative to non-treated cells (**a, b, Figure 4.7**).

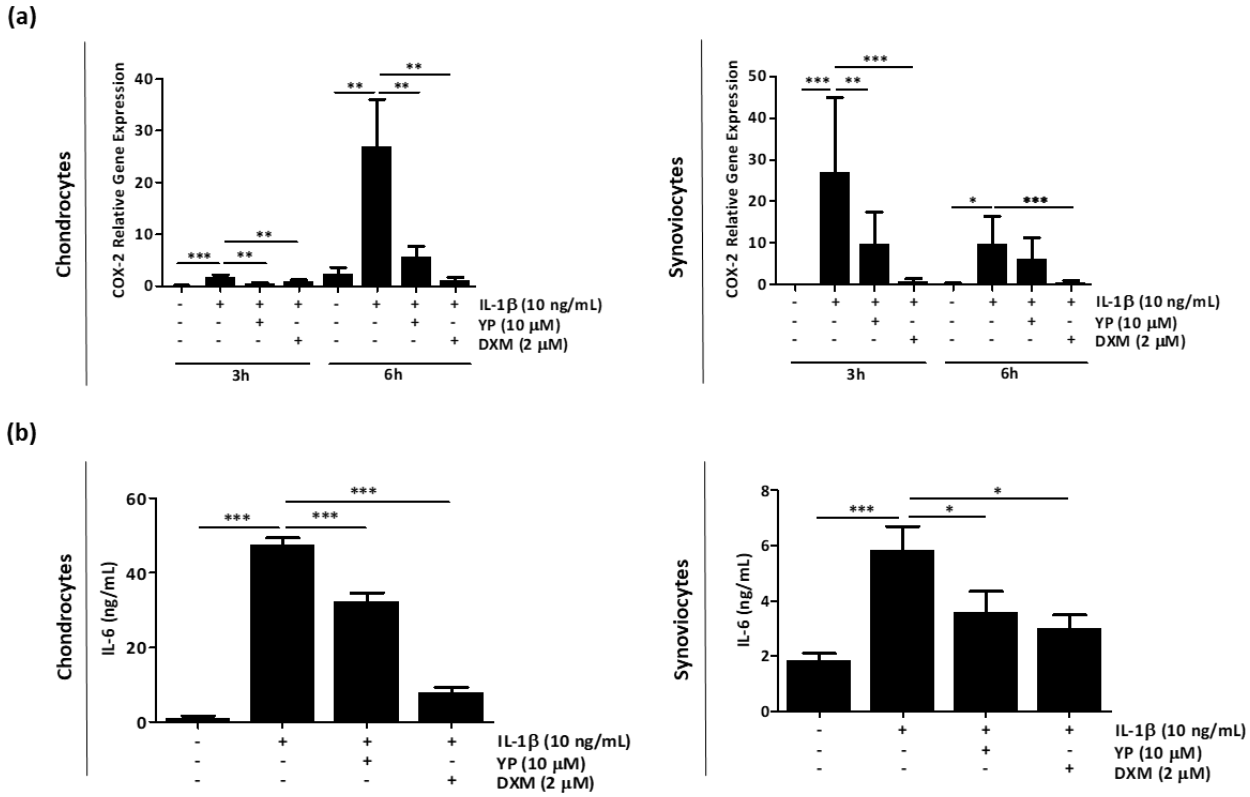

Figure 4.7 YP reduces the levels of inflammatory markers in articular-derived cells stimulated with IL-1β (a, b). Primary chondrocytes and synoviocytes were pre-treated with 10 μM YP for 24h, followed by stimulation with 10 ng/mL IL-1β during different time points. (a) Relative gene expression of the inflammatory marker COX-2 was determined by qPCR, at 3h and 6h post IL-1β stimulation in chondrocytes and synoviocytes. (b) Levels of IL-6 in cell culture media 6h post IL-1β stimulation, determined by ELISA. Cells treated with 2 μM dexamethasone (DXM) were used as a positive anti-inflammatory control. Data are presented as means of at least three independent experiments. All graphs show mean ±SD. One-way Anova and multiple comparisons were achieved with the Dunnett's test. Statistical significance was defined as $p \leq 0.05$ (*), $p \leq 0.005$ (**) and $p \leq 0.0005$ (***).

Interestingly, YP pre-treatment of chondrocytes and synoviocytes stimulated with HAP, resulted in a similar downregulation of the inflammatory marker COX-2 (**Figure 4.8**).

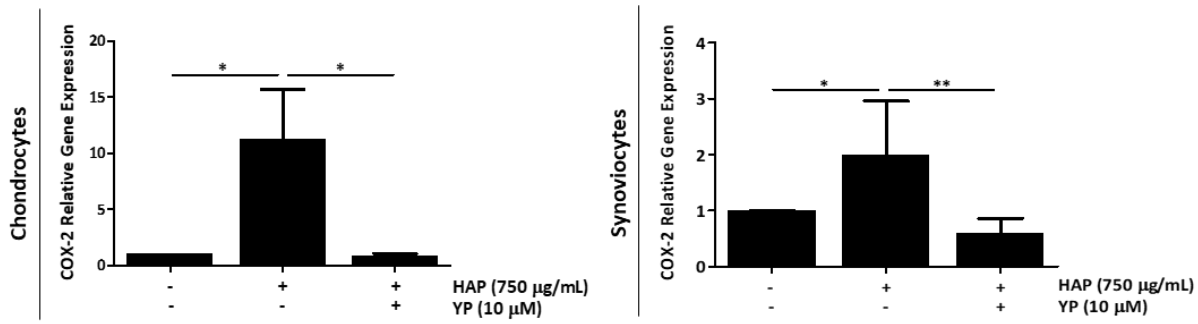

Figure 4.8 YP downregulates the inflammatory marker COX-2 in articular-derived cells stimulated with HAP. Primary chondrocytes and synoviocytes were pre-treated with 10 µM YP for 24h, followed by stimulation with 750 µg/mL HAP during 6h. Relative gene expression of COX-2 was determined by qPCR, at 6h post HAP stimulation in chondrocytes and synoviocytes. Data are presented as means of two independent experiments, with duplicates. All graphs show mean ±SD. One-way Anova and multiple comparisons were achieved with the Dunnett's test. Statistical significance was defined as $p \leq 0.05$ (*) and $p \leq 0.005$ (**).

No cytotoxicity was observed in chondrocytes and synoviocytes, when treated with different YP concentrations or HAP concentrations (**Figure 4.9**).

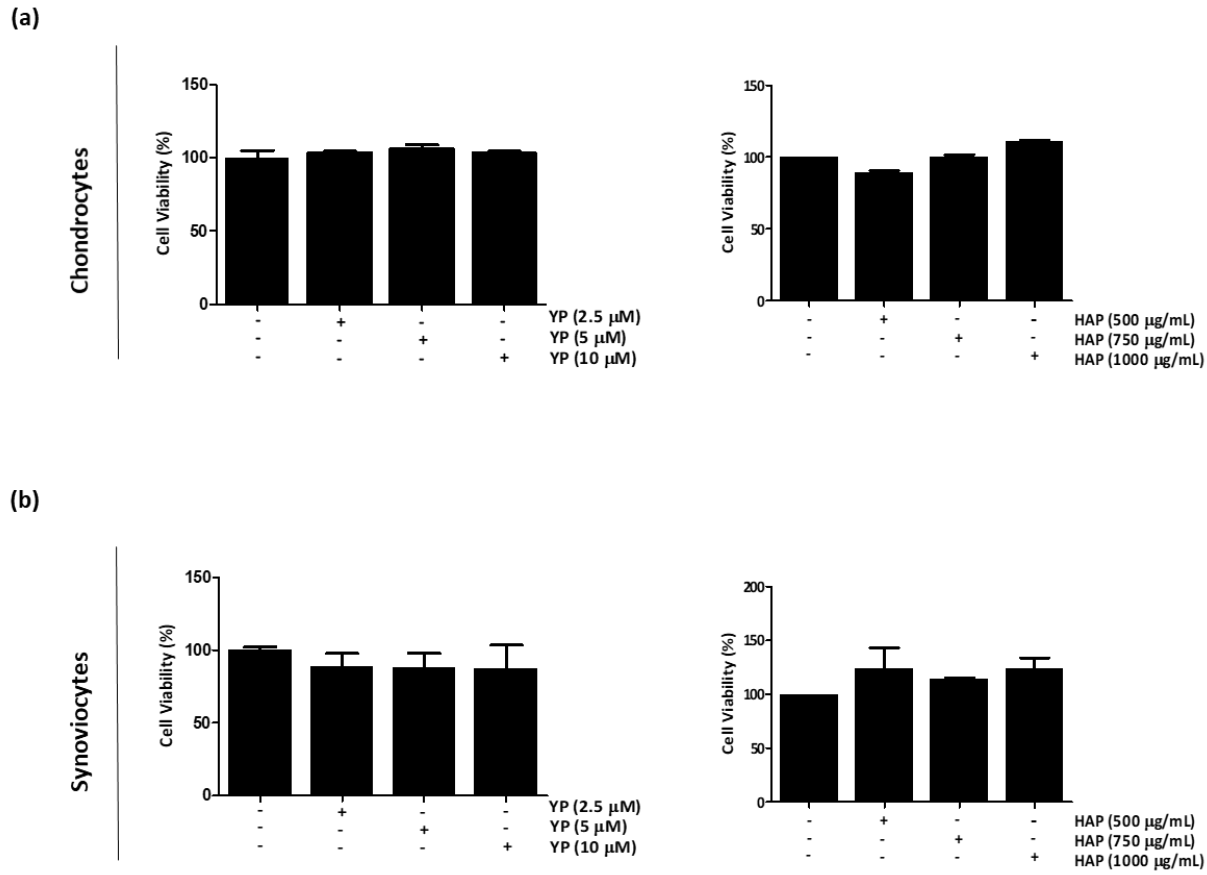

Figure 4.9 Viability of human primary chondrocytes (a) and synoviocytes (b) exposed to different amentadione (YP) concentrations for 24 h and exposed to different hydroxyapatite (HAP) concentrations for 72 h. Control (Ctr) corresponds to culture media of non-treated cells.

These results demonstrate a promising anti-inflammatory effect of YP in the articular OA cell system model, through downregulation of inflammatory genes, either when stimulated with IL-1β or treated with the mineralizing agent HAP.

4.3.3 YP modulates cartilage homeostasis under mineralizing conditions in the *ex-vivo* cartilage explant model

The effect of YP in response to HAP stimulation was assessed in *ex vivo* assays, using cartilage tissue explants, classified as normal- to early-OA tissues through the modified Mankin score (258), as previously depicted in Chapter 3.

The results showed that stimulated explants expressed higher levels of ECM-related genes, collagen-10 (Col10), runt-related transcription factor-2 (Runx2) and membrane metalloprotease-3 (MMP3) (**Figure 4.10**) and of the catabolic OA marker MMP3 and of the inflammatory marker IL-6, responsible for ECM degradation (**Figure 4.11**). Pre-treatment of human cartilage explants with YP resulted not only in the down-regulation of the differentiation and ECM-related genes (**Figure 4.10**), but also decreased levels of the OA marker MMP3 and of the inflammatory marker IL-6 (**Figure 4.11**), relative to stimulated explants.

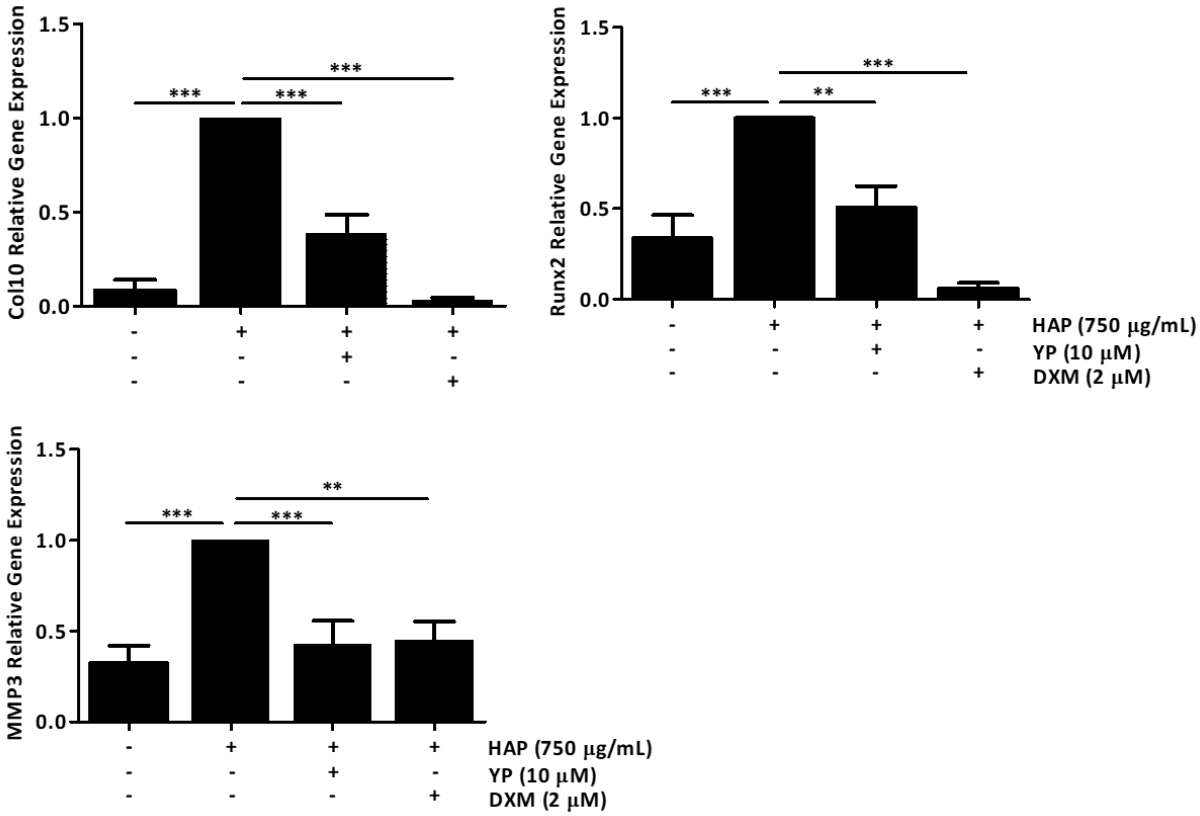

Figure 4.10 YP downregulates cell differentiation and extracellular matrix degradation markers associated with OA in the *ex vivo* cartilage explant model under HAP stimulation. Human cartilage explants were pre-treated with 10µM YP for 24h, followed by 72h of 750 µg/mL HAP stimulation. Relative gene expression of Col10, Runx2 and MMP3 was determined by qPCR. DXM indicates treatments with 2 µM dexamethasone. Data are presented as means of at least three independent experiments. All graphs show mean ±SD. One-way Anova and multiple comparisons were achieved with the Dunnett's test. Statistical significance was defined as $p \leq 0.005$ (**) and $p \leq 0.0005$ (***).

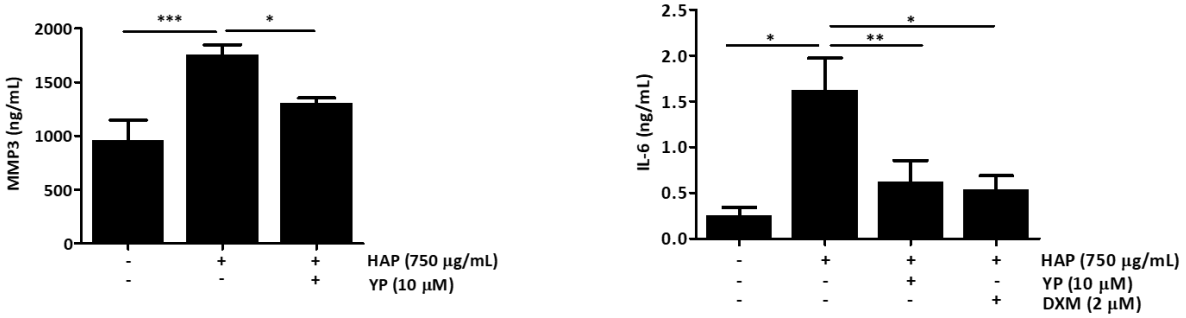

Figure 4.11 YP downregulates pro-inflammatory marker levels associated with OA in the HAP-stimulated *ex vivo* cartilage explant model. Human cartilage explants were pre-treated with 10µM YP for 24h, followed by 72h of 750 µg/mL HAP stimulation, and levels of MMP3 and IL-6 accumulation in the culture media were determined by ELISA. DXM indicates treatments with 2 µM dexamethasone. Data are presented as means of at least three independent experiments. All graphs show mean ±SD. One-way Anova and multiple comparisons were achieved with the Dunnett's test. Statistical significance was defined as $p \leq 0.05$ (*), $p \leq 0.005$

(**) and $p \leq 0.0005$ (***).

4.3.4. YP function as a protective agent against cartilage deterioration under OA promoting conditions in an explant-based co-culture OA model

The *ex vivo* explant-based co-culture OA model previously developed in Chapter 3, was used to study the effects of YP in the complex crosstalk of cartilage and synovial membrane. YP pre-treatment of human cartilage explants co-cultured with primary human synoviocytes and stimulated with IL-1β, consistently diminished the increased gene expression of COX-2, IL-6 and MMP3 in cartilage explants (**Figure 4.12**).

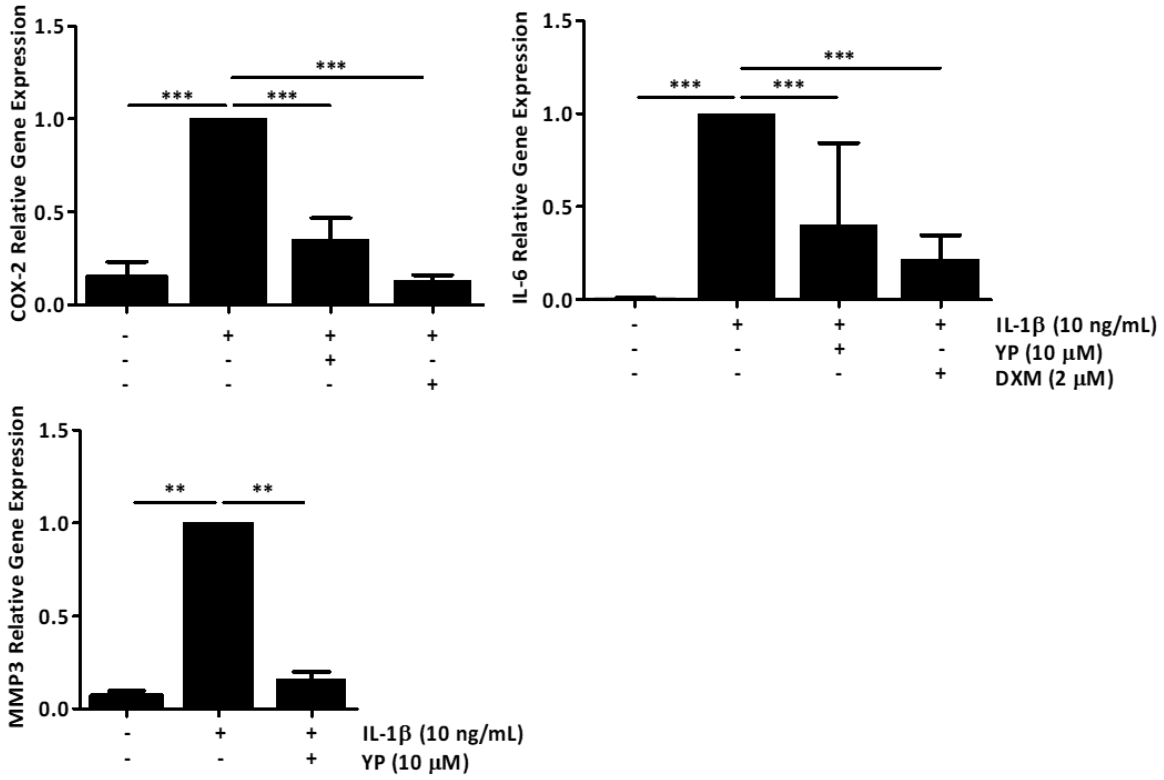

Figure 4.12. YP downregulates pro-inflammatory and ECM degradation markers associated with OA in the explant-based co-culture OA model under inflammatory stimulation with IL-1β. Cartilage explants co-cultured with human primary synoviocytes were pre-treated with 10 μM YP for 24h, followed by 24h of 10 ng/mL IL-1β stimulation. Relative gene expression of COX-2, IL-6 and MMP3 in cartilage explants were determined by qPCR. DXM indicates treatments with 2 μM dexamethasone. Data are presented as means of at least three independent experiments. One-way Anova and multiple comparisons were achieved with the Dunnett's test. All graphs show mean ± SD. Statistical significance was defined as $p \leq 0.05$ (*), $p \leq 0.005$ (**) and $p \leq 0.0005$ (***).

In a similar way, increased levels of MMP3 and IL-6 in the cell culture media of co-culture cartilage explants treated with HAP were reduced with the YP pre-treatment (**Figure 4.13**).

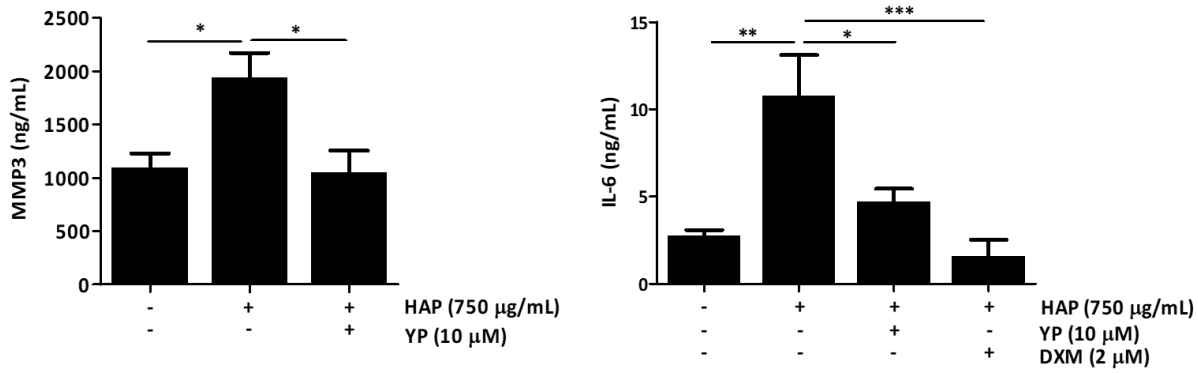

Figure 4.13 YP decreases the production of ECM degradation and pro-inflammatory markers in the explant-based co-culture OA model under mineralizing conditions. Cartilage explants co-cultured with human primary synoviocytes were pre-treated with 10 µM YP 24h, followed by 72h of 750 µg/mL HAP stimulation. Levels of MMP3 and IL-6 accumulation in the co-culture media were determined by ELISA. DXM indicates treatments with 2 µM dexamethasone. Data are presented as means of at least three independent experiments. One-way Anova and multiple comparisons were achieved with the Dunnett's test. All graphs show mean ± SD. Statistical significance was defined as $p \leq 0.05$ (*), $p \leq 0.005$ (**) and $p \leq 0.0005$ (***).

Overall, considering the effects of YP at cartilage tissue level, evaluated using the cartilage explants and the explant-based co-culture models, the results suggest that YP exerts a cartilage protective effect, by reducing inflammatory reactions and preventing chondrocyte differentiation towards extracellular matrix mineralization and degradation.

4.3.5 YP downregulates NF-kB expression and inhibits IkBα phosphorylation in primary chondrocyte cells

Since YP was able to downregulate several pro-inflammatory mediators known to be directly regulated by the NF-kB signaling pathway, we investigated whether the anti-inflammatory action of YP was due to its effect on NF-kB transcription and phosphorylation of its inhibitor IkBα.

In human primary articular chondrocytes, pre-treated with YP for 24h followed by IL-1β stimulation, NF-kB expression was significantly downregulated at all-time points tested (**Figure 4.14**).

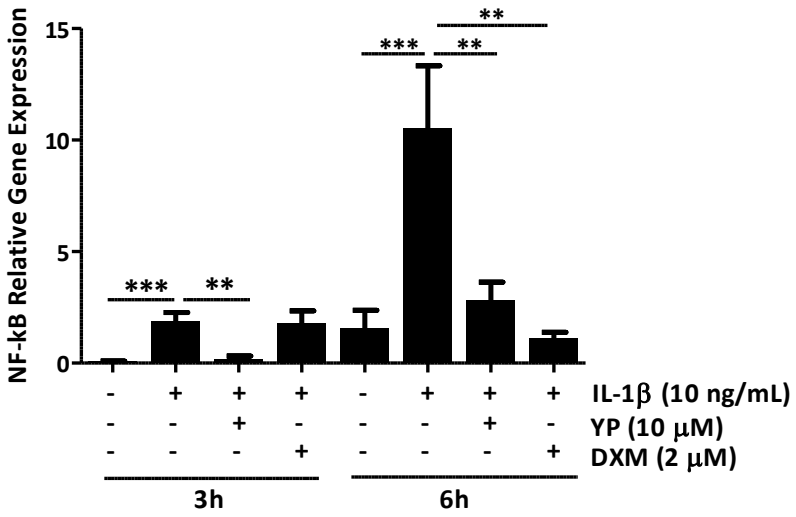

Figure 4.14 YP downregulates NF-kB expression in IL-1β-stimulated primary articular chondrocytes. Relative gene expression of NF-kB was determined by qPCR at 3h and 6h post 10 ng/mL IL-1β stimulation. Data is presented as mean of three independent experiments. Graph shows mean ±SD. One-way Anova and multiple comparisons were achieved with the Dunnett's test. Statistical significance was defined as $p \leq 0.005$ (**) and $p \leq 0.0005$ (***).

To determine the effect of YP in IkBα phosphorylation (pIkBα), known to precede NF-kB nuclear translocation, an initial experiment was performed under IL-1β stimulation, and pIkBα was evaluated at different times of exposition to the stimuli. Western blot analysis of chondrocyte protein extracts indicated increased levels of pIkBα from 30 min to 60 min of IL-1β treatment (**Figure 4.15**).

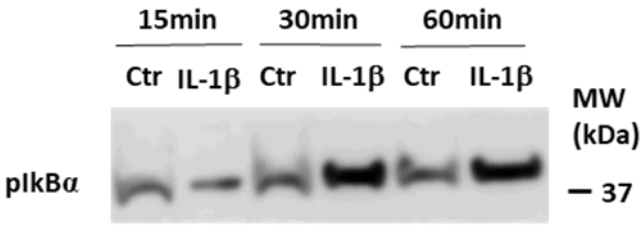

Figure 4.15 Indication on the time point with increased pIkBα after IL-1β stimulation. 20 μg of total protein extracts of chondrocytes cultured in control (Ctr) and treated with 10 ng/mL IL-1β for different time points, were analysed by Western blot to detect pIkBα. Position of relevant molecular mass marker (kDa) is indicated on the right side.

Based on that, detection of pIkBα in chondrocytes pre-treated with YP for 24h followed by 30 min IL-1β stimulation suggests a reduction of pIkBα in the YP treated chondrocytes relatively to the untreated and IL-1β stimulated cells (**a, Figure 4.16**). Specific ELISA assays measuring pIkBα and total IkBα at 30 min shown that YP treatment reduces the ratio of

pIkBα/total IkBα (**b, Figure 4.16**), strongly indicating an effect of YP on IkBα phosphorylation.

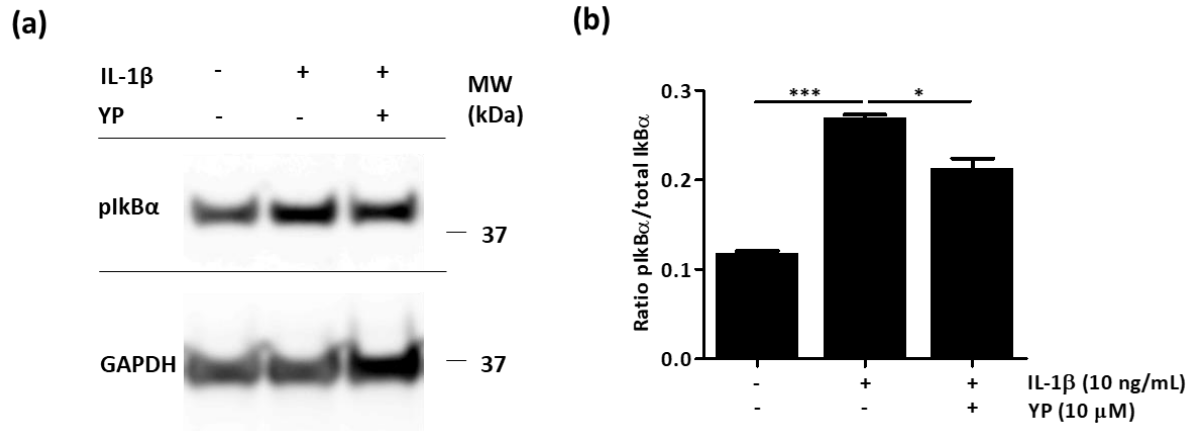

Figure 4.16 YP downregulates inhibits IkBα phosphorylation in IL-1β-stimulated primary articular chondrocytes. (a) Total protein extracts of chondrocytes cultured in untreated conditions, stimulated with 10 ng/mL IL-1β for 30 minutes, and pre-treated with YP (10 μM) followed by 30 minutes of 10 ng/mL IL-1β treatment, were analysed by Western blot to detect pIkBα. Position of relevant molecular mass marker (kDa) is indicated on the right side and GAPDH was used as loading control. (b) The pIkBα ratio (pIkBα/total IkBα) was determined in total protein extracts of chondrocytes cultured in control conditions (Ctr); 30 min of IL-1β (10 ng/ml) treatment; and pre-treated with YP for 24 h followed by 30 min of IL-1β stimulation (YP), by measuring the content of total and pIkBα with the specific InstantOne ELISA assay kit. Data is presented as mean of two out of four representative experiments. Graph shows mean ±SD. One-way Anova and multiple comparisons were achieved with the Dunnett's test. Statistical significance was defined as $p \leq 0.05$ (*) and $p \leq 0.0005$ (***).

These results demonstrate an anti-inflammatory effect of YP in articular chondrocytes, by downregulation of NF-kB expression, and inhibition of its activation through modulation of IkBα phosphorylation, and consequent downregulation of several NF-kB-related target genes.

4.4 Discussion

The main aim in this chapter was to explore the potential activity of a series of pure meroditerpenoids isolated from the brown alga *C. usneoides* (283). The first activity studies concerning the meroditerpenoids YP, Cyd G, Cyd K and Cy C, are indicative of some capacity of diminishing the inflammatory response of THP-1 MoM, promoted by IL-1β and HAP. Among those, YP was selected and its activity profile analysed throughout the activity screening pipeline, described in Chapter 3. YP is able to decrease inflammation, cell differentiation and extracellular matrix (ECM) degradation in the *in vitro*/ *ex vivo* OA model

systems included in the pipeline. The workflow includes increasing levels of complexity, from 2D monolayer cultures of THP-1 MoM, primary chondrocytes and synoviocytes, to *ex vivo* culture of human cartilage explants and a newly developed OA explant-based co-culture model. This co-culture model was developed to mimic the crosstalk between cartilage explants and synoviocytes occurring in the OA context of cartilage degradation and inflammation interplay and closely resembling the *in vivo* joint interplay. YP consistently promoted a protective effect under pro-inflammatory and mineralizing stimuli. These results bring new evidence on the health benefits of YP as a protective OA agent by attenuating cartilage degrading processes under known OA promoting stimuli, with consequent cartilage maintenance promoting effects, with potential therapeutic application.

YP has previously shown to have anti-inflammatory properties associated with the inhibition of TNFα in LPS-activated human macrophages (283). In the present study, we demonstrated that YP was able to counteract inflammation, cell differentiation and ECM degradation, induced not only by IL-1β but also by hydroxyapatite, in all OA models, including primary articular cells, cartilage explants and *ex vivo* explant-based co-culture systems. These effects were demonstrated at multiple levels. Through downregulation of master players involved in pro-inflammatory reactions, such as NF-kB, COX-2 and IL-6, and the ECM catabolic marker MMP3, YP is directly contributing to preserve cartilage homeostasis, by avoiding ECM disruption and cartilage collapse. Similarly, the capacity to downregulate crucial genes involved in chondrocyte differentiation such as Col10 and Runx2, suggests YP as an inhibitor of chondrocytes hypertrophic differentiation. The resulting decrease of apoptosis and ECM mineralization, indirectly contributes to a consequent decrease of pro-inflammatory reactions, ultimately preserving cartilage homeostasis. Although our studies were not directed to evaluate the effect of YP as a structural cartilage-modifying drug, its capacity to inhibit early molecular events leading to joint deterioration, suggests YP as a potential disease modifying OA drug, worth to be further investigated.

Also, this YP protective role might represent a promising alternative to the anti-inflammatory drugs commercially available to manage symptomatology associated with OA and chronic autoimmune and inflammatory diseases, mostly based on NSAIDs target to inactivate COX enzymes (COX-1 and COX-2) (284), or biologics targeting crucial pro-inflammatory cytokines such as TNFα and IL-1β (295-296). Although some effectiveness has been shown in slowing inflammatory reactions, the growing list of adverse side effects and the high percentage of patients presenting no response to these treatments, clearly demonstrate the urgent need for safer and more effective anti-inflammatory drugs. In this field, natural derived

products, such as YP, have been considered as promising and valid alternatives. Some examples are the tetracyclic triterpenoid glycoside Ginsenoside Rb1 (G-Rb1) and curcumin, which have shown both *in vitro* and *in vivo*, the capacity of targeting the production of several pro-inflammatory species and promoting the synthesis of anti-inflammatory mediators, with cartilage protective effects (297-300).

Considering the pivotal role of NF-kB as a major regulator of inflammation, many strategies have been developed to block NF-kB signaling in a variety of inflammatory disease settings (289). Although in the context of OA these strategies are still in their infancy, the crucial role of NF-kB signaling mediating inflammatory responses, but also the hypertrophic conversion of articular cartilage chondrocytes, leading to ECM damage and cartilage destruction, is of paramount importance in the disease context (265,302). Various terpenoids, monoterpenoids, sesquiterpenoids, diterpenoids, sesterterpenoids, triterpenoids, tetraterpenoids and polyterpenoids inhibit NF-kB signaling pathway through IkB phosphorylation, DNA binding and p65 translocation (291). An anticipated benefit of the study of a single chemical entity, such as YP, may be the convenience to understand its molecular mechanism. Our results demonstrate that YP is able to downregulate NF-kB expression and decrease IkBα phosphorylation in chondrocytes, strongly suggesting that YP cartilage protective properties are associated, at least in part, with the inhibition of NF-kB nuclear translocation and consequent decreased activation of catabolic pathways, including expression of cytokines and chemokines, inflammatory mediators, matrix degrading enzymes, and regulators of chondrocytes differentiation. In agreement, YP treatments consistently decreased levels of COX-2 and IL-6, MMP3, Col10 and Runx2 in cartilage tissue, clearly demonstrating the potential of YP in ameliorating cartilage homeostasis and integrity, a good rationale for the exploitation of YP in the treatment of OA.

4.5 Acknowledgements

Acknowledges to Prof. Eva Eva Zubía, Faculty of Marine and Environmental Sciences, University of Cadiz, for the pure marine derived compounds tested in this study: YP, Cyd G, Cyd K and Cy C.

Sincere gratitude to the Departamento de Ortopedia do Hospital Particular do Algarve - Gambelas (Faro, Portugal) for their collaboration, which made the collection of human biological material for this study possible. In particular, we extend our profound appreciation

to Doctor Acácio Ramos, who played a crucial role in collecting the control and osteoarthritic biological samples, as well as providing valuable clinical information about the subjects. Doctor Acácio Ramos showed great interest in this project and was always available to address any questions related to osteoarthritis medical aspects. We also extend our thanks to Dr. Maria M. Carvalho, Dr. Henrique Cruz and Dr. João Paulo Sousa, from the same medical team for their availability and collaboration in this study.

We acknowledge Dr. Joana Magalhães and Dr. Francisco Blanco, from Unidad de Medicina Regenerativa, Grupo de Investigación en Reumatología (GIR), Instituto de Investigación Biomédica de A Coruña (INIBIC), Complejo Hospitalario Universitario de A Coruña (CHUAC), and Centro de Investigación Biomédica en Red (CIBER), Madrid for the primary cell cultures of synoviocytes and chondrocytes. A special thanks to Dr. Joana Magalhães for her appreciated help in the evaluation of the human cartilage explants collected and used in this study. We would like to thank Dr. Joana Magalhães for all the support and participation during this PhD, with very useful advices and encouragement.

Furthermore, we would like to acknowledge the support of Doctor José Enriquez and technician Alexandra Teixeira from Centro Hospitalar do Algarve (Departamento de Anatomia Patológica, Faro, Portugal). Their assistance has been of immense value. We are grateful to Doctor José Enriquez, the head of the department, for allowing this collaboration and providing expertise in analysing several histological characterization results. We also thank Alexandra Teixeira for her contributions in tissue paraffin embedding and some of the tissue sectioning in this chapter.

All primary antibodies used in this chapter were kindly provided by GenoGla Diagnostics (Universidade do Algarve, Faro, Portugal) or VitaK BV (University of Maastricht, Maastricht, The Netherlands).

Part of the work presented in this chapter represents our published results in Araujo, N. *et al*. (271).

Chapter 5

General conclusions and future perspectives

Chapter 5- General conclusions and future perspectives

Osteoarthritis (OA) remains as the most prevalent form of degenerative joint disorders. It is characterized by damage to the articular cartilage, accompanied by tissue inflammation, extracellular matrix (ECM) mineralization, and abnormal bone formation (304-306) Very often, OA occurrence remains undetected for many years, leading to irreversible damage to the cartilage. To worsened the situation, there are currently no effective disease-modifying drugs available to treat OA (292). Given the complex nature of OA and its underlying pathophysiologic mechanisms, it is crucial to achieve a deeper understanding of the molecular factors and pathways involved in the disease development and progression (292). The identification of new molecular targets, along with improvements in preclinical drug development testing, are essential in the search for new active compounds to prevent or manage OA.

In this study, in Chapter 2, novel data was obtained by assessing on the functional potential of encapsulated vitamin K-dependent protein (VKDP), Gla-rich protein (GRP), more specifically its uncarboxylated form (ucGRP), in the OA context. The aim was to explore the functionality of the encapsulated protein as a potential therapeutic strategy for OA, in THP-1 macrophages and articular cells. Further, the anti-inflammatory capacity of the marine-derived compound Amentadione was investigated, using a novel preclinical drug development pipeline here developed, aiming to mimic early stage OA.

Although bioactivity of ucGRP has been observed at various levels, its eventual use as a therapeutic agent is limited by its low solubility at physiological pH. The approach to overcome this limitation was based on the encapsulation of ucGRP using chitosan-tripolyphosphate (CS-TPP) nanoparticles, taking advantage of the beneficial biological properties of CS. In addition to its high capacity of incorporating and releasing a variety of drugs, such as proteins, peptides, vitamins, and other bioactive compounds (246-248,307) studies have demonstrated chondroprotective properties of chitosan and its ability to inhibit cartilage degradation and inflammation in the synovial membrane (201-202), making it a potential synergistic partner for OA treatment. For that, the first part of this research was focused on the incorporation of ucGRP into the GRP-loaded FC/TPP nanoparticles (FCNG) formulation, through well-established procedures for CS-TPP nanoparticle production and protein encapsulation (239). Nanoencapsulation of ucGRP was further confirmed by flow cytometry.

The characterization of CS–TPP nanoparticles exhibited a nanoscale size range, varying

from 120 to 150 nm, and there was no significant difference in size between FCNG and FCNP nanoparticles, despite the high association efficiency of ucGRP. This can be attributed to the small size and low concentration of GRP that was uploaded onto the nanoparticles. Although the nanoparticles were successfully accomplished, the synthetic yield could, in the future, be further optimized by regulating chitosan concentrations and molecular weight, the degree of CS acetylation, and the CS/TPP molar ratio (238). FCNP and FCNG intense fluorescence emission formulations allow their easy detection to be quickly tracked intra- and extracellularly, which is a tool extensively used and suitable for several applications, including biomedical and pharmacological applications (235).

When the functionality of the encapsulated GRP in the chitosan-based nanoparticle (FCNG) as a potential therapeutic strategy for OA was assessed in LPS stimulated THP-1 MoM and IL-1β treated chondrocytes, results demonstrated that FCNG was non-cytotoxic and effectively act as an anti-inflammatory mediator. Indeed, FCNG treatment resulted in a response to pro-inflammatory mediators involved in several chronic inflammatory diseases (CIDs), such as LPS used to stimulate THP-1 macrophages, and IL-1β to activate articular chondrocytes. It is important to highlight that FCNG have shown the capacity to restrain the inflammatory response in activated macrophages and human cultured chondrocytes. These results are also indicative of an effective delivery system for GRP with the retention of the protein anti-inflammatory activity. In fact, although the mechanism of action of FCNG in different cell-specific inflammatory conditions remains unclear, cytometry data demonstrates the presence of FCNG in THP1-MoM cells after a 2-hour incubation, and a notable increase in intra- and extracellular GRP levels after 24 hours in THP1-MoM. These findings strongly support that the FCNG formulation facilitates sustained and prolonged delivery of ucGRP. The observed results align with previous findings in this study, that indicate minimal GRP release from nanoparticles when incubated in cell culture media, likely due to protein desorption from the nanoparticles surface (238). This suggests that the majority of GRP remains entrapped within the matrix of FCNG, being released in a constant and slow release rate (295) indicative of enhanced biological stability.

Importantly, and in concordance with literature (309-312), results show the anti-inflammatory activity of FCNP in all *in vitro* cell systems tested, strengthening the beneficial use of the CS excipient by fulfilling requirements and adding a synergetic therapeutic effect to GRP anti-inflammatory activity. The overall reduction in pro-inflammatory mediators point out to a promising therapeutic potential for FCNG in the treatment of chronic inflammatory diseases (CIDs).

This study also revealed that although the γ-carboxylation of Gla-rich protein (GRP) was essential for its anti-mineralization effect (164,166,168,178), it is not required for its anti-inflammatory activity in THP-1 MoM cells, consistent with previous findings in chondrocytes and synoviocytes (178,209). Both uncarboxylated GRP (ucGRP) and carboxylated GRP (cGRP) treatments resulted in decrease of the inflammatory response. However, the anti-inflammatory effect of ucGRP in THP-1 MoM seemed to be more prolonged and independent of the concentration compared to cGRP treatment (203). This suggests that GRP mechanisms of action as an anti-calcifying or anti-inflammatory agent still impact the inflammation-calcification relationship. Specifically, cGRP prevents chondrocyte differentiation towards a mineralizing and hypertrophic phenotype (76), reducing the probability of inflammatory events, while ucGRP promotes cartilage homeostasis and prevents ectopic calcification potentiation.

Overall, this study has successfully shown that incorporating GRP into CS-TPP nanoparticles yields a novel, stable, and biodegradable formulation of ucGRP with favourable physicochemical properties for biomedical applications. Importantly, this formulation retains the anti-inflammatory activity of GRP, enhancing the potential of GRP for treating various inflammation-related diseases. Moreover, this opens the way for future improvements in GRP nanoparticle technology, ultimately enabling a more effective anti-inflammatory therapy approach.

Further, in Chapter 3, a novel preclinical drug development pipeline for osteoarthritis was established, to screen potential new OA drugs. This pipeline was designed to evaluate the anti-mineralizing and anti-inflammatory potential of compounds in OA, as inflammation plays an important role by interacting with calcification in a cycle of extracellular matrix (ECM) degradation, apoptosis and mineral deposition in OA.

The synoviocyte and chondrocyte OA cell systems (173) were found to be effective for screening OA-related activities, such as inflammation and calcification. In response to inflammatory and mineralizing stimuli, treatment with IL-1β or HAP respectively, the primary articular cell systems showed increased expression of specific pathological markers associated with OA, including COX-2, NF-KB, and IL-6.

For a deeper understanding into cartilage degradation driven by inflammation, a human explant cartilage model was included in the workflow. To better mimick the articular context, we developed a more complex *ex vivo* 3D OA co-culture model combining human cartilage explants and synoviocytes. This 3D OA co-culture model was integrated into the final step of the pipeline to mimic early OA disease stages, providing a powerful tool for evaluating potential active compounds during the preclinical stage of drug development. This model allowed us to

study cell interactions and the role of the extracellular matrix.

Results from this 3D co-culture model indicated that treatment with inflammatory stimuli and hydroxyapatite nanocrystals induced cartilage catabolic processes and inflammation, evidenced by the expression of known markers. Treatment with hydroxyapatite also led to cartilage calcification and degradation, as evidenced by the overexpression of Col10 and Runx2 and the deposition of mineralized material in the ECM.

Furthermore, the up-regulation of COX-2, IL-6, and MMP3 in response to HAP and IL-1β highlighted the detrimental potential of calcification in OA. These results align with recent data showing that BCPs upregulate IL-6 in *in vivo* murine OA models, which in turn induces the expression of genes involved in calcification, promoting a positive loop of BCP formation (247). Increased BCP and IL-6 levels were associated with cartilage degradation through the activation of matrix-degrading enzymes in chondrocytes (247).

Overall, the results obtained from the developed 3D co-culture OA model clearly demonstrated its potential for studying the interplay between cartilage degradation and inflammation, which is critical in the drug development of potential anti-osteoarthritic compounds.

The final part of this research was concentrated on investigating the meroterpenoid compound YP, derived from the brown alga *Cystoseira usneoides*, as a potential therapeutic agent for osteoarthritis (OA). In Chapter 4, a series of *in vitro* and *ex vivo* experiments took place, using the newly established drug development pipeline. The results consistently demonstrated that YP effectively reduced inflammation, cell differentiation, and extracellular matrix (ECM) degradation along the screening biological pipeline model, described in Chapter 3. YP exhibited protective effects against pro-inflammatory and mineralizing stimuli, supporting its potential as a therapeutic agent for OA.

OA is characterized by cartilage loss and synovial membrane inflammation, and this study shows that YP targeted crucial molecular events associated with cartilage homeostasis disruption and inflammation, which contribute to disease progression. Specifically, YP decreased the expression of major regulators involved in pro-inflammatory reactions, such as NF-kB, COX-2, and IL-6, as well as ECM catabolic marker MMP3. Furthermore, YP inhibited chondrocyte differentiation towards hypertrophy, which led to decreased apoptosis and ECM mineralization, ultimately preserving cartilage homeostasis.

One of the key mechanisms underlying YP beneficial effects is its ability to downregulate NF-kB expression and decrease IkBα phosphorylation in chondrocytes. This inhibition leads to reduced activation of catabolic pathways, including the expression of

cytokines, chemokines, inflammatory mediators, matrix-degrading enzymes, and regulators of chondrocyte differentiation.

Overall, YP presents encouraging results as it inhibits early molecular events that contribute to joint deterioration. In addition to its anti-inflammatory effects, YP showed promise as a cartilage-protective agent, making it a potential candidate disease-modifying OA drug. While the current study demonstrates promising results in *in vitro* and *ex vivo* models, further translational research is necessary. Preclinical investigations employing animal models, including both genetically modified and wild-type mouse models, are widely used for toxicological assessments, exploring molecular mechanisms underlying OA, and to investigate genetic factors and specific genes involved in cartilage degeneration, bone remodeling, and inflammation (298). If preclinical in aimal models succeed, clinical trials in humans would be further required to validate the safety and efficacy of YP as a potential OA treatment in human.

In the context of future research perspectives for the management and improvement of OA treatment, we propose exploring some topics based on the evidence presented in this work.

The anti-inflammatory and anti-calcification effects of FCNG containing ucGRP should be further evaluated in *in vivo* OA mouse models. These studies will provide critical insights into the therapeutic potential of this nanoformulation and its safety profile. cGRP should be also encapsulated and detailed pharmacokinetic studies are necessary to understand the release kinetics of ucGRP or cGRP from FCNG *in vivo*. These studies could help optimize the dosing treatment and frequency of administration for effective results. Further investigations should be conducted to establish the optimal activity window for FCNG administration. This will involve determining the appropriate concentration and dosing frequency to achieve maximal anti-inflammatory and anti-calcification effects, first *in vitro* and further *in vivo* OA models, first in OA mouse models and then in clinical trials.

Various preclinical studies have provided clinical evidence of the preventive role of vitamin K1 in relation to OA. Low plasma levels of vitamin K1 have been linked to an increased prevalence and progression of OA (132-134). Additionally, clinical studies have shown an association between low vitamin K1 levels and joint cartilage loss (135-136). These findings underline the significance of vitamin K in maintaining bone and cartilage health, particularly in preventing OA and its progression. An important element in this context is the VKDP GRP. GRP plays a crucial role in preventing ectopic calcification and protecting articular cartilage, under pathological conditions like osteoarthritis and inflammatory arthritis (174,178). Considering the biological activity of cGRP, particularly in the context of OA, and the role of Vitamin K in its γ-carboxylation, it is worthy to explore vitamin K supplementation as a

beneficial and cost-effective strategy for preventing or treating OA. In line with that, encapsulation of GRP and Vitamin K might present a promising approach to ensure adequate Vitamin K levels for optimal function. Furthermore, this initiative can be seen as a combination therapy approach, in the sense that encapsulation of both elements may provide Vitamin K to act as co-factor in the carboxylation of GRP, but also to behave as an independent anti-inflammatory agent (174,178). By the potential synergistic effects of GRP and Vitamin K, this approach may promote bone and cartilage health, reducing the risk of developing OA or slow its progression effectively. Nanoencapsulation of Vitamin K within nanoliposome systems has been investigated (299). Liposomes are versatile lipid-based vesicles that can encapsulate both hydrophobic and hydrophilic substances due to their unique bilayer structure. This ability to encapsulate a wide range of compounds (300), makes liposomes a promising approach to synergistically incorporate both active compounds,Vitamin K and GRP, within a single system.

In summary, future research in this direction should investigate the potential benefits of vitamin K supplementation, either independently or in combination with GRP encapsulation, as a means to enhance bone and cartilage health, ultimately leading to improved OA management and treatment strategies.

References

1. World Health Organization. Osteoarthritis [Internet]. FactSheets; Detail; Osteoarthritis. 2023 [cited 2023 Sep 27]. Available from: https://www.who.int/news-room/fact-sheets/detail/osteoarthritis
2. StatPearls Publishing. Chronic Inflammation [Internet]. Pahwa; R, Goyal; A, Jialal I, editors. 2023. [updated 2023 Aug 7; cited 2023 Set 7]. Available from: https://www.ncbi.nlm.nih.gov/books/NBK493173/
3. Woodell-May JE, Sommerfeld SD. Role of Inflammation and the Immune System in the Progression of Osteoarthritis. J Orthop Res. 2020;38(2):253–7.
4. Hunter DJ, Bierma-Zeinstra S. Osteoarthritis. Lancet. 2019;393(10182):1745–59.
5. Loeser RF, Goldring SR, Scanzello CR, Goldring MB. Osteoarthritis: A Disease of the Joint as an Organ. Arthritis Rheum. 2012;64(6):1697–707.
6. Luong M-LN, Cleveland RJ, Nyrop KA, Callahan LF. Social determinants and osteoarthritis outcomes. Aging health. 2012;8(4):413–37.
7. Veronese N, Cereda E, Maggi S, Luchini C, Solmi M, Smith T, et al. Osteoarthritis and mortality: A prospective cohort study and systematic review with meta-analysis. Semin Arthritis Rheum. 2016;46(2):160–7.
8. Centers for Disease Control and Prevention. Osteoarthristis (OA) [Internet]. 2020. p. [updated 2020 Jul 27; cited 2023 Set 7]. Available from: https://www.cdc.gov/arthritis/basics/osteoarthritis.htm
9. Alliance OA, Centers for Disease Control and Prevention, Foundation A. A National Public Health Agenda for Osteoarthritis : 2020 Update. 2020;1–23.
10. Woolf AD, Pfleger B. Burden of major musculoskeletal conditions. Bull World Health Organ. 2003;81(9):646–54.
11. Veronese N, Trevisan C, De Rui M, Bolzetta F, Maggi S, Zambon S, et al. Association of Osteoarthritis with Increased Risk of Cardiovascular Diseases in the Elderly: Findings from the Progetto Veneto Anziano Study Cohort. Arthritis Rheumatol. 2016;68(5):1136–44.
12. Lee Y, Lee SH, Lim SM, Baek SH, Ha IH. Mental health and quality of life of patients with osteoarthritis pain: The sixth Korea National Health and Nutrition Examination Survey (2013–2015). PLoS One. 2020;15(11 November):1–17.
13. Piva SR, Susko AM, Khoja SS, Josbeno DA, Fitzgerald GK, Toledo FGS. Links between osteoarthritis and diabetes: Implications for management from a physical activity perspective. Vol. 31, Clinics in Geriatric Medicine. 2015. p. 67–87.
14. Beaudart C, Biver E, Bruyère O, Cooper C, Al-Daghri N, Reginster JY, et al. Quality of life assessment in musculo-skeletal health. Aging Clin Exp Res. 2018;30(5):413–8.
15. Abramoff B, Caldera FE. Osteoarthritis: Pathology, Diagnosis, and Treatment Options. Med Clin North Am. 2020;104(2):293–311.
16. Pereira D, Peleteiro B, Araújo J, Branco J, Santos RA, Ramos E. The effect of osteoarthritis definition on prevalence and incidence estimates: A systematic review. Osteoarthr Cartil. 2011;19(11):1270–85.
17. Alami S, Boutron I, Desjeux D, Hirschhorn M, Meric G, Rannou F, et al. Patients' and practitioners' views of knee osteoarthritis and its management: A qualitative interview study. Vol. 6, PLoS ONE. 2011.
18. Word Health Organization. Global Health Estimates [Internet]. 2019. Available from: https://www.who.int/data/global-health-estimates
19. Safiri S, Kolahi AA, Smith E, Hill C, Bettampadi D, Mansournia MA, et al. Global, regional and national burden of osteoarthritis 1990-2017: A systematic analysis of the Global Burden of Disease Study 2017. Ann Rheum Dis. 2020;1–10.

20. Prieto-Alhambra D, Judge A, Javaid MK, Cooper C, Diez-Perez A, Arden NK. Incidence and risk factors for clinically diagnosed knee, hip and hand osteoarthritis: Influences of age, gender and osteoarthritis affecting other joints. Ann Rheum Dis. 2014;73(9):1659–64.
21. Yu D, Peat G, Bedson J, Jordan KP. Annual consultation incidence of osteoarthritis estimated from population-based health care data in England. Rheumatol (United Kingdom). 2015;54(11):2051–60.
22. Quicke JG, Conaghan PG, Corp N, Peat G. Osteoarthritis year in review 2021: epidemiology & therapy. Osteoarthr Cartil. 2022;30(2):196–206.
23. Global Burden of Disease. Global Burden of Disease Study 2019 (GBD 2019) Results [Internet]. 2019. [updated 2023 Set 71; cited 2022 Nov 4]. Available from: https://www.healthdata.org/research-analysis/gbd
24. James SL, Abate D, Abate KH, Abay SM, Abbafati C, Abbasi N, et al. Global, regional, and national incidence, prevalence, and years lived with disability for 354 Diseases and Injuries for 195 countries and territories, 1990-2017: A systematic analysis for the Global Burden of Disease Study 2017. Lancet. 2018;392(10159):1789–858.
25. Cui A, Li H, Wang D, Zhong J, Chen Y, Lu H. Global, regional prevalence, incidence and risk factors of knee osteoarthritis in population-based studies. EClinicalMedicine. 2020;29–30:100587.
26. Yahaya I, Wright T, Babatunde OO, Corp N, Helliwell T, Dikomitis L, et al. Prevalence of osteoarthritis in lower middle- and low-income countries: a systematic review and meta-analysis. Rheumatol Int. 2021;41(7):1221–31.
27. Branco M, Nogueira P, Contreiras T. Uma observação sobre estimativas da prevalência de algumas doenças crónicas, em Portugal Continental. 2005.
28. Liga Portuguesa Contra as Doenças Reumáticas (LPCDR). Estatisticas das Doenças Reumáticas [Internet]. 2013.[updated 2023 Jun 19; cited 2023 Set 7]. Available from: http://www.lpcdr.org.pt/index.php?option=com_content&view=cate gory&id=69&Itemid=128.
29. Branco JC, Rodrigues AM, Gouveia N, Eusébio M, Ramiro S, Machado PM, et al. Prevalence of rheumatic and musculoskeletal diseases and their impact on health-related quality of life, physical function and mental health in Portugal: Results from EpiReumaPt- a national health survey. RMD Open. 2016;2(1).
30. Kluzek S, Sanchez-Santos MT, Leyland KM, Judge A, Spector TD, Hart D, et al. Painful knee but not hand osteoarthritis is an independent predictor of mortality over 23 years follow-up of a population-based cohort of middle-aged women. Ann Rheum Dis. 2016;75(10):1749–56.
31. Cleveland RJ, Alvarez C, Schwartz TA, Losina E, Renner JB, Jordan JM, et al. The impact of painful knee osteoarthritis on mortality: a community-based cohort study with over 24 years of follow-up. Osteoarthr Cartil. 2019;27(4):593–602.
32. Turkiewicz A, Kiadaliri AA, Englund M. Cause-specific mortality in osteoarthritis of peripheral joints. Osteoarthr Cartil. 2019;27(6):848–54.
33. Hoy DG, Smith E, Cross M, Sanchez-Riera L, Buchbinder R, Blyth FM, et al. The global burden of musculoskeletal conditions for 2010: An overview of methods. Ann Rheum Dis. 2014;73(6):982–9.
34. Chen A, Gupte C, Akhtar K, Smith P, Cobb J. The Global Economic Cost of Osteoarthritis: How the UK Compares. Arthritis. 2012;2012:1–6.
35. Altman R, Alarcon G, Appelrouth D, Bloch D, Borenstein K, Brandt K, et al. The american college of rheumatology criteria for the classification and reporting of osteoarthritis of the hand. Arthritis Rheum. 1990;33(11):1601–10.
36. Altman R, Asch E, Bloch D, Bole G, Borenstein D, Brandt K, et al. The american college

of rheumatology criteria for the classification and reporting of osteoarthritis of the hip. Osteoarthr Rheum. 1991;34(5):505–14.
37. Kohn MD, Sassoon AA, Fernando ND. Classifications in Brief: Kellgren-Lawrence Classification of Osteoarthritis. Clin Orthop Relat Res. 2016;474(8):1886–93.
38. Riddle DL, Jiranek WA, Hull JR. Validity and reliability of radiographic knee osteoarthritis measures by arthroplasty surgeons. Orthopedics. 2013;36(1):25–32.
39. Guermazi A, Hayashi D, Roemer F, Felson DT, Wang K, Lynch J, et al. Severe radiographic knee osteoarthritis - does Kellgren and Lawrence grade 4 represent end stage disease? - the MOST study. Osteoarthr Cartil. 2015;23(9):1499–505.
40. Zhang Q, Li H, Zhang Z, Yang F, Chen J. Serum metabolites as potential biomarkers for diagnosis of knee osteoarthritis. Dis Markers. 2015;2015.
41. Flemming DJ, Gustas-French CN. Rapidly Progressive Osteoarthritis: a Review of the Clinical and Radiologic Presentation. Curr Rheumatol Rep. 2017;19(7).
42. Hana S, Aicha BT, Selim D, Ines M, Rawdha T. Clinical and Radiographic Features of Knee Osteoarthritis of Elderly Patients. Curr Rheumatol Rev. 2018;14(2):181–7.
43. Pereira D, Ramos E, Branco J. Osteoarthritis. Acta Med Port. 2015;28(Jan-Feb):99–106.
44. Sinusas K. Osteoarthritis:Diagnosis and treatment. Am Fam Physician. 2012;85(1):49–56.
45. Hanada M, Takahashi M, Furuhashi H, Koyama H, Matsuyama Y. Elevated erythrocyte sedimentation rate and high-sensitivity C-reactive protein in osteoarthritis of the knee: relationship with clinical findings and radiographic severity. Ann Clin Biochem. 2016;53(5):548–53.
46. Karande SP, Kini S. Osteoarthritis: Clinical and Radiological Correlation. J Assoc Physicians India. 2018;66(7):37–9.
47. Hayashi D, Roemer FW, Guermazi A. Imaging for osteoarthritis. Ann Phys Rehabil Med. 2016;59(3):161–9.
48. Okano T, Mamoto K, Di Carlo M, Salaffi F. Clinical utility and potential of ultrasound in osteoarthritis. Radiol Medica. 2019;124(11):1101–11.
49. Hayashi D, Roemer FW, Guermazi A. Magnetic resonance imaging assessment of knee osteoarthritis: current and developing new concepts and techniques. Clin Exp Rheumatol. 2019;37(5):88–95.
50. Glyn-Jones S, Palmer AJR, Agricola R, Price AJ, Vincent TL, Weinans H, et al. Osteoarthritis. Lancet. 2015;386(9991):376–87.
51. Khan M, Khanna V, Adill A, Ayeni OR, Bedi A, Bhandari M. Knee osteoarthritis: when arthroscopy can help Moin. Pol Arch Intern Med. 2018;128(2):121–5.
52. Ishijima M, Kaneko H, Kaneko K. The evolving role of biomarkers for osteoarthritis. Ther Adv Musculoskelet Dis. 2014;6(4):144–53.
53. Lotz M, Martel-Pelletier J, Christiansen C, Brandi ML, Bruyère O, Chapurlat R, et al. Value of biomarkers in osteoarthritis: Current status and perspectives. Ann Rheum Dis. 2013;72(11):1756–63.
54. Spil WE van, Drossaers-Bakker KW, Lafeber FPJG. Associations of CTX-II with biochemical markers of bone turnover raise questions on its tissue origin: data from CHECK, a cohort study of early osteoarthritis. Ann Rheum Dis. 20163;72(1):29–36.
55. Mehana ESE, Khafaga AF, El-Blehi SS. The role of matrix metalloproteinases in osteoarthritis pathogenesis: An updated review. Life Sci. 2019;234(June):116786.
56. Rocha FAC, Ali SA. Soluble biomarkers in osteoarthritis in 2022: year in review. Osteoarthr Cartil. 2023;31(2):167–76.
57. Szilagyi I, Vallerga C, Waarsing JH, Schiphof D, Bierma-Zeinstra SMA, Van Meurs J. Op0111 Plasma Proteomics Identifies Crtac1 As Biomarker for Osteoarthritis Severity and Progression. Ann Rheum Dis. 2021;80(Suppl 1):61.1-62.

58. Bay-Jensen AC, Bihlet A, Byrjalsen I, Andersen JR, Riis BJ, Christiansen C, et al. Serum C-reactive protein metabolite (CRPM) is associated with incidence of contralateral knee osteoarthritis. Sci Rep. 2021;11(1):1–10.
59. Roos EM, Arden NK. Strategies for the prevention of knee osteoarthritis. Nat Rev Rheumatol. 2016;12(2):92–101.
60. Yucesoy B, Charles LE, Baker B, Burchfiel CM, Branch MB, Effects H, et al. Occupational and genetic risk factors for osteoarthritis: A review Berran. Work. 2015;50(2):261–73.
61. Hunziker EB, Quinn TM, Häuselmann HJ. Quantitative structural organization of normal adult human articular cartilage. Osteoarthr Cartil. 2002;10(7):564–72.
62. Long F, Ornitz DM. Development of the endochondral skeleton. Cold Spring Harb Perspect Biol. 2013;5(1):1–20.
63. Knecht S, Vanwanseele B, Stüssi E. A review on the mechanical quality of articular cartilage - Implications for the diagnosis of osteoarthritis. Clin Biomech. 2006;21(10):999–1012.
64. Jurvelin J, Saamanen A-M, Arokoski J, Helminen HJ, Kiviranta I, Tammi M. Biomechanical properties of the canine knee articular cartilage as related to matrix proteoglycans and collagen. Eng Med. 1988;17(4):157–62.
65. Madry H, Luyten FP, Facchini A. Biological aspects of early osteoarthritis. Knee Surgery, Sport Traumatol Arthrosc. 2012;20(3):407–22.
66. Houard X, Goldring MB, Berenbaum F. Homeostatic mechanisms in articular cartilage and role of inflammation in osteoarthritis. Curr Rheumatol Rep. 2013;15(11).
67. Jr DWH, R L Brower KJJ. Articular cartilage. Anatomy, injury, and repair. Clin Pod Med Surg. 2001;18(1):35–53.
68. Goldring MB, Otero M, Plumb DA, Dragomir C, Favero M, El Hachem K, et al. Roles of inflammatory and anabolic cytokines in cartilage metabolism: Signals and multiple effectors converge upon MMP-13 regulation in osteoarthritis. Vol. 21, European Cells and Materials. 2011. p. 202–20.
69. Van der Kraan PM, Van den Berg WB. Chondrocyte hypertrophy and osteoarthritis: Role in initiation and progression of cartilage degeneration? Osteoarthr Cartil. 2012;20(3):223–32.
70. Dreier R. Hypertrophic differentiation of chondrocytes in osteoarthritis: The developmental aspect of degenerative joint disorders. Arthritis Res Ther. 2010;12(5).
71. Scanzello CR, Goldring SR. The Role of Synovitis in Osteoarthritis pathogenesis. Bone. 2012;51(2):249–57.
72. Konttinen YT, Čeponis A, Meri S, Vuorikoski A, Kortekangas P, Sorsa T, et al. Complement in acute and chronic arthritides: Assessment of C3c, C9, and protectin (CD59) in synovial membrane. Vol. 55, Annals of the Rheumatic Diseases. 1996;888–94.
73. Thielen NGM, Van der Kraan PM, Van Caam APM. TGFβ/BMP Signaling Pathway in Cartilage Homeostasis. Cells. 2019;8(9).
74. Mathiessen A, Conaghan PG. Synovitis in osteoarthritis: Current understanding with therapeutic implications. Arthritis Res Ther. 2017;19(1):1–9.
75. Ea H, Lioté F. Diagnosis and Clinical Manifestations of Calcium Pyrophosphate and Basic Calcium Phosphate Crystal Deposition Diseases Hang-Korng. Rheum Dis Clin NA. 2017;40(2):207–29.
76. Ea HK, Nguyen C, Bazin D, Bianchi A, Guicheux J, Reboul P, et al. Articular cartilage calcification in osteoarthritis: Insights into crystal-induced stress. Arthritis Rheum. 2011;63(1):10–8.
77. Vilder EY De, Vanakker OM. From variome to phenome: Pathogenesis, diagnosis and

management of ectopic mineralization disorders. World J Clin Cases. 2015;3(7):556.
78. Giachelli CM. Ectopic calcification: Gathering hard facts about soft tissue mineralization. Am J Pathol. 1999;154(3):671–5.
79. Felson DT, Anderson JJ, Naimark A, Kannel W, Meenan RF. The prevalence of chondrocalcinosis in the elderly and its association with knee osteoarthritis: the Framingham Study. J Rheumatol. 1989;16(9):1241–5.
80. Nalbant S, Martinez JAM, Kitumnuaypong T, Clayburne G, Sieck M, Schumacher HR. Synovial fluid features and their relations to osteoarthritis severity: New findings from sequential studies. Osteoarthr Cartil. 2003;11(1):50–4.
81. Liote F, Ea H. Clinical implications of pathogenic calcium crystals. Curr Opin Rheumatol. 2014;26(2):192–6.
82. Fuerst M, Niggemeyer O, Lammers L, Schäfer F, Lohmann C, Rüther W. Articular cartilage mineralization in osteoarthritis of the hip. BMC Musculoskelet Disord. 2009;10(1):1–8.
83. Molloy ES, Morgan MP, Doherty GA, Mcdonnell B, Hilliard M, Byrne JO, et al. Mechanism of basic calcium phosphate crystal-stimulated cyclo-oxygenase-1 up-regulation in osteoarthritic synovial fibroblasts. Rheumatol. 2008;(April):965–71.
84. Liu YZ, Jackson AP, Cosgrove SD. Contribution of calcium-containing crystals to cartilage degradation and synovial inflammation in osteoarthritis. Osteoarthr Cartil. 2009;17(10):1333–40.
85. Taruc-uy RL, Lynch SA. Diagnosis and Treatment of Osteoarthritis. Prim Care Clin Off Pract. 2013;December(40(4)):821–36.
86. Fernandes L, Hagen KB, Bijlsma JWJ, Andreassen O, Christensen P, Conaghan PG, et al. EULAR recommendations for the non-pharmacological core management of hip and knee osteoarthritis. Ann Rheum Dis. 2013;72(7):1125–35.
87. Colletti A, Cicero AFG. Nutraceutical approach to chronic osteoarthritis: From molecular research to clinical evidence. Int J Mol Sci. 2021;22(23).
88. Machado GC, Maher CG, Ferreira PH, Pinheiro MB, Lin CC, Day RO, et al. Efficacy and safety of paracetamol for spinal pain and osteoarthritis : systematic review and meta-analysis of randomised placebo controlled trials. Br Med J. 2015;Mar 31(350):h1225.
89. Smith SR, Deshpande BR, Collins JE, Katz JN, Losina E. Comparative pain reduction of oral non-steroidal anti-in fl ammatory drugs and opioids for knee osteoarthritis : systematic analytic review. Osteoarthr Cartil. 2016;24(6):962–72.
90. Bannuru RR, Schmid CH, Kent DM, Vaysbrot EE, Wong JB, McAlindon TE. Comparative effectiveness of pharmacologic interventions for knee osteoarthritis: a systematic review and network meta-analysis. Ann Intern Med. 2015;162(1):46–54.
91. Rannou F, Pelletier J, Martel-pelletier J. Efficacy and safety of topical NSAIDs in the management of osteoarthritis: Evidence from real-life setting trials and surveys. Semin Arthritis Rheum. 2016;45(4):S18–21.
92. Honvo G, Reginster JY, Rabenda V, Geerinck A, Mkinsi O. Safety of Symptomatic Slow - Acting Drugs for Osteoarthritis : Outcomes of a Systematic Review and Meta - Analysis. Vol. 36, Drugs & Aging. 2019. 65–99 p.
93. Guedes V, Castro JP, Brito I. Topical capsaicin for pain in osteoarthritis: A literature review. Reumatol Clin. 2018;14(1):40–5.
94. Migliorini F, Driessen A, Quack V, Sippel N, Cooper B, Mansy Y El, et al. Comparison between intra-articular infiltrations of placebo, steroids, hyaluronic and PRP for knee osteoarthritis: a Bayesian network meta-analysis. Arch Orthop Trauma Surg. 2021;141(9):1473–90.
95. Micheloni MRGM, Perusi MBF. Clinical comparison of oral administration and viscosupplementation of hyaluronic acid (HA) in early knee osteoarthritis.

Musculoskelet Surg. 2020;
96. Quinn RH, Murray JN, Pezold R, Sevarino KS. Surgical Management of Osteoarthritis of the Knee. J Am Acad Orthop Surg. 2018;26(9):e191–3.
97. Samvelyan HJ, Hughes D, Stevens C, Staines KA. Models of Osteoarthritis: Relevance and New Insights. Calcif Tissue Int. 2021;109(3):243–56.
98. Lee JI, Sato M, Kim HW, Mochida J. Transplantatation of scaffold-free spheroids composed of synovium-derived cells and chondrocytes for the treatment of cartilage defects of the knee. Eur Cell Mater. 2011;22(ext 2320):275–90.
99. Alizadeh-Osgouei M, Li Y, Wen C. A comprehensive review of biodegradable synthetic polymer-ceramic composites and their manufacture for biomedical applications. Bioact Mater. 2019;4(1):22.
100. Deplaine H, Lebourg M, Ripalda P, Vidaurre A, Mora G, Pr F, et al. Biomimetic hydroxyapatite coating on pore walls improves osteointegration of poly (L -lactic acid) scaffolds. J Biomed Mater Res - Part B Appl Biomater. 2013;101B(1):173–86.
101. Deplaine H, Lebourg M, Ripalda P, Vidaurre A, Sanz-Ramos P, Mora G, et al. Biomimetic hydroxyapatite coating on pore walls improves osteointegration of poly(L-lactic acid) scaffolds. J Biomed Mater Res - Part B Appl Biomater. 2013 Jan;101 B(1):173–86.
102. van Lent PLEM, van den Berg WB. Mesenchymal stem cell therapy in osteoarthritis: Advanced tissue repair or intervention with smouldering synovial activation? Arthritis Res Ther. 2013;15(2):1–2.
103. Xue J, Feng B, Zheng R, Lu Y, Zhou G, Liu W, et al. Engineering ear-shaped cartilage using electrospun fibrous membranes of gelatin/polycaprolactone. Biomaterials. 2013;34(11):2624–31.
104. Ozeki K, Hoshino T, Aoki H, Masuzawa T. Phase Composition of Sputtered Film from a Mixture Target of Hydroxyapatite and Strontium-apatite. J Mater Sci Technol. 2013;29(1):1–6.
105. Van Hong Thien D, Hsiao SW, Ho MH, Li CH, Shih JL. Electrospun chitosan/hydroxyapatite nanofibers for bone tissue engineering. J Mater Sci. 2013;48(4):1640–5.
106. Kim SE, Park JH, Cho YW, Chung H, Jeong SY, Lee EB, et al. Porous chitosan scaffold containing microspheres loaded with transforming growth factor-β1: Implications for cartilage tissue engineering. J Control Release. 2003;91(3):365–74.
107. Cao P, Li Y, Tang Y, Ding C, Hunter DJ. Pharmacotherapy for knee osteoarthritis: current and emerging therapies. Expert Opin Pharmacother. 2020;21(7):797–809.
108. Răduț R, Crăciun AM, Silaghi CN. Bone Markers in Arthropathies. Acta Clin Croat. 2019;58(4):716–25.
109. Karsdal MA, Michaelis M, Ladel C, Siebuhr AS, Bihlet AR, Andersen JR, et al. Disease-modifying treatments for osteoarthritis (DMOADs) of the knee and hip: lessons learned from failures and opportunities for the future. Osteoarthr Cartil. 2016;24(12):2013–21.
110. Carlson AK, Rachel A. Rawle, Adams E, Greenwood MC, Bothner B, June RK. Application of Global Metabolomic Profiling of Synovial Fluid for Osteoarthritis Biomarkers. Biochem Biophys Res Commun. 2018;499(2):182–8.
111. Carlson AK, Rawle RA, Wallace CW, Brooks EG, Greenwood MC, Olmer M, et al. Characterization of synovial fluid metabolomic phenotypes of cartilage morphological changes associated with osteoarthritis. Osteoarthr Cartil. 2019;27(8):1174–84.
112. Honek J. Preclinical research in drug development. Med Writ. 2017;26(4):5–8.
113. Rothbauer M, Reihs EI, Fischer A, Windhager R. A Progress Report and Roadmap for Microphysiological Systems and Organ-On-A-Chip Technologies to Be More Predictive Models in Human (Knee) Osteoarthritis. 2022;10(June):1–17.

114. Ingber DE. Human organs-on-chips for disease modelling, drug development and personalized medicine. Nat Rev Genet. 2022;23(August):467–91.
115. Houtman E, van Hoolwerff M, Lakenberg N, Suchiman EHD, van der Linden-van der Zwaag E, Nelissen RGHH, et al. Human Osteochondral Explants: Reliable Biomimetic Models to Investigate Disease Mechanisms and Develop Personalized Treatments for Osteoarthritis. Rheumatol Ther. 2021;8(1):499–515.
116. Brandt KD. Animal models of osteoarthritis. Biorheology. 2022;39(1–2):221–35.
117. Makarczyk MJ, Gao Q, He Y, Li Z, Gold MS, Hochberg MC, et al. Current Models for Development of Disease-Modifying Osteoarthritis Drugs. Tissue Eng - Part C Methods. 2021;27(2):124–38.
118. Conway R, Mccarthy GM, Conway R. Calcium-Containing Crystals and Osteoarthritis : an Unhealthy Alliance. Curr Rheumatol Rep. 2018;Mar 8(20 (3)):13.
119. Stock M, Schett G. Vitamin k-dependent proteins in skeletal development and disease. Int J Mol Sci. 2021;22(17).
120. Shearer M, Newman P. Metabolism and cell biology of vitamin K. Thromb Haemost. 2008;100:530–47.
121. Walther B, Karl JP, Booth SL, Boyaval P. Menaquinones , Bacteria , and the Food Supply : The Relevance of Dairy and Fermented Food Products to Vitamin K Requirements. Adv Nutr. 2013;4:463–73.
122. Okano T, Nakagawa K, Kamao M. In vivo metabolism of vitamin K: in relation to the conversion of vitamin K1 to MK-4. Clin Calcium. 2009;19(12):1779–87.
123. Simes DC, Viegas CSB, Araújo N, Marreiros C. Vitamin K as a diet supplement with impact in human health: Current evidence in age-related diseases. Nutrients. 2020;12(1).
124. Nakagawa K, Hirota Y, Sawada N, Yuge N, Watanabe M, Uchino Y, et al. Identification of UBIAD1 as a novel human menaquinone-4 biosynthetic enzyme. Nature. 2010;468(7320):117–21.
125. Nowicka B, Kruk J. Occurrence, biosynthesis and function of isoprenoid quinones. Biochim Biophys Acta - Bioenerg. 2010;1797(9):1587–605.
126. Xv F an, Chen J, Duan L, Li S. Research progress on the anticancer effects of vitamin K2 (Review). Oncol Lett. 2018;15:8926–34.
127. Markowska A, Antoszczak M, Markowska J, Huczyński A. Role of Vitamin K in Selected Malignant Neoplasms in Women. Nutrients. 2022;14(16):1–10.
128. Fusaro M, Cianciolo G, Brandi ML, Ferrari S, Nickolas TL, Tripepi G, et al. Vitamin K and osteoporosis. Nutrients. 2020;12(12):1–13.
129. Simes DC, Viegas CSB, Araújo N, Marreiros C. Vitamin K as a powerful micronutrient in aging and age-related diseases: Pros and cons from clinical studies. Int J Mol Sci. 2019;20(17).
130. Misra D, Booth SL, Tolstykh I, Felson DT, Nevitt MC, Lewis CE, et al. Vitamin K Deficiency Is Associated with Incident Knee Osteoarthritis. Am J Med. 2013;126:243–8.
131. Oka C, Akune T, Muraki S, En-yo Y, Yoshida M, Saika A, et al. Association of low dietary vitamin K intake with radiographic knee osteoarthritis in the Japanese elderly population : dietary survey in a population-based cohort of the ROAD study. J Orthop Sci. 2009;14:687–92.
132. Shea MK, Kritchevsky SB, Hsu F, Nevitt M, Booth SL, Kwoh CK, et al. The association between vitamin K status and knee osteoarthritis features in older adults: The Health, Aging and Body Composition Study. Osteoarthr Cartil. 2016;23:370–8.
133. Houston DK, Tooze JA, Neiberg RH, Hausman DB, Johnson MA, Cauley JA, et al. 25-hydroxyvitamin D status and change in physical performance and strength in older adults. Am J Epidemiol. 2012;176(11):1025–34.

134. Sunnerhagen, Drakenberg MT, Forsen S, Stenflo J. Effect of Ca2+ on the structure of vitamin K-dependent coagulation factors. Haemostasis. 1996;1:45–53.
135. Ellison EH, Castellino FJ. Adsorption of Vitamin K-Dependent Blood Coagulation Proteins To Spread Phospholipid Monolayers as Determined from Combined Measurements of the Surface Pressure and Surface Protein Concentration †. Biochemistry. 1998;2960(97):7997–8003.
136. Hoang QQ, Sicheri F, Howard AJ, Yang DSC. Bone recognition mechanism of porcine osteocalcin from crystal structure. Nature. 2003;425(6961):977–80.
137. Schurgers LJ, Cranenburg ECM, Vermeer C. Matrix Gla-protein: the calcification inhibitor in need of vitamin K. Thromb Haemost. 2008;4:593–603.
138. Hauschka P V, Lian JB, Gallop PM. Direct identification of the calcium-binding amino acid, y-carboxyglutamate, in mineralized tissue. Proc Nat Acad Sci USA. 1975;72(10):3925–9.
139. Katagiri T, Takahashi N. Regulatory mechanisms of osteoblast and osteoclast.pdf. 2002;(March):147–59.
140. Zoch ML, Clemens TL, Riddle RC. New Insights into the Biology of Osteocalcin. Bone. 2016;27:915–8.
141. Neve A, Corrado A, Cantatore FP. Osteocalcin: Skeletal and extra-skeletal effects. J Cell Physiol. 2013;228:1149–53.
142. Mizokami A, Kawakubo-Yasukochi T, Hirata M. Osteocalcin and its endocrine functions. Biochem Pharmacol. 2017;132(February):1–8.
143. Booth SL, Broe KE, Gagnon DR, Tucker KL, Hannan MT, McLean RR, et al. Vitamin K intake and bone mineral density in women and men. Am J Clin Nutr. 2003;77(2):512–6.
144. Naito K, Watari T, Obayashi O, Katsube S, Nagaoka I, Kaneko K. Relationship between serum undercarboxylated osteocalcin and hyaluronan levels in patients with bilateral knee osteoarthritis. Int J Mol Med. 2012;29(5):756–60.
145. Luo G, Ducy P, McKee MD, Pinero GJ, Loyer E, Behringer RR, et al. Spontaneous calcification of arteries and cartilage in mice lacking matrix GLA protien. Vol. 386, Nature. 1997. p. 78–81.
146. Egloff C, Hügle T, Valderrabano V. Biomechanics and pathomechanisms of osteoarthritis. Swiss Med Wkly. 2012;142(July):1–14.
147. Zebboudj AF, Imura M, Boström K. Matrix GLA protein, a regulatory protein for bone morphogenetic protein-2. J Biol Chem. 2002;277(6):4388–94.
148. Gheorghe SR, Craciun AM. Matrix Gla protein in tumoral pathology. Clujul Med. 2016;89:319–21.
149. Bjorklund G, Svanberg E, Dadar M, David JC, Salvatore C, Dominic JH, et al. The role of matrix Gla protein (MGP) in vascular calcification. Curr Med Chem. 2018;
150. Wallin R, Schurgers LJ, Loeser RF. Biosynthesis of the vitamin K-dependent matrix Gla protein (MGP) in chondrocytes: A fetuin-MGP protein complex is assembled in vesicles shed from normal but not from osteoarthritic chondrocytes. Osteoarthr Cartil. 2010;18(8):1096–103.
151. Heiss A, Duchesne A, Denecke B, Gro J, Yamamoto K, Renne T, et al. Structural Basis of Calcification Inhibition by a2-HS Glycoprotein/Fetuin-A. Biol Chem. 2003;278(15):13333–41.
152. Smith ER, Hanssen E, McMahon LP, Holt SG. Fetuin-A-Containing Calciprotein Particles Reduce Mineral Stress in the Macrophage. PLoS One. 2013;8(4).
153. Roy ME, Nishimoto SK. Matrix Gla protein binding to hydroxyapatite is dependent on the ionic environment: Calcium enhances binding affinity but phosphate and magnesium decrease affinity. Bone. 2002;31(2):296–302.

154. Sweatt A, Sane DC, Hutson SM, Wallin R. Matrix Gla protein (MGP) and bone morphogenetic protein-2 in aortic calcified lesions of aging rats. J Thromb Haemost. 2003;1(1):178–85.
155. Yagami K, Suh JY, Enomoto-Iwamoto M, Koyama E, Abrams WR, Shapiro IM, et al. Matrix GLA protein is a developmental regulator of chondrocyte mineralization and, when constitutively expressed, blocks endochondral and intramembranous ossification in the limb. J Cell Biol. 1999;147(5):1097–108.
156. Schurgers LJ, Joosen IA, Laufer EM, Chatrou MLL, Herfs M, Winkens MHM, et al. Vitamin K-Antagonists Accelerate Atherosclerotic Calcification and Induce a Vulnerable Plaque Phenotype. PLoS One. 2012;7:e43229.
157. Viegas CSB, Simes DC, Laize V, Williamson MK, Price PA, Cancela ML. Gla-rich Protein (GRP), A New Vitamin K-dependent Protein Identified from Sturgeon Cartilage and Highly Conserved. Biol Chem. 2008;283(52):36655–64.
158. Viegas CSB, Cavaco S, Neves PL, Ferreira A, João A, Williamson MK, et al. Gla-rich protein is a novel vitamin K-dependent protein present in serum that accumulates at sites of pathological calcifications. Am J Pathol. 2009;175(6):2288–98.
159. Viegas CSB, Herfs M, Rafael MS, Enriquez JL, Teixeira A, Luís IM, et al. Gla-Rich Protein Is a Potential New Vitamin K Target in Cancer : Evidences for a Direct GRP-Mineral Interaction. Biomed Res Int. 2014;2014.
160. Viegas CSB, Rafael MS, Enriquez JL, Teixeira A, Vitorino R, Luís IM, et al. Gla-rich protein acts as a calcification inhibitor in the human cardiovascular system. Arterioscler Thromb Vasc Biol. 2015;35(2):399–408.
161. Willems BA, Furmanik M, Caron MMJ, Chatrou MLL, Kusters DHM, Welting TJM, et al. Ucma/GRP inhibits phosphate-induced vascular smooth muscle cell calcification via SMAD-dependent BMP signalling. Sci Rep. 2018;8(1):1–11.
162. Dhore CR, Cleutjens JPM, Lutgens E, Cleutjens KBJM, Geusens PPM, Kitslaar PJEHM, et al. Differential expression of bone matrix regulatory proteins in human atherosclerotic plaques. Arterioscler Thromb Vasc Biol. 2001;21(12):1998–2003.
163. Viegas CSB, Santos L, Macedo AL, Matos AA, Silva AP, Neves PL, et al. Chronic kidney disease circulating calciprotein particles and extracellular vesicles promote vascular calcification: A role for GRP (Gla-Rich Protein). Arterioscler Thromb Vasc Biol. 2018;38(3):575–87.
164. Grady SO, Morgan MP. Microcalcifications in breast cancer: From pathophysiology to diagnosis and prognosis. BBA - Rev Cancer. 2018;1869(March):310–20.
165. Evrard S, Delanaye P, Kamel S, Cristol JP, Cavalier E, Arnaud J, et al. Vascular calcification: From pathophysiology to biomarkers. Clin Chim Acta. 2014;438:401–14.
166. Pasch A, Farese S, Gräber S, Wald J, Richtering W, Floege J, et al. Nanoparticle-Based Test Measures Overall Propensity for Calcification in Serum. J Am Soc Nephrol. 2012;23:1744–52.
167. Surmann-schmitt C, Dietz U, Kireva T, Adam N, Park J, Tagariello A, et al. Ucma , a Novel Secreted Cartilage-specific Protein with Implications in Osteogenesis. Biol Chem. 2008;283(11):7082–93.
168. Neacsu CD, Grosch M, Tejada M, Winterpacht A, Paulsson M, Wagener R, et al. Ucmaa (Grp-2) is required for zebrafish skeletal development. Evidence for a functional role of its glutamate γ-carboxylation. Matrix Biol. 2011;30(7–8):369–78.
169. Seuffert F, Weidner D, Baum W, Schett G, Stock M. Upper zone of growth plate and cartilage matrix associated protein protects cartilage during inflammatory arthritis. Arthritis Res Ther. 2018;20(1):1–13.
170. Stock M, Menges S, Eitzinger N, Geßlein M, Botschner R, Wormser L, et al. A dual role for UCMA in osteoarthritis- Inhibition of aggrecanases and promotion of bone turnover.

Arthritis Rheumatol. 2016;
171. Okuyan HM, Terzi MY, Karaboğa İ, Doğan S, Kalacı A. In vivo protective effects of UCMA against cartilage degeneration in monosodium iodoacetate-induced osteoarthritis model. Can J Physiol Pharmacol. 2020;I(1):45–8.
172. Sokolove J, Lepus CM. Role of inflammation in the pathogenesis of osteoarthritis: Latest findings and interpretations. Ther Adv Musculoskelet Dis. 2013;5(2):77–94.
173. Cavaco S, Viegas CSB, Rafael MS, Ramos A, Magalhães J, Blanco FJ, et al. Gla-rich protein is involved in the cross-talk between calcification and inflammation in osteoarthritis. Cell Mol Life Sci. 2016;73:1051–65.
174. Rafael MS, Cavaco S, Viegas CSB, Santos S, Ramos A, Willems BAG, et al. Insights into the association of Gla-rich protein and osteoarthritis, novel splice variants and γ-carboxylation status. Mol Nutr Food Res. 2014;58(8):1636–46.
175. Okuyan HM, Terzi MY, Ozcan O, Kalaci A. Association of UCMA levels in serum and synovial fluid with severity of knee osteoarthritis. Int J Rheum Dis. 2019;22(10):1884–90.
176. Jha RK, Zi-Rong X. Biomedical compounds from marine organisms. Mar Drugs. 2004;2(3):123–46.
177. Kiuru P, Valeria D'Auria M, Muller CD, Tammela P, Vuorela H, Yli-Kauhaluoma J. Exploring marine resources for bioactive compounds. Planta Med. 2014;80(14):1234–46.
178. Marine Pharmacology [Internet]. 2023 [cited 2022 Aug 12]. p. [updated 2023 Aug 14; cited 2023 Set 7]. Available from: https://www.marinepharmacology.org/approved
179. Monfort J, Pelletier JP, Garcia-Giralt N, Martel-Pelletier J. Biochemical basis of the effect of chondroitin sulphate on osteoarthritis articular tissues. Ann Rheum Dis. 2008;67(6):735–40.
180. Miller KL, Clegg DO. Glucosamine and chondroitin sulfate. Rheum Dis Clin North Am. 2011;37(1):103–18.
181. Volpi N. Chondroitin sulfate safety and quality. Molecules. 2019;24(8).
182. Jomphe C, Gabriac M, Hale TM, Héroux L, Trudeau LÉ, Deblois D, et al. Chondroitin sulfate inhibits the nuclear translocation of nuclear factor-kappaB in interleukin-1beta-stimulated chondrocytes. Basic Clin Pharmacol Toxicol. 2008;102(1):59–65.
183. De Los Reyes C, Ortega MJ, Zbakh H, Motilva V, Zubía E. Cystoseira usneoides: A Brown Alga Rich in Antioxidant and Anti-inflammatory Meroditerpenoids. J Nat Prod. 2016;79(2):395–405.
184. Cranenburg ECM, Schurgers LJ, Uiterwijk HH, Beulens JWJ, Dalmeijer GW, Westerhuis R, et al. Vitamin K intake and status are low in hemodialysis patients. Kidney Int. 2012;82(5):605–10.
185. Bito T, Teng F, Watanabe F. Bioactive Compounds of Edible Purple Laver Porphyra sp. (Nori). J Agric Food Chem Agric Food Chem. 2017;65:10685–92.
186. Tarento TDC, Mcclure DD, Vasiljevski E, Schindeler A, Dehghani F, Kavanagh JM. Microalgae as a source of vitamin K1. Algal Res. 2018;36:77–87.
187. Johnson TW, Shen G, Zybailov B, Kolling D, Reategui R, Beauparlant S, et al. Recruitment of a foreign quinone into the A1 site of photosystem I. I. Genetic and physiological characterization of phylloquinone biosynthetic pathway mutants in Synechocystis sp. PCC 6803. J Biol Chem. 2000;275:8523–30.
188. Collins MD, Jones D. Distribution of isoprenoid quinone structural types in bacteria and their taxonomic implications. MicrobiolRev. 1981;45:316–54.
189. Mimuro M, Tsuchiya T, Inoue H, Sakuragi Y, Itoh Y, Gotoh T, et al. The secondary electron acceptor of photosystem I in Gloeobacter violaceus PCC 7421 is menaquinone-4 that is synthesized by a unique but unknown pathway. FEBS Lett. 2005;579(17):3493–

6.
190. Ikeda Y, Komura M, Watanabe M, Minami C, Koike H, Itoh S, et al. Photosystem I complexes associated with fucoxanthin-chlorophyll-binding proteins from a marine centric diatom, Chaetoceros gracilis. Biochim Biophys Acta. 2008;1777:351–61.
191. Bolton-Smith C, Price RJ, Fenton ST, Harrington DJ, Shearer MJ. Compilation of a provisional UK database for the phylloquinone (vitamin K1) content of foods. Br J Nutr. 2000;83(4):389–99.
192. Roeck-holtzhauer Y De, Quere I, Claire C. Vitamin analysis of five planktonic microalgae and one macroalga. J Appl Phycol. 1991;3:259–64.
193. Qin Y. A comparison of alginate and chitosan fibres. Med Device Technol. 2004;15(1):34–7.
194. Kim IY, Seo SJ, Moon HS, Yoo MK, Park IY, Kim BC, et al. Chitosan and its derivatives for tissue engineering applications. Biotechnol Adv. 2008;26(1):1–21.
195. Comblain F, Rocasalbas G, Gauthier S, Henrotin Y. Chitosan: A promising polymer for cartilage repair and viscosupplementation. Biomed Mater Eng. 2017;28(s1):S209–15.
196. Hamza RZ, Al-Salmi FA, El-Shenawy NS. Chitosan and lecithin ameliorate osteoarthritis symptoms induced by monoiodoacetate in a rat model. Molecules. 2020;25(23).
197. Viegas C, Araújo N, Marreiros C, Simes D. The interplay between mineral metabolism, vascular calcification and inflammation in Chronic Kidney Disease (CKD): Challenging old concepts with new facts. Aging (Albany NY). 2019;11(12).
198. Frallonardo P, Ramonda R, Peruzzo L, Scanu A, Galozzi P, Tauro L, et al. Basic calcium phosphate and pyrophosphate crystals in early and late osteoarthritis: relationship with clinical indices and inflammation. Clin Rheumatol. 2018;37(10):2847–53.
199. Carlson AK, McCutchen CN, June RK. Mechanobiological implications of articular cartilage crystals. Curr Opin Rheumatol. 2017;29(2):157–62.
200. Ummarino A, Gambaro FM, Kon E, Andón FT. Therapeutic manipulation of macrophages using nanotechnological approaches for the treatment of osteoarthritis. Nanomaterials. 2020;10(8):1–24.
201. Piscaer TM, Müller C, Mindt TL, Lubberts E, Verhaar JAN, Krenning EP, et al. Imaging of activated macrophages in experimental osteoarthritis using folate-targeted animal single-photon-emission computed tomography/computed tomography. Arthritis Rheum. 2011;63(7):1898–907.
202. Kraus VB, McDaniel G, Huebner JL, Stabler T V., Pieper CF, Shipes SW, et al. Direct in vivo evidence of activated macrophages in human osteoarthritis. Osteoarthr Cartil. 2016;24(9):1613–21.
203. B Viegas CS, ben Costa RM, cia Santos L, Videira PA, Silva Z, Araú jo N, et al. Gla-rich protein function as an anti-inflammatory agent in monocytes/ macrophages: Implications for calcification-related chronic inflammatory diseases. PLoS One. 2017;12(5):e0177829.
204. Rizeq BR, Younes NN, Rasool K, Nasrallah GK. Synthesis, bioapplications, and toxicity evaluation of chitosan-based nanoparticles. Int J Mol Sci. 2019;20(22).
205. Dash M, Chiellini F, Ottenbrite RM, Chiellini E. Chitosan - A versatile semi-synthetic polymer in biomedical applications. Prog Polym Sci. 2011;36(8):981–1014.
206. Senapati S, Mahanta AK, Kumar S, Maiti P. Controlled drug delivery vehicles for cancer treatment and their performance. Signal Transduct Target Ther. 2018;3(1):1–19.
207. Mohebbi S, Nezhad MN, Zarrintaj P, Jafari SH, Gholizadeh SS, Saeb MR, et al. Chitosan in Biomedical Engineering: A Critical Review. Curr Stem Cell Res Ther. 2019;14(2):93–116.
208. Bellich B, D'Agostino I, Semeraro S, Gamini A, Cesàro A. "The good, the bad and the

ugly" of chitosans. Vol. 14, Marine Drugs. 2016.
209. He C, Hu Y, Yin L, Tang C, Yin C. Effects of particle size and surface charge on cellular uptake and biodistribution of polymeric nanoparticles. Biomaterials. 2010;31(13):3657–66.
210. Elzoghby AO, Samy WM, Elgindy NA. Protein-based nanocarriers as promising drug and gene delivery systems. J Control Release. 2012;161(1):38–49.
211. Oprenyeszk F, Sanchez C, Dubuc JE, Maquet V, Henrist C, Compère P, et al. Chitosan enriched three-dimensional matrix reduces inflammatory and catabolic mediators production by human chondrocytes. PLoS One. 2015;10(5):1–17.
212. Reginster JY, Neuprez A, Lecart MP, Sarlet N, Bruyere O. Role of glucosamine in the treatment for osteoarthritis. Rheumatol Int. 2012;32(10):2959–67.
213. Nagaoka I, Tsuruta A, Yoshimura M. Chondroprotective action of glucosamine, a chitosan monomer, on the joint health of athletes. Int J Biol Macromol. 2019;132:795–800.
214. Qaqish RB, Amiji MM. Synthesis of a fluorescent chitosan derivative and its application for the study of chitosan-mucin interactions. Carbohydr Polym. 1999;38(2):99–107.
215. Yadu NV, Raghvendra KM, Aswathy V, Parvathy P, Sunija S, Neelakandan M, et al. Chitosan as Promising Materials for Biomedical Application: Review. Res Dev Mater Sci. 2017;2(4):170–85.
216. Noble JE, Bailey MJA. Quantitation of Protein. Vol. 463, Methods in Enzymology. 2009. 73–95 p.
217. Calvo P, Remuñán-López C, Vila-Jato JL, Alonso MJ. Novel hydrophilic chitosan-polyethylene oxide nanoparticles as protein carriers. J Appl Polym Sci. 1997;63(1):125–32.
218. Burguera EF, Vela-Anero Á, Magalhães J, Meijide-Faílde R, Blanco FJ. Effect of hydrogen sulfide sources on inflammation and catabolic markers on interleukin 1β-stimulated human articular chondrocytes. Osteoarthr Cartil. 2014;22(7):1026–35.
219. Cillero-Pastor B, Martin MA, Arenas J, Lápez-Armada MJ, Blanco FJ. Effect of nitric oxide on mitochondrial activity of human synovial cells. BMC Musculoskelet Disord. 2011;12(1):42.
220. Viegas CSB, Santos L, Macedo AL, Matos AA, Silva AP, Neves PL, et al. Chronic Kidney Disease Circulating Calciprotein Particles and Extracellular Vesicles Promote Vascular Calcification: A Role for GRP (Gla-Rich Protein). Arterioscler Thromb Vasc Biol. 2018;38(3):575–87.
221. Tintut Y, Patel J, Territo M, Saini T, Parhami F, Demer LL. Monocyte/macrophage regulation of vascular calcification in vitro. Circulation. 2002;105(5):650–5.
222. Rahmati M, Mobasheri A, Mozafari M. Inflammatory mediators in osteoarthritis: A critical review of the state-of-the-art, current prospects, and future challenges. Bone. 2016 Apr;85:81–90.
223. Legein B, Temmerman L, Biessen EAL, Lutgens E. Inflammation and immune system interactions in atherosclerosis. Cell Mol Life Sci. 2013;70(20):3847–69.
224. Viegas CSB, Araújo N, Carreira J, Pontes JF, Macedo AL, Vinhas M, et al. Nanoencapsulation of Gla-Rich Protein (GRP) as a Novel Approach to Target Inflammation. Int J Mol Sci. 2022;23(9).
225. Hillaireau H, Couvreur P. Nanocarriers' entry into the cell: Relevance to drug delivery. Cell Mol Life Sci. 2009;66(17):2873–96.
226. Aderem A, Underhill DM. Mechanisms of phagocytosis in macrophages. Annu Rev Immunol. 1999;17:593–623.
227. Johnson CI, Argyle DJ, Clements DN. In vitro models for the study of osteoarthritis. Vet J. 2016;209:40–9.

228. Kapoor M, Martel-Pelletier J, Lajeunesse D, Pelletier JP, Fahmi H. Role of proinflammatory cytokines in the pathophysiology of osteoarthritis. Nat Rev Rheumatol. 2011;7(1):33–42.
229. Takano S, Uchida K, Miyagi M, Inoue G, Aikawa J, Fujimaki H, et al. Synovial macrophage-derived IL-1β regulates the calcitonin receptor in osteoarthritic mice. Clin Exp Immunol. 2016;183(1):143–9.
230. Sun ARJ, Friis T, Sekar S, Crawford R, Xiao Y, Prasadam I. Is Synovial Macrophage Activation the Inflammatory Link Between Obesity and Osteoarthritis? Curr Rheumatol Rep. 2016;18(9).
231. Bondeson J, Blom AB, Wainwright S, Hughes C, Caterson B, Van Den Berg WB. The role of synovial macrophages and macrophage-produced mediators in driving inflammatory and destructive responses in osteoarthritis. Arthritis Rheum. 2010;62(3):647–57.
232. Al-Qadi S, Grenha A, Carrión-Recio D, Seijo B, Remuñán-López C. Microencapsulated chitosan nanoparticles for pulmonary protein delivery: In vivo evaluation of insulin-loaded formulations. J Control Release. 2012;157(3):383–90.
233. Grenha A, Seijo B, Remuñán-López C. Microencapsulated chitosan nanoparticles for lung protein delivery. Eur J Pharm Sci. 2005;25(4–5):427–37.
234. Mohammed MA, Syeda JTM, Wasan KM, Wasan EK. An overview of chitosan nanoparticles and its application in non-parenteral drug delivery. Pharmaceutics. 2017;9(4).
235. Caprifico AE, Polycarpou E, Foot PJS, Calabrese G. Biomedical and Pharmacological Uses of Fluorescein Isothiocyanate Chitosan-Based Nanocarriers. Macromol Biosci. 2021;21(1):1–27.
236. Zhao J, Wu J. Preparation and Characterization of the Fluorescent Chitosan Nanoparticle Probe. Chinese J Anal Chem. 2006;34(11):1555–9.
237. Fan W, Yan W, Xu Z, Ni H. Formation mechanism of monodisperse, low molecular weight chitosan nanoparticles by ionic gelation technique. Colloids Surf B Biointerfaces. 2012;90(1):21–7.
238. Gan Q, Wang T. Chitosan nanoparticle as protein delivery carrier-Systematic examination of fabrication conditions for efficient loading and release. Colloids Surfaces B Biointerfaces. 2007;59(1):24–34.
239. Poth N, Seiffart V, Gross G, Menzel H, Dempwolf W. Biodegradable chitosan nanoparticle coatings on titanium for the delivery of BMP-2. Biomolecules. 2015;5(1):3–19.
240. De Campos AM, Diebold Y, Carvalho ELS, Sánchez A, Alonso MJ. Chitosan nanoparticles as new ocular drug delivery systems: In vitro stability, in vivo fate, and cellular toxicity. Pharm Res. 2004;21(5):803–10.
241. Pant A, Negi JS. Novel controlled ionic gelation strategy for chitosan nanoparticles preparation using TPP-β-CD inclusion complex. Eur J Pharm Sci. 2018;112(1):180–5.
242. Sreekumar S, Goycoolea FM, Moerschbacher BM, Rivera-Rodriguez GR. Parameters influencing the size of chitosan-TPP nano- and microparticles. Sci Rep. 2018;8(1):1–11.
243. Huang M, Ma Z, Khor E, Lim LY. Uptake of FITC-chitosan nanoparticles by A549 cells. Pharm Res. 2002;19(10):1488–94.
244. Stannus O, Jones G, Cicuttini F, Parameswaran V, Quinn S, Burgess J, et al. Circulating levels of IL-6 and TNF-α are associated with knee radiographic osteoarthritis and knee cartilage loss in older adults. Osteoarthr Cartil. 2010;18(11):1441–7.
245. Ashford S, Williard J. Osteoarthritis: A review. Nurse Pract. 2014;39(5):1–8.
246. Fábio dos Santos Duarte Lana J, Lima Rodrigues B. Osteoarthritis as a Chronic Inflammatory Disease: A Review of the Inflammatory Markers. Osteoarthr Biomarkers

Treat. 2019;
247. Nasi S, So A, Combes C, Daudon M, Busso N. Interleukin-6 and chondrocyte mineralisation act in tandem to promote experimental osteoarthritis. Ann Rheum Dis. 2016;75(7):1372–9.
248. Wang J, Wang X, Cao Y, Huang T, Song DX, Tao HR. Therapeutic potential of hyaluronic acid/chitosan nanoparticles for the delivery of curcuminoid in knee osteoarthritis and an in vitro evaluation in chondrocytes. Int J Mol Med. 2018;42(5):2604–14.
249. Blanco FJ. Osteoarthritis: something is moving. Reumatol Clin. 2014;10(1):4–5.
250. Robinson WH, Lepus CM, Wang Q, Raghu H, Mao R, Lindstrom TM, et al. Low-grade inflammation as a key mediator of the pathogenesis of osteoarthritis. Nat Rev Rheumatol. 2016;12(10):580–92.
251. Ledford BYH. 4 Ways To Fix Clinical Trial. Nature. 2011;477(29):526–8.
252. Khoruzhenko AI. 2D- and 3D-cell culture. Biopolym Cell. 2011;27(1):17–24.
253. McCoy AM. Animal Models of Osteoarthritis: Comparisons and Key Considerations. Vet Pathol. 2015;52(5):803–18.
254. Zheng W, Feng Z, You S, Zhang H, Tao Z, Wang Q, et al. Fisetin inhibits IL-1β-induced inflammatory response in human osteoarthritis chondrocytes through activating SIRT1 and attenuates the progression of osteoarthritis in mice. Int Immunopharmacol. 2017;45:135–47.
255. Wei FY, Lee JK, Wei L, Qu F, Zhang JZ. Correlation of insulin-like growth factor 1 and osteoarthritic cartilage degradation: a spontaneous osteoarthritis in guinea-pig. Eur Rev Med Pharmacol Sci. 2017;21(20):4493–500.
256. Choi MC, Jo J, Park J, Kang HK, Park Y. NF-κb signaling pathways in osteoarthritic cartilage destruction. Cells. 2019;8(7):1–21.
257. Chomczynski P, Sacchi N. The single-step method of RNA isolation by acid guanidinium thiocyanate-phenol-chloroform extraction: Twenty-something years on. Nat Protoc. 2006;1(2):581–5.
258. Pritzker KPH, Gay S, Jimenez SA, Ostergaard K, Pelletier JP, Revell K, et al. Osteoarthritis cartilage histopathology: Grading and staging. Osteoarthr Cartil. 2006;14(1):13–29.
259. López-Senra E, Casal-Beiroa P, López-Álvarez M, Serra J, González P, Valcarcel J, et al. Impact of prevalence ratios of chondroitin sulfate (CS)- 4 and -6 isomers derived from marine sources in cell proliferation and chondrogenic differentiation processes. Mar Drugs. 2020;18(2).
260. Rosenberg L. Chemical basis for the histological use of safranin O in the study of articular cartilage. J Bone Jt Surg Am. 1971;53(1):69–82.
261. Viegas CSB, Cavaco S, Neves PL, Ferreira A, João A, Williamson MK, et al. Gla-rich protein is a novel vitamin K-dependent protein present in serum that accumulates at sites of pathological calcifications. Am J Pathol. 2009;175(6):2288–98.
262. Pascual Garrido C, Hakimiyan AA, Rappoport L, Oegema TR, Wimmer MA, Chubinskaya S. Anti-apoptotic treatments prevent cartilage degradation after acute trauma to human ankle cartilage. Osteoarthr Cartil. 2009;17(9):1244–51.
263. Hernandez-Santana A, Yavorskyy A, Loughran ST, McCarthy GM, McMahon GP. New approaches in the detection of calcium-containing microcrystals in synovial fluid. Bioanalysis. 2011;3(10):1085–91.
264. Corr EM, Cunningham CC, Helbert L, McCarthy GM, Dunne A. Osteoarthritis-associated basic calcium phosphate crystals activate membrane proximal kinases in human innate immune cells. Arthritis Res Ther. 2017;19(1):1–13.
265. Nadra I, Mason JC, Philippidis P, Florey O, Smythe CDW, McCarthy GM, et al.

Proinflammatory activation of macrophages by basic calcium phosphate crystals via protein kinase C and MAP kinase pathways: A vicious cycle of inflammation and arterial calcification? Circ Res. 2005;96(12):1248–56.
266. Wojdasiewicz P, Poniatowski ŁA, Szukiewicz D. The role of inflammatory and anti-inflammatory cytokines in the pathogenesis of osteoarthritis. Mediators Inflamm. 2014;2014.
267. Jung YK, Han MS, Park HR, Lee EJ, Jang JA, Kim GW, et al. Calcium-phosphate complex increased during subchondral bone remodeling affects earlystage osteoarthritis. Sci Rep. 2018;8(1):1–10.
268. Rose BJ, Kooyman DL. A Tale of Two Joints: The Role of Matrix Metalloproteases in Cartilage Biology. Dis Markers. 2016;2016.
269. Ismail HM, Yamamoto K, Vincent TL, Nagase H, Troeberg L, Saklatvala J. Interleukin-1 acts via the JNK-2 signaling pathway to induce aggrecan degradation by human chondrocytes. Arthritis Rheumatol. 2015;67(7):1826–36.
270. Hall AC. The Role of Chondrocyte Morphology and Volume in Controlling Phenotype—Implications for Osteoarthritis, Cartilage Repair, and Cartilage Engineering. Curr Rheumatol Rep. 2019;21(8).
271. Araujo N, Viegas CSB, Zubfa E, Magalhaes J, Ramos A, Carvalho MM, et al. Amentadione from the Alga Cystoseira usneoides as a Novel Osteoarthritis Protective Agent in an Ex Vivo Co-Culture OA Model. Mar Drugs. 2020;18(12).
272. Sutton S, Clutterbuck A, Harris P, Gent T, Freeman S, Foster N, et al. The contribution of the synovium, synovial derived inflammatory cytokines and neuropeptides to the pathogenesis of osteoarthritis. Vet J. 2009;179(1):10–24.
273. Abramson SB, Attur M, Amin AR, Clancy R. Nitric oxide and inflammatory mediators in the perpetuation of osteoarthritis. Curr Rheumatol Rep. 2001;3(6):535–41.
274. Mobasheri A. The future of osteoarthritis therapeutics: Targeted pharmacological therapy topical collection on osteoarthritis. Curr Rheumatol Rep. 2013;15(10).
275. Henrotin Y, Mobasheri A. Natural Products for Promoting Joint Health and Managing Osteoarthritis. Curr Rheumatol Rep. 2018;20(11):1–9.
276. Suroowan S, Mahomoodally F. Herbal Products for Common Auto-Inflammatory Disorders - Novel Approaches. Comb Chem High Throughput Screen. 2018;21(3):161–74.
277. Castrogiovanni P, Trovato FM, Loreto C, Nsir H, Szychlinska MA, Musumeci G. Nutraceutical supplements in the management and prevention of osteoarthritis. Int J Mol Sci. 2016;17(12).
278. Stoppoloni D, Politi L, Leopizzi M, Gaetani S, Guazzo R, Basciani S, et al. Effect of glucosamine and its peptidyl-derivative on the production of extracellular matrix components by human primary chondrocytes. Osteoarthr Cartil. 2015;23(1):103–13.
279. Paul AT, Gohil VM, Bhutani KK. Modulating TNF-α signaling with natural products. Drug Discov Today. 2006;11(15–16):725–32.
280. Wang G, Tang W, Bidigare RR. Terpenoids as therapeutic drugs and pharmaceutical agents. Nat Prod Drug Discov Ther Med. 2005;197–227.
281. De Los Reyes C, Zbakh H, Motilva V, Zubía E. Antioxidant and anti-inflammatory meroterpenoids from the brown alga Cystoseira usneoides. J Nat Prod. 2013;76(4):621–9.
282. Zbakh H, Talero E, Avila J, Alcaide A, De Los Reyes C, Zubía E, et al. The algal meroterpene 11-hydroxy-1′-O-methylamentadione ameloriates dextran sulfate sodium-induced colitis in mice. Mar Drugs. 2016;14(8):1–14.
283. Zbakh H, Zubía E, de los Reyes C, Calderón-Montaño JM, López-Lázaro M, Motilva V. Meroterpenoids from the brown alga cystoseira usneoides as potential anti-inflammatory

and lung anticancer agents. Mar Drugs. 2020;18(4).
284. Zweers MC, de Boer TN, van Roon J, Bijlsma JWJ, Lafeber FPJG, Mastbergen SC. Celecoxib: Considerations regarding its potential disease-modifying properties in osteoarthritis. Arthritis Res Ther. 2011;13(5).
285. Aitken D, Laslett LL, Pan F, Haugen IK, Otahal P, Bellamy N, et al. A randomised double-blind placebo-controlled crossover trial of HUMira (adalimumab) for erosive hand OsteoaRthritis – the HUMOR trial. Osteoarthr Cartil. 2018;26(7):880–7.
286. Rider P, Carmi Y, Cohen I. Biologics for Targeting Inflammatory Cytokines, Clinical Uses, and Limitations. Int J Cell Biol. 2016;2016(iv).
287. Cheng W, Wu D, Zuo Q, Wang Z, Fan W. Ginsenoside Rb1 prevents interleukin-1 beta induced inflammation and apoptosis in human articular chondrocytes. Int Orthop. 2013;37(10):2065–70.
288. Jurenka JS. Anti-inflammatory properties of curcumin, a major constituent of Curcuma longa: a review of preclinical and clinical research. Altern Med Rev. 2009;14(2):141–53.
289. Marcu KB, Otero M, Olivotto E, Borzi RM, Goldring MB. NF-kappaB signaling: multiple angles to target OA. Curr Drug Targets. 2010;11(5):599–613.
290. Olivotto E, Otero M, Marcu KB, Goldring MB. Pathophysiology of osteoarthritis: Canonical NF-κB/IKKβ-dependent and kinase-independent effects of IKKα in cartilage degradation and chondrocyte differentiation. RMD Open. 2015;1(Suppl 1):1–6.
291. Jain H, Dhingra N, Narsinghani T, Sharma R. Insights into the mechanism of natural terpenoids as NF-κB inhibitors: An overview on their anticancer potential. Exp Oncol. 2016;38(3):158–68.
292. Fibel KH. State-of-the-Art management of knee osteoarthritis. World J Clin Cases. 2015;3(2):89.
293. Rosenthal AK. Crystals, inflammation, and osteoarthritis. Curr Opin Rheumatol. 2011;23(2):170–3.
294. Kim Y, Zharkinbekov Z, Raziyeva K, Tabyldiyeva L, Berikova K, Zhumagul D, et al. Chitosan-Based Biomaterials for Tissue Regeneration. Pharmaceutics. 2023;15(3).
295. Mi FL, Shyu SS, Peng CK. Characterization of ring-opening polymerization of genipin and pH-dependent cross-linking reactions between chitosan and genipin. J Polym Sci Part A Polym Chem. 2005;43(10):1985–2000.
296. Azuma K, Osaki T, Minami S, Okamoto Y, Puoci F. Anticancer and Anti-Inflammatory Properties of Chitin and Chitosan Oligosaccharides. J Funct Biomater 2015, Vol 6, Pages 33-49. 2015;6(1):33–49.
297. Jhundoo HD, Siefen T, Liang A, Schmidt C, Lokhnauth J, Béduneau A, et al. Anti-Inflammatory Activity of Chitosan and 5-Amino Salicylic Acid Combinations in Experimental Colitis. Pharmaceutics. 2020;12(11):1–16.
298. Cope PJ, Ourradi K, Li Y, Sharif M. Models of osteoarthritis: the good, the bad and the promising. Osteoarthr Cartil. 2019;27(2):230–9.
299. Mohammadi MA, Farshi P, Ahmadi P, Ahmadi A, Yousefi M, Ghorbani M, et al. Encapsulation of Vitamins Using Nanoliposome: Recent Advances and Perspectives. Adv Pharm Bull. 2023;13(1):48–68.
300. Aguilar-Pérez KM, Avilés-Castrillo JI, Medina DI, Parra-Saldivar R, Iqbal HMN. Insight Into Nanoliposomes as Smart Nanocarriers for Greening the Twenty-First Century Biomedical Settings. Front Bioeng Biotechnol. 2020;8(December):1–23.
301. Martel-Pelletier J, Barr AJ, Cicuttini FM, Conaghan PG, Cooper C, Goldring MB, et al. Osteoarthritis. Nat Rev Dis Prim. 2016;2.

Thesis Outline - Manuscripts

- Gla-rich protein function as an anti-inflammatory agent in monocytes/macrophages: implications for calcification-related chronic inflammatory diseases, Carla S. B. Viegas, Rúben M. Costa, Lúcia Santos, Paula A. Videira, Zélia Silva, Nuna Araújo, Anjos L. Macedo, António P. Matos, Cees Vermeer, Dina C. Simes (2017) PLoS ONE 12(5): e0177829. https://doi.org/10.1371/journal.pone.0177829

- Use of an innovative system and nanotechnology-based strategy for therapeutic applications of Gla-rich protein (GRP), Carla Viegas, Evelina Edelweiss, Justine Schneider, Christine SchaefferReiss, Arnaud Poterszman, Marta Rafael, Nuna Araújo, Anjos Macedo, António Alves de Matos & Dina Simes (2019) Annals of Medicine, 51:sup1, 38-38. DOI: 10.1080/07853890.2018.1561804.

- Amentadione is a new modulating agent for osteoarthritis in an ex-vivo co-culture preclinical assay, Nuna Araújo, Carla Viegas, Inês Perrolas, Rúben Costa, Joana Magalhães, Francisco Blanco, Acácio Ramos, Maria Miguel, Cees Vermeer, Eva Zubía & Dina Simes (2019) Annals of Medicine, 51:sup1, 43-43. DOI: 10.1080/07853890.2018.1561895.

- Vitamin K as a Powerful Micronutrient in Aging and Age-Related Diseases: Pros and Cons from Clinical Studies, Simes DC, Viegas CSB, Araújo N, Marreiros C. (2019) Int J Mol Sci.;20(17):4150. DOI:10.3390/ijms20174150. 9

- The interplay between mineral metabolism, vascular calcification and inflammation in Chronic Kidney Disease (CKD): challenging old concepts with new facts, Viegas C, Araújo N, Marreiros C, Simes D. (2019) Aging (Albany NY). 11(12):4274-4299. https://www.ncbi.nlm.nih.gov/pmc/articles/PMC6628989/

- Vitamin K as a Diet Supplement with Impact in Human Health: Current Evidence in Age-Related Diseases, Simes, D.C.; Viegas, C.S.B.; Araújo, N.; Marreiros, C (2020) Nutrients, 12, 138. https://doi.org/10.3390/md18010040

- Nanoencapsulation of Gla-Rich Protein (GRP) as a Novel Approach to Target Inflammation, Viegas, C.S.B.; Araújo, N.; Carreira, J.; Pontes, J.F.; Macedo, A.L.; Vinhas, M.; Moreira, A.S.; Faria, T.Q.; Grenha, A.; de Matos, A.A.; Schurgers, L.; Vermeer, C.; Simes, D.C. (2022) Int. J. Mol. Sci., 23, 4813. https://doi.org/10.3390/ijms2309481